

**Roles of Interphase Node Protein Nod1 and UNC-13/Munc13 Protein  
Ync13 during Fission Yeast Cytokinesis**

**Dissertation**

Presented in Partial Fulfillment of the Requirements for the Degree Doctor of Philosophy  
in the Graduate School of The Ohio State University

By

Yihua Zhu, B.S.

Graduate Program in Molecular Genetics

The Ohio State University

2017

Dissertation Committee

Dr. Jian-Qiu Wu, Advisor

Dr. Stephen Osmani

Dr. Hay-Oak Park

Dr. Dmitri Kudryashov

Copyright by

Yihua Zhu

2017

## **Abstract**

Cytokinesis is a complicated yet important cellular process that divides the mother cell into two daughter cells. Fission yeast serves as a model organism to study cytokinesis, not only because of its relatively small size and ease for genetic manipulation but also because of the conservation during the cytokinesis process between yeast and human. In both organisms, cells assemble an actomyosin contractile ring at a predefined division site, and the ring constricts and guides furrow ingression and extracellular matrix formation. Although multiple reported protein complexes and signaling pathways contributed to successful cytokinesis, discoveries of novel components always shed new light on the mechanisms and regulation of cytokinesis. In this work, I discuss the roles of two previously uncharacterized proteins in cytokinesis.

In fission yeast, the contractile ring is formed by a group of protein assemblies called nodes at the medial cortex. Nod1 is one of the components in the nodes and the contractile ring. I found Nod1 binds to another node component, the Rho Guanine nucleotide exchange factor Gef2, which is essential to both proteins for their localization and function in division site positioning. During the later stage of cytokinesis, Gef2 and Nod1 stabilize the contractile ring during ring constriction and affect the recruitment of the SIN pathway component Sid2 to the division site. The putative Gef2 GEF domain bind to Rho1, Rho4 and Rho5 GTPases in vitro. Taken together, our data indicate that

Nod1 and Gef2 function cooperatively in a protein complex to regulate fission yeast cytokinesis.

The yeast Unc-13/Munc13 protein Ync13 is another novel protein that localizes to the division site by interacting with lipids. Cells without Ync13 fail to grow on rich medium and have severe cell wall defects that lead to cell lysis. I found Ync13 affects the localization and dynamics of cell wall synthases and the upstream Rho GTPases dependent cell integrity pathway via altering the location of both exocytosis and endocytosis at the division site. Thus, Ync13 serves as a vital link between membrane trafficking and cell wall integrity during the late stage of cytokinesis.

## **Dedication**

This dissertation is dedicated to my wife Yuting Shou, who continuously supported and encouraged me during my PhD study.

## **Acknowledgements**

I thank my parents for their consistent support to my life and study at the United States.

I thank the people in Wu lab, Dr. Valerie Coffman, Dr. I-Ju Lee, Dr. Damien Laporte, Dr. Yanfang Ye, Dr. Ning Wang, Dr. Reshma Davidson, Dr. Mo Wang, Yajun Liu and Ken Gerien for keeping a comfortable lab environment and providing useful suggestions to my projects. I thank Kristyn Gumper, Vedud Purde, and Menglin Chen for giving me the opportunity to work with them during their first year rotation. I thank Joanne Hynn for helping my projects as an undergraduate assistant. I thank other undergraduate students in the Wu lab for making medium and organizing lab supplies.

I thank the people in Department of Molecular Genetics. I thank my Committee, Dr. Stephen Osmani, Dr. Hay-Oak Park and Dr. Dmitri Kudryashov for giving critical thoughts and suggestion to my PhD study. I thank people in Dr. Anita Hopper lab, Dr. Jim Hopper lab, Dr. Stephen Osmani lab, Dr. Hay-Oak Park lab and Dr. Paul Herman lab for sharing reagents and equipment. I thank Dr. David Bisaro and Dr. Anna Alonso for letting me do first year rotation in their labs. I thank Dr. Robin Wharton and Dr. Susan Cole for their roles at graduate student committee. I thank the MG staff Debbie Dotter, Jessie Siegman, Eduardo Acosta and Dameyon Shipley for providing help and support in all kinds of events and meetings.

I thank Bo Zhang, Yao Wan, Qian Shi, Daokun Sun, Xiangnan Guan, Chaojie Wang, Xiao Zhou and Huayang Liu for being supportive for my academic and personal

life. I thank Tianyu Cao, Qiuwan Wang, Shengjie Sun, Yibo Zhang and Yi Rong for being excellent roommates and good friends. I thank Yi Wang, Chen Ge, Kaiwen Zhang, Heting Li, Prashanth Ramesh for being good friends during my life at Columbus.

Finally, I want to thank Dr. Jian-Qiu Wu for the continuous guidance and advice during my PhD study. I thank him for being a role model of diligent and passionate science researcher, and for developing my critical thinking and experimental skills which I will carry for the rest of my career.

## Vita

- 2009 ..... B.S. Biological Science, Fudan University
- 2009-2010 ..... Assistant Researcher, Fudan University
- 2010-2014 ..... Graduate Teaching/Research Associate  
The Ohio State University
- 2014-2016 ..... Pelotonia Fellowship,  
The Ohio State University
- 2016-2017 ..... Graduate Teaching/Research Associate  
The Ohio State University

## Publications

- Wang, N., Wang M., **Zhu Y.-H.**, Grosel T.W., Sun D., Kudryashov D.S., Wu J.-Q..  
2015. The Rho-GEF Gef3 interacts with the septin complex and activates the  
GTPase Rho4 during fission yeast cytokinesis. *Mol. Biol. Cell* 26(2):238-255
- Wang, N., Lo Presti L., **Zhu Y.-H.**, Kang M., Wu Z., Martin S.G., Wu J.-Q.. 2014. The  
novel proteins Rng8 and Rng9 regulate the myosin-V Myo51 during fission yeast  
cytokinesis. *J. Cell Biol.* 205(3):357-375
- Zhu, Y.-H.** & Wu J.-Q.. 2013. Cell-size control: Complicated. *Cell Cycle* 13(5):693-694

**Zhu, Y.-H.,** Ye Y., Wu Z. and Wu J.-Q.. 2013. Cooperation between Rho-GEF Gef2 and its binding partner Nod1 in the regulation of fission yeast cytokinesis. *Mol. Biol. Cell.* 24:3187-3204

## **Field of Study**

Major Field: Molecular Genetics

## Table of Contents

Abstract.....	ii
Dedication.....	iv
Acknowledgements.....	v
Vita.....	vii
Table of Contents.....	ix
List of Figures.....	xiii
List of Tables.....	xv
List of Abbreviations.....	xvi
Chapter 1: Introduction.....	1
Chapter 2: Cooperation between Rho-GEF Gef2 and Its Binding Partner Nod1 in the Regulation of Fission Yeast Cytokinesis.....	10
2.1 Abstract.....	10
2.2 Introduction.....	11
2.3 Materials and methods.....	14
2.3.1 Strains, genetic, molecular, and cellular methods.....	14
2.3.2 Microscopy and data analysis.....	15
2.3.3 FRAP analysis.....	17
2.3.4 IP and Western blotting.....	18
2.3.5 Yeast two-hybrid assays.....	18
2.3.6 Protein purification and the interaction between Gef2 and Rho GTPases.....	19

2.4 Results.....	20
2.4.1 Nod1 is a Gef2 related protein that localizes to cortical nodes and the contractile ring20	
2.4.2 Nod1 regulates division-site positioning cooperatively with Polo kinase Plo1 .....	23
2.4.3 Nod1 and Gef2 are interdependent on their C-termini for localization to cortical nodes .....	24
2.4.4 Nod1 physically interacts with Gef2 through their C-termini .....	28
2.4.5 The F-BAR protein Cdc15 recruits Nod1 and Gef2 to the contractile ring through its interaction with the Nod1 N-terminus .....	28
2.4.6 Nod1 and Gef2 affect the contractile-ring stability during late cytokinesis .....	30
2.4.7 Nod1 and Gef2 suppress mutants in the SIN pathway and affect Sid2 kinase localization.....	34
2.4.8 Gef2 interacts with Rho GTPases in vitro and is involved in Rho4 localization.....	37
2.5 Discussion.....	40
2.5.1 The roles of Rho GTPases during cytokinesis .....	41
2.5.2 Localization of Nod1 and Gef2 during the cell cycle .....	42
2.5.3 Nod1 and Gef2 coordinate with F-BAR protein Cdc15 to maintain contractile-ring stability.....	43
2.5.4 Nod1 and Gef2 suppress the SIN pathway .....	44
2.6 Acknowledgements.....	46
 Chapter 3: Involvement of the UNC-13/Munc13 Protein Ync13 in Endocytosis during Fission	
Yeast Cytokinesis .....	57
3.1 Abstract.....	57
3.2 Introduction.....	57
3.3 Materials and methods .....	63
3.3.1 Strains, genetic, molecular, and cellular methods.....	63

3.3.2 Confocal microscopy and image analysis.....	65
3.3.3 Photobleaching, FRAP, and FLIP analysis.....	68
3.3.4 Superresolution microscopy.....	69
3.3.5 Electron microscopy.....	69
3.3.6 Plasmid construction and protein purification.....	70
3.3.7 Protein-lipid overlay assays.....	71
3.3.8 Liposome cofloatation, clustering, and copelleting assays.....	72
3.3.9 Simultaneous lipid mixing and content mixing assays.....	73
3.4 Results.....	74
3.4.1 Ync13 localizes to the division site during cytokinesis.....	74
3.4.2 Ync13 depends on the contractile ring for localization and interacts with membrane lipids.....	76
3.4.3 Ync13 MHD and C2 domains did not promote lipid mixing or lipid clustering.....	80
3.4.4 Ync13 is essential for cell integrity.....	81
3.4.5 Roles of Ync13 in localizations of cell wall enzymes glucan synthases and glucanase.....	87
3.4.6 Ync13 collaborates with the exocyst complex to mediate exocytosis at the division site.....	89
3.4.7 Does Ync13 regulate exocytosis mediated by the TRAPP-II complex?.....	92
3.4.8 Ync13 is important for selecting endocytic site at the division plane.....	94
3.4.9 Septin deletion partially rescues <i>ync13Δ</i> cells.....	98
3.5 Discussion.....	98
3.5.1 A novel role of UNC-13/Munc13 protein family in cytokinesis.....	99
3.5.2 Roles of Ync13 in spatial regulation of cell wall enzymes and membrane trafficking during cytokinesis.....	101
3.5.3 Ync13 domains for its localization and functions.....	103

3.5.4 Septins as possible regulators of endocytosis .....	103
3.6 Acknowledgement .....	104
Chapter 4: Conclusions and Future Directions .....	116
4.1 The role of putative Rho GEF Gef2 and its binding partner Nod1 during early and late cytokinesis .....	116
4.2 The novel role of UNC-13/Munc13 protein during cytokinesis .....	118
References.....	121

## List of Figures

Figure 1.1 Cytokinesis in fission yeast. ....	3
Figure 2.1 Nod1 colocalizes with Gef2 in cortical nodes and the contractile ring and shares similar function with Gef2 in division-site selection. ....	22
Figure 2.2 Nod1 and Gef2 are interdependent on their C-termini for cortical node localization and partially interdependent for localization to the contractile ring. ....	25
Figure 2.3 Nod1 and Gef2 physically interact through their C-termini. ....	27
Figure 2.4 The F-BAR protein Cdc15 recruits or stabilizes Nod1 and Gef2 localization to the division site by interaction with Nod1 N-terminus. ....	29
Figure 2.5 Nod1 and Gef2 affect contractile-ring stability. ....	32
Figure 2.6 Gef2 affects contractile-ring stability during cytokinesis. ....	33
Figure 2.7 <i>nod1</i> $\Delta$ and <i>gef2</i> $\Delta$ suppress SIN mutants by reducing cell lysis. ....	35
Figure 2.8 <i>nod1</i> $\Delta$ and <i>gef2</i> $\Delta$ suppress SIN mutant <i>cdc7-24</i> by reducing cell lysis. ....	36
Figure 2.9 Gef2 GEF domain binds to GTPases Rho1, Rho4, and Rho5 in vitro. ....	38
Figure 2.10 Model of Nod1 and Gef2 localizations and interactions with other proteins on the cytoplasmic side of the plasma membrane during the cell cycle. ....	40
Figure 3.1 Ync13 localizes to the division site. ....	75
Figure 3.2 Localization dependence and domain analyses of Ync13. ....	77

Figure 3.3 Ync13 depends on the contractile ring for localization and interacts with membrane lipids.....	79
Figure 3.4 Ync13 interacts with lipids but does not promote vesicle fusion.....	80
Figure 3.5 <i>ync13Δ</i> is lethal due to cell lysis.....	82
Figure 3.6 Ync13 coordinates with Rho1 GTPase dependent cell integrity pathway during cytokinesis.....	84
Figure 3.7 Synthetic interactions between mutations in <i>ync13</i> and cell wall enzymes. ....	86
Figure 3.8 Ync13 affects the distribution of cell wall enzymes on the division plane. ....	88
Figure 3.9 Cooperation between Ync13 and exocyst during cytokinesis. ....	91
Figure 3.10 Involvement of Ync13 in exocytosis and endocytosis. ....	92
Figure 3.11 Ync13 affects localizations and dynamics of TRAPP-II complex and Rab11 GTPase Ypt3 at the division plane during cytokinesis. ....	93
Figure 3.12 Sites of endocytosis at the division plane is compromised in <i>ync13Δ</i> cells..	95
Figure 3.13 Deletion of septin partially rescues <i>ync13Δ</i> . ....	97
Figure 3.14 Roles of Ync13 in cytokinesis. ....	99

## List of Tables

Table 2.1 Genetic interactions of <i>nod1Δ</i> with other mutations affecting cytokinesis and cell-size control.....	48
Table 2.2 <i>S. pombe</i> strains used in Chapter 2 .....	50
Table 3.1 Genetic interactions between <i>ync13</i> mutants and other mutants affecting cytokinesis and membrane trafficking.....	106
Table 3.2 Strains used in Chapter 3 .....	109

## List of Abbreviations

aa, amino acid

BFA, Brefeldin A

CME, clathrin mediated endocytosis

CIE, clathrin independent endocytosis

CIP, cell integrity pathway

DH, DBL-homology

DIC, differential interference contrast

EMM5S, Edinburgh minimal medium plus five supplements

FL, full length

FLIP, fluorescence loss in photobleaching

FRAP, fluorescence recovery after photobleaching

GEF, guanine nucleotide exchange factor

IP, immunoprecipitation

MBC, methyl benzimidazole-2-yl carbamate

mECitrine, monomeric enhanced Citrine

mEGFP, monomeric enhanced GFP

MHD, Munc13 homology domain

PALM, photoactivated localization microscopy

PB, phloxin B

PH, Pleckstrin homology

ROI, region of interest

SIN, septation initiation network

SPB, spindle pole body

tdTomato, tandem Tomato

TRAPP-II, Transport Protein Particle II

wt, wild type

## Chapter 1: Introduction

Cytokinesis is the cellular process that physically separates the mother cells into two daughter cells. To ensure successful cytokinesis, cells must first define a division site, where actin filaments and myosin complexes assemble the actomyosin contractile ring (Pollard, 2010; Pollard and Wu, 2010; Lee *et al.*, 2012). The contractile ring connects with the plasma membrane and guides the cleavage furrow during ring constriction. Cell division misregulations often lead to cytokinesis failure and eventually cell death or oncogenesis (Fujiwara *et al.*, 2005; Ganem *et al.*, 2007). It is thus important to understand the mechanisms and regulations of cytokinesis.

Our lab uses *Schizosaccharomyces pombe* as the model organism to study cytokinesis. Fission yeast shares many conserved features and protein components with animal cells during the progression of cytokinesis. Its relatively fast growth, smaller size, and haploid genome provide convenience for genetic manipulation and microscopy (Pollard and Wu, 2010). One can easily quantify the global and local levels for a protein of interest as well as its dynamics and interactions in vivo (Wu and Pollard, 2005; Coffman *et al.*, 2013; Coffman and Wu, 2014).

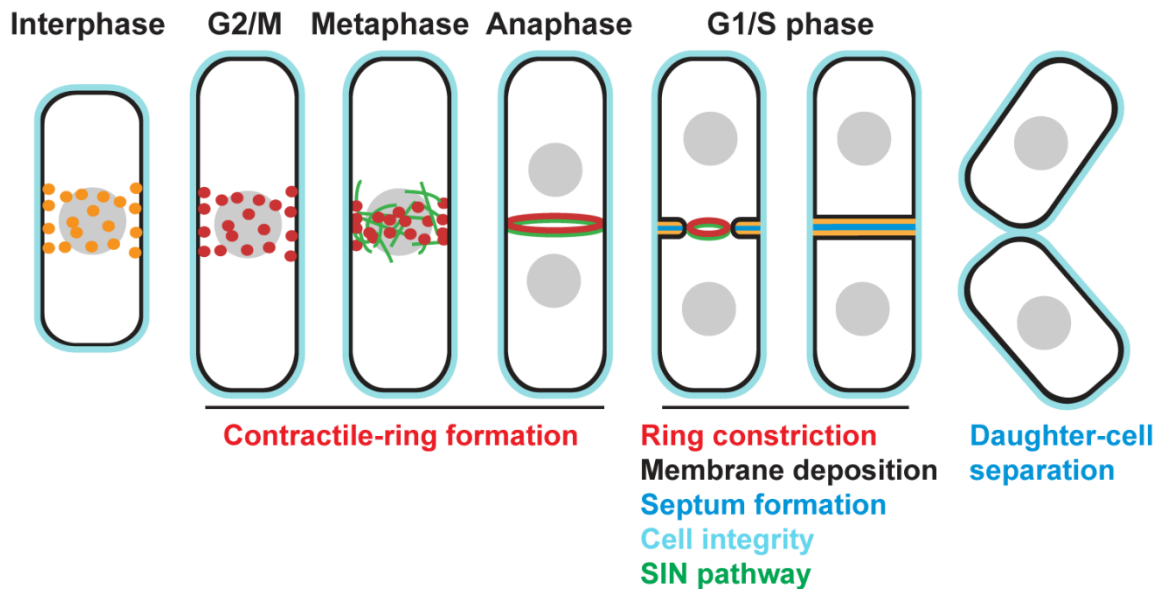
In fission yeast, cytokinesis starts with the formation of a zone of protein complexes called nodes at the medial cortex during interphase (Bähler *et al.*, 1998; Almonacid *et al.*, 2009; Lee *et al.*, 2012) (Figure 1.1). These nodes are the precursors of the contractile ring and are involved in mitotic entry and cell size control (Almonacid *et*

*al.*, 2009; Moseley *et al.*, 2009; Bhatia *et al.*, 2013; Deng and Moseley, 2013). There are two types of interphase nodes (Akamatsu *et al.*, 2014). The type I nodes, including the Anillin Mid1, and the SAD kinases Cdr1 and Cdr2, arrive at the cell cortex first (Almonacid *et al.*, 2009; Lee and Wu, 2012; Saha and Pollard, 2012b, a; Bhatia *et al.*, 2013). The components of type II nodes include the node protein Blt1, the Rho guanine nucleotide exchange factor (GEF) Gef2 and the kinesin Klp8, which join the type I nodes to form the interphase nodes (Ye *et al.*, 2012; Guzman-Vendrell *et al.*, 2013; Goss *et al.*, 2014). Among them, Mid1 plays a central role in division site position. During the G2/M transition, more Mid1 exit from the nuclei and join the nodes after the POLO kinase Plo1 phosphorylation (Bähler *et al.*, 1998; Almonacid *et al.*, 2011). This process is also coordinated by the type II node Gef2 and its binding partner Nod1, which stabilize Mid1 localization at the medial cortex (Jourdain *et al.*, 2013; Zhu *et al.*, 2013). Mid1 then recruits the downstream myosin II complex proteins, the IQGAP Rng2, the F-BAR protein Cdc15 and the formin Cdc12 in a hierarchy way to form the cytokinesis nodes (Laporte *et al.*, 2011). The mature cytokinesis nodes coalesce to the contractile ring through a search, capture, pull and release mechanism (Wu *et al.*, 2006; Vavylonis *et al.*, 2008; Ojkic *et al.*, 2011). Recent advances have shed more lights on the contractile ring formation through revealing the node structure by super-resolution microscopy and 3D simulations of ring assembly with or without Mid1 (Bidone *et al.*, 2014, 2015; Laplante *et al.*, 2016).

During the later stages of cytokinesis, the contractile ring starts to constrict and guides membrane invagination and extracellular matrix (ECM) formation (Pollard and

Wu, 2010; D'Avino *et al.*, 2015). Multiple components and pathways are reported to participate in the later stage of cytokinesis (Figure 1.1).

**Figure 1.1 Cytokinesis in fission yeast.**



During interphase, node proteins localize to the medial cortex. They mature into cytokinesis nodes at G2/M transition by recruiting myosin II complex and formins. The cytokinesis nodes then condense into the contractile ring. Multiple pathways contribute to the later stages of cytokinesis to promote membrane invagination and septum formation. Finally, the primary septum is digested, which leads to daughter-cell separation. Adapted from Lee *et al.*, 2012.

**ECM:** The ECM components are produced by cells to provide mechanical support and sense environment signaling (Jordan *et al.*, 2011; D'Avino *et al.*, 2015). The contributions from the ECM are limited in current models explaining cytokinesis. However, studies have reported that cell anchorage to the ECM by integrins are necessary for cytokinesis in adherent cells (Pellinen *et al.*, 2008; De Franceschi *et al.*, 2015). Hemicentin, a component of ECM in *C. elegans*, stabilizes the cleavage furrow during

cytokinesis (Vogel *et al.*, 2011; Xu and Vogel, 2011). In fungi, the ECM exists in the form of cell wall and septum (Cole, 1996; Sipiczki, 2007; Roncero and Sánchez, 2010). Whereas they are common features in fungi, the composition and structure of the septum and cell wall vary in different species (Cole, 1996; Walther and Wendland, 2003). In *S. pombe*, the septum is a three layered structure where a primary septum composed of linear  $\beta$ -1,3-glucan is sandwiched by two secondary septa mainly consisting of 1,6 branched  $\beta$ -1,3-glucan and  $\alpha$ -1,3-glucan (Cortés *et al.*, 2002; Cortés *et al.*, 2005; Cortés *et al.*, 2007; Roncero and Sánchez, 2010; Cortés *et al.*, 2012). During cytokinesis, the septum physically compartmentalizes the mother cell into two daughter cells and serves as new cell walls after cell separation to protect the cell integrity (Sipiczki, 2007; Roncero and Sánchez, 2010). Although the contractile ring constriction is important, it is now believed that septum formation by cell wall synthases provides the dominant force to promote furrow ingression during fission yeast cytokinesis (Proctor *et al.*, 2012; Stachowiak *et al.*, 2014; Thiyagarajan *et al.*, 2015; Zhou *et al.*, 2015).

**Rho GTPases:** Rho GTPases are small molecule switches that play important roles in many cellular processes including cytokinesis (Imamura *et al.*, 1997; García *et al.*, 2006b; Hall, 2012; Jordan and Canman, 2012; Mardilovich *et al.*, 2012). The Rho guanine nucleotide exchange factors (GEFs) are molecules that activate Rho GTPases by switching the hydrolyzed GDP for GTP. In animal cells, the activated RhoA/Rho1 GTPase recruits formins to the division site and activates myosin II to assemble the contractile ring (Piekny *et al.*, 2005; Su *et al.*, 2011; Hall, 2012; Jordan and Canman, 2012; Thumkeo *et al.*, 2013). In *S. pombe*, all six Rho GTPases (Rho1-5 and Cdc42), and seven Rho GEFs (Rgf1-3, Gef1-3, and Scd1) are actively involved in cytokinesis through

different pathways (García *et al.*, 2006b). Cdc42 regulates cell polarity, morphology, and septation (Coll *et al.*, 2003; Hirota *et al.*, 2003; Rincón *et al.*, 2007). Rho1 and Rho2 mediate the cell integrity pathway to activate the downstream  $\beta$ -glucan synthases Bgs1 and Bgs4 and  $\alpha$ -glucan synthase Ags1 at the division site for septum formation (Arellano *et al.*, 1996; Calonge *et al.*, 2000; Tajadura *et al.*, 2004; Nakano *et al.*, 2005; García *et al.*, 2006a; Rincón *et al.*, 2006). Rho3 is a regulator of exocytosis and Rho4 controls the glucanases Eng1 and Agn1 localizations for primary septum degradation (Kita *et al.*, 2011; Munoz *et al.*, 2014; Doi *et al.*, 2015; Pérez *et al.*, 2015; Wang *et al.*, 2015). A recent study suggested that Rho4 and Rho5 may also interact with Pck2 and regulate cell integrity pathway (Doi *et al.*, 2015). Out of the seven Rho GEFs, Rgf1-3 are the Rho GEFs for Rho1 while Gef1 and Scd1 activate Cdc42 (Coll *et al.*, 2003; Hirota *et al.*, 2003; Tajadura *et al.*, 2004; Morrell-Falvey *et al.*, 2005; Mutoh *et al.*, 2005; García *et al.*, 2009; Davidson *et al.*, 2015; Wei *et al.*, 2016). Until recently, the Rho substrates for Gef2 and Gef3 were unclear. Our lab has found that Gef3 activates Rho4 for promoting the formation and degradation of the septum (Wang *et al.*, 2015). In this work, I discovered that Gef2 is a potential GEF for Rho1, Rho4, and Rho5, and it stabilizes the contractile ring in addition to its role during early cytokinesis (Zhu *et al.*, 2013)(Chapter 2).

**SIN pathway:** The septum initiation network (SIN) pathway signals the constriction of the contractile ring in fission yeast (Krapp and Simanis, 2008; Johnson *et al.*, 2012; Simanis, 2015). The SIN pathway is homologous to the mitotic exit network (MEN) pathway in budding yeast and the HIPPO pathway in animal cells (Bedhomme *et al.*, 2008; Baro *et al.*, 2017; Foltman and Sánchez-Díaz, 2017). It is triggered by the POLO kinase Plo1 phosphorylation on the GTPase Spg1 at the spindle pole body (SPB).

The signal is passed along and expanded through a protein kinase cascade (Cerutti and Simanis, 1999; Furge *et al.*, 1999; Guertin *et al.*, 2000; Hou *et al.*, 2000; Mehta and Gould, 2006). Eventually, the activated downstream kinase Sid2 and its binding partner Mob1 join the contractile ring from the SPB, and phosphorylate the Cdc14 phosphatase Clp1 and the formin Cdc12 to promote ring constriction and septum formation (Sparks *et al.*, 1999; Hou *et al.*, 2000; Wachtler *et al.*, 2006; Chen *et al.*, 2008; Hachet and Simanis, 2008; Bohnert *et al.*, 2013). The SIN pathway also helps set the division plane in new daughter cells through phosphorylating the type I node protein Cdr2 (Pu *et al.*, 2015; Rincón *et al.*, 2017), which sheds new light on SIN regulation of cytokinesis.

**Endocytosis:** Membrane trafficking maintains the dynamics and integrity of the division plane. Exocytosis provides the enzymes and membrane needed for furrow ingression, cell wall formation and degradation, and endocytosis recycles the unwanted materials back to cytoplasm (Montagnac *et al.*, 2008; Tang, 2012; Jurgens *et al.*, 2015; Nakayama, 2016). The inhibition of membrane trafficking caused slower furrow ingression, furrow regression and cytokinesis failure (Skop *et al.*, 2001; Albertson *et al.*, 2005; Boucrot and Kirchhausen, 2007; Giansanti *et al.*, 2015; Wang *et al.*, 2016). The clathrin mediated endocytosis is one of the major pathways that retrieve proteins and lipids from the targeted plasma membrane (Weinberg and Drubin, 2012; Goode *et al.*, 2015; Lu *et al.*, 2016). The establishment of endocytic patches is well studied in budding yeast (Weinberg and Drubin, 2012; Goode *et al.*, 2015; Lu *et al.*, 2016). The early coat proteins including the clathrin and the Eps15 protein Edel arrive at the endocytic site, and recruit the downstream components including Pan1, the Huntingtin interacting protein-1 related protein End4/Sla2, the actin filament nucleator Arp2/3 complex and its

activator WASP (Naqvi *et al.*, 1998; Duncan *et al.*, 2001; Iwaki *et al.*, 2004; D'Agostino and Goode, 2005; Boeke *et al.*, 2014; Toshima *et al.*, 2015; Toshima *et al.*, 2016; Lu and Drubin, 2017). The membrane invagination and fission occur as results of forces from the actin network, membrane and coat proteins (Goode *et al.*, 2015; Lu *et al.*, 2016).

However, how cells define endocytosis sites are unclear. Previously our lab showed that the endocytic patches emerged along the cleavage furrow with a preference at the rim of the division plane during fission yeast cytokinesis (Wang *et al.*, 2016). It is intriguing to understand the distribution and regulation of endocytosis during cytokinesis.

**Exocytosis:** Exocytosis towards the division site is assisted by a multi-subunit complex called the exocyst (TerBush *et al.*, 1996; Martin-Cuadrado *et al.*, 2005; He and Guo, 2009). The exocyst is first found in budding yeast. Regulated by Rho GTPase Rho1, Rho3, Cdc42 and Rab GTPase Sec4, the exocyst interacts with SNARE proteins and brings vesicles in proximity to the targeted membrane for fusion (Adamo *et al.*, 1999; Guo *et al.*, 1999; Guo *et al.*, 2001; Zhang *et al.*, 2001; He and Guo, 2009; Wu and Guo, 2015; Lepore *et al.*, 2016). The exocyst complex is essential for the cell plate maturation and membrane fusion during plant cytokinesis (Wu *et al.*, 2013; Zarsky *et al.*, 2013; Rybak *et al.*, 2014; Jurgens *et al.*, 2015). The *Drosophila* exocyst is required for the membrane addition during anaphase cell elongation and cleavage furrow ingression (Giansanti *et al.*, 2015; Holly *et al.*, 2015). During animal cell cytokinesis, the exocyst, together with Rab and Arf GTPases, participates in the membrane addition, remodeling and abscission (Fielding *et al.*, 2005; Gromley *et al.*, 2005; Tang, 2012; Neto *et al.*, 2013). The fission yeast exocyst interacts with septins and Rho4 GTPase and controls the proper distribution of cell wall lytic enzyme Eng1 and Agn1 at the rim of division plane

(Martin-Cuadrado *et al.*, 2005; Sipiczki, 2007; Pérez *et al.*, 2015). Unlike their homologs in animal cells, the exocyst complex does not follow the furrow ingression in fission yeast but stays at the rim of the division plane instead (Martin-Cuadrado *et al.*, 2005; Pérez *et al.*, 2015). Thus, alternative exocytosis pathways should exist during cytokinesis. The TRAPP-II complex is a potential candidate to facilitate exocytosis during fission yeast cytokinesis (Wang *et al.*, 2016). The TRAPP-II complex regulates vesicle trafficking at Golgi in budding yeast and plants, but is later found to participate in cytokinesis in *Drosophila* and plant cells as well (Robinett *et al.*, 2009; Rybak *et al.*, 2014). In *S. pombe*, the TRAPP-II complex localizes to the leading edge of the cleavage furrow and cooperates with the exocyst to ensure an even membrane deposition and cargo delivery along the division plane (Wang *et al.*, 2016).

After vesicle delivery, the fusion process requires the assembly of the SNARE complex (Harbury, 1998; Chen and Scheller, 2001; Gromley *et al.*, 2005; Li *et al.*, 2006). Before the t-SNARE syntaxin forms a four helix bundle with t-SNARE SNAP-25 and v-SNARE synaptobrevin, it is usually in an inhibitory “closed” conformation with the Sec1/Munc18 protein (Scott *et al.*, 2004; Lu *et al.*, 2008; McNew, 2008; Rizo and Sudhof, 2012; Archbold *et al.*, 2014). The release of this “closed” conformation needs the Unc13/Munc13 family proteins (Rizo and Sudhof, 2012; James and Martin, 2013; Kabachinski *et al.*, 2013; Rizo and Xu, 2015). First discovered in *C. elegans*, the Unc13/Munc13 family proteins are essential priming factors in higher eukaryotes (Brose *et al.*, 1995; Betz *et al.*, 1996; Aravamudan *et al.*, 1999; Yang *et al.*, 2002; Rossner *et al.*, 2004). The MUN domain, a characteristic feature of this family, opens the closed conformation of syntaxin-Munc18 for the SNARE complex assembly (Madison *et al.*,

2005; Pei *et al.*, 2009; Yang *et al.*, 2015; Liu *et al.*, 2016; Xu *et al.*, 2017). The mouse homolog Munc13-1 also functions as a vesicle tether besides its role in the priming stage (Liu *et al.*, 2016; Xu *et al.*, 2017). In fungi, however, a C2 domain locates inside the MUN domain and separates the MUN domain into MHD1 and MHD2 domains (Kao *et al.*, 2006; Pei *et al.*, 2009). The exact functions of Unc13/Munc13 family proteins in yeast remain unclear. The only study reported Git1, a distant Unc13/Munc13 family protein in fission yeast, is involved in cAMP signaling (Kao *et al.*, 2006). In this work, we found that another Unc13/Munc13 family protein Ync13 participates in the later stages of cytokinesis. Deletion of Ync13 led to severe cell wall defects that caused cell lysis. Ync13 maintained the distribution and dynamics of multiple proteins and pathways including the cell wall synthases, the Rho GTPase dependent cell integrity pathway, the TRAPP-II mediated exocytosis and the clathrin mediated endocytosis. (Chapter 3)

## **Chapter 2: Cooperation between Rho-GEF Gef2 and Its Binding**

### **Partner Nod1 in the Regulation of Fission Yeast Cytokinesis**

Derived from: **Zhu, Y.-H.**, Y. Ye, Z. Wu and J.-Q. Wu. Cooperation between Rho-GEF Gef2 and its binding partner Nod1 in the regulation of fission yeast cytokinesis. *Mol. Biol. Cell.* 24:3187-204

#### **2.1 Abstract**

Cytokinesis is the last step of the cell-division cycle, which requires precise spatial and temporal regulation to ensure genetic stability. Rho guanine nucleotide exchange factors (Rho GEFs) and Rho GTPases are among the key regulators of cytokinesis. We previously found that putative Rho-GEF Gef2 coordinates with Polo kinase Plo1 to control the medial cortical localization of anillin-like protein Mid1 in fission yeast. Here we show that an adaptor protein Nod1 colocalizes with Gef2 in the contractile ring and its precursor cortical nodes. Like *gef2* $\Delta$ , *nod1* $\Delta$  has strong genetic interactions with various cytokinesis mutants involved in division-site positioning, suggesting a role of Nod1 in early cytokinesis. We find that Nod1 and Gef2 interact through the C-termini, which is important for their localization. The contractile-ring localization of Nod1 and Gef2 also depends on the interaction between Nod1 and the F-BAR protein Cdc15, where the Nod1/Gef2 complex plays a role in contractile-ring maintenance and affects the septation initiation network. Moreover, Gef2 binds to purified GTPases Rho1, Rho4, and Rho5 in

vitro. Taken together, our data indicate that Nod1 and Gef2 function cooperatively in a protein complex to regulate fission yeast cytokinesis.

## 2.2 Introduction

Cytokinesis is the last step of the cell cycle and essential for cell proliferation and differentiation. Most proteins and key events in cytokinesis are evolutionarily conserved from fungal to human cells (Pollard and Wu, 2010; Green *et al.*, 2012; Lee *et al.*, 2012; Wloka and Bi, 2012). In the fission yeast *Schizosaccharomyces pombe*, anillin-related protein Mid1 plays a crucial role in early stages of cytokinesis (Chang *et al.*, 1996; Sohrmann *et al.*, 1996; Bähler *et al.*, 1998a; Paoletti and Chang, 2000; Lee and Wu, 2012; Saha and Pollard, 2012a). Mid1 resides in the nucleus and in protein complexes called nodes at the medial cortex during interphase (Bähler *et al.*, 1998a; Paoletti and Chang, 2000; Almonacid *et al.*, 2011). Together with the DYRK kinase Pom1, these medial nodes control cell size and mitotic entry (Martin and Berthelot-Grosjean, 2009; Moseley *et al.*, 2009; Hachet *et al.*, 2011). During G2/M transition, more Mid1 is released from the nucleus to the cortical nodes by Polo kinase Plo1 via phosphorylation of Mid1 (Bähler *et al.*, 1998a; Almonacid *et al.*, 2011). These Mid1 nodes mature into cytokinesis nodes by recruiting other proteins such as IQGAP Rng2, myosin-II, F-BAR protein Cdc15, and formin Cdc12 (Wu *et al.*, 2003, 2006; Motegi *et al.*, 2004; Almonacid *et al.*, 2011; Laporte *et al.*, 2011; Padmanabhan *et al.*, 2011). Then the nodes and actin filaments condense into a compact ring through a search, capture, pull, and release mechanism (Vavylonis *et al.*, 2008; Chen and Pollard, 2011; Ojkic *et al.*, 2011; Laporte *et al.*, 2012). The compact ring matures and constricts, guiding the formation of a

division septum (Pollard and Wu, 2010; Proctor *et al.*, 2012). The cell is then divided into two daughter cells with the degradation of primary septum.

The F-BAR protein Cdc15 is essential for cytokinesis (Fankhauser *et al.*, 1995; Carnahan and Gould, 2003; Roberts-Galbraith *et al.*, 2009, 2010; Arasada and Pollard, 2011). In early cytokinesis, Mid1 recruits Cdc15 to cytokinesis nodes, which in turn recruits the formin Cdc12 to nucleate actin filaments (Carnahan and Gould, 2003; Kovar *et al.*, 2003; Laporte *et al.*, 2011). Cdc15 is also essential for contractile-ring maturation and assembly regulated by the septation initiation network (SIN) pathway (Wachtler *et al.*, 2006; Hachet and Simanis, 2008; Laporte *et al.*, 2012). During late cytokinesis, Cdc15 and another F-BAR protein Imp2 recruit C2-domain protein Fic1 and paxillin Px11 to ensure the maintenance and integrity of the contractile ring (Pinar *et al.*, 2008; Roberts-Galbraith *et al.*, 2009).

The contractile ring and septation/septum formation are regulated by the SIN pathway that is composed of a GTPase and a kinase cascade (Wachtler *et al.*, 2006; Hachet and Simanis, 2008; Krapp and Simanis, 2008; Johnson *et al.*, 2012). The SIN proteins locate at the spindle pole body (SPB) via scaffold proteins Cdc11 and Sid4 (Chang and Gould, 2000; Krapp *et al.*, 2001; Tomlin *et al.*, 2002; Morrell *et al.*, 2004). SIN pathway signaling is controlled by the activation of the GTPase Spg1 by Polo kinase, and the inactivation by the two component GTPase-activating proteins Cdc16 and Byr4 (Schmidt *et al.*, 1997; Furge *et al.*, 1998, 1999; Jwa and Song, 1998; Tanaka *et al.*, 2001; Krapp *et al.*, 2008). The GTP-bound Spg1 interacts with kinase Cdc7 and causes its redistribution to the new SPB (Fankhauser and Simanis, 1994; Cerutti and Simanis, 1999; Mehta and Gould, 2006). The downstream kinases and their binding partners including

Sid1-Cdc14 and Sid2-Mob1 are then activated and recruited onto the SPB (Fankhauser and Simanis, 1993; Balasubramanian *et al.*, 1998; Sparks *et al.*, 1999; Guertin *et al.*, 2000; Hou *et al.*, 2000; Salimova *et al.*, 2000). Activated Sid2-Mob1 is then relocalized to the contractile ring to promote contractile-ring constriction and septum formation (Jin *et al.*, 2006 ; Chen *et al.*, 2008)

Besides the equivalents of the SIN pathway, MEN and Hippo pathways, Rho GTPase Rho1/RhoA and its activators, the Rho guanine nucleotide exchange factor (GEF; Ect2, Pebble, etc.) are involved in division-site specification and contractile-ring formation by activating myosin-II and actin assembly in budding yeast and animal cells (Lehner, 1992; Imamura *et al.*, 1997; O'Keefe *et al.*, 2001; Tolliday *et al.*, 2002; Bement *et al.*, 2005; Yuce *et al.*, 2005; Nishimura and Yonemura, 2006; Yoshida *et al.*, 2006; Watanabe *et al.*, 2010; Su *et al.*, 2011). In contrast, Rho GTPases in *S. pombe* are only found to regulate later stages of cytokinesis and cell polarity (García *et al.*, 2006b; Pérez and Rincón, 2010). Fission yeast has six Rho GTPases (Cdc42 and Rho1-5) and seven Rho GEFs (Gef1-3, Rgf1-3, and Scd1). Cdc42, regulated by Gef1 and Scd1, is essential for cell polarity and morphology (Coll *et al.*, 2003; Hirota *et al.*, 2003; Rincón *et al.*, 2007). Rho-GEFs Rgf1-3 activate Rho1, which is essential for cell-wall synthesis, septum formation, and cell polarization (Tajadura *et al.*, 2004; Morrell-Falvey *et al.*, 2005; Mutoh *et al.*, 2005; García *et al.*, 2006a, 2009; Wu *et al.*, 2010). Rho2 is involved in cell morphology and septum formation by regulating cell wall  $\alpha$ -glucan biosynthesis (Calonge *et al.*, 2000). Rho3 regulates exocytosis (Nakano *et al.*, 2002; Wang *et al.*, 2003; Kita *et al.*, 2011). Rho4 controls the secretion of lytic enzymes for septum degradation (Nakano *et al.*, 2003; Santos *et al.*, 2003, 2005). Rho5 is a paralogue of Rho1

and shares similar functions (Nakano *et al.*, 2005; Rincón *et al.*, 2006). GEFs that regulate Rho2-5 GTPases are unknown except that Rgf1 and Rgf2 might weakly interact with Rho5 (Mutoh *et al.*, 2005).

Recently, we and others found that the putative Rho-GEF Gef2 localizes to cortical nodes and coordinates with Polo kinase Plo1 to regulate division-site selection (Moseley *et al.*, 2009; Ye *et al.*, 2012; Guzman-Vendrell *et al.*, 2013). In *gef2Δ plo1* double mutants, Mid1 localization to the cortical nodes and the contractile ring is severely affected and the division site is misplaced. In addition, these studies showed that Gef2 interacts with Mid1 N-terminus (Ye *et al.*, 2012; Guzman-Vendrell *et al.*, 2013), which is essential for Mid1 function (Almonacid *et al.*, 2009, 2011; Lee and Wu, 2012). However, the substrates GTPases for Gef2 and the regulation of Gef2 are largely unknown.

Here we show that Nod1 forms a complex with Gef2 to regulate cytokinesis. Nod1 and Gef2 are interdependent for their localization to cortical nodes and the contractile ring. Their localization at the contractile ring also depends on the physical interaction between Nod1 and the F-BAR protein Cdc15. Like *gef2Δ*, *nod1Δ* suppresses SIN mutants by reducing cell lysis. In addition, the GEF domain of Gef2 interacts with GTPases Rho1, Rho4, and Rho5 in vitro. Thus, it is possible that the Gef2/Nod1 complex may activate and function through Rho GTPases during cytokinesis.

## **2.3 Materials and methods**

### **2.3.1 Strains, genetic, molecular, and cellular methods**

Strains used in Chapter 2 are listed in Table 2.2. We used PCR-based gene targeting and standard yeast genetics to construct strains (Moreno *et al.*, 1991; Bähler *et al.*, 1998b).

All tagged and truncation strains are regulated under endogenous promoters or 5' UTR and integrated into native chromosomal loci, except the overexpression strains that are integrated at native loci under the control of *3nmt1* or *41nmt1* promoter, which is repressed by thiamine (Maundrell, 1990).

Nod1 C-terminal truncations and Nod1 overexpression were constructed as previously described (Bähler *et al.*, 1998b). For N-terminal truncations, *nod1* 5' UTR - 300 to +3 bp was cloned into pFA6a-kanMX6-P3nmt1-mECitrine at *Bgl*III and *Pac*I sites to replace the *3nmt1* promoter. The resulting plasmid (JQW560) was then used as the template for PCR amplification and gene targeting. Primers were designed according to desired truncation sites and the PCR products were transformed into wt cells. The resulting strains were sequenced. Some *kanMX6* marker at 5' end of *nod1* or *gef2* gene was looped out by crossing the strains to wt cells.

To test the functionalities of tagged FL Nod1, both N- and C-terminally tagged Nod1 strains were crossed to *plol-ts18*. Double mutants had <10% abnormal septa at 25°C, which is similar to *plol-ts18* single mutant but different from the ~95% abnormal septa in *plol-ts18 nod1Δ*. Thus, both N- and C-terminally tagged Nod1 are functional.

For DNA staining, cells were incubated with 10 µg/ml Hoechst 33258 for 10 min in the dark before imaging in the DAPI channel as described (Wu *et al.*, 2011).

### **2.3.2 Microscopy and data analysis**

Strains were restreaked from -80°C stock and grown 1-2 days on yeast extract plus five supplements (YE5S) plates at 25°C. Cells were then inoculated and kept in exponential phase for ~48 h at 25°C except where noted. Before microscopy, cells were washed in Edinburgh minimal medium plus five supplements (EMM5S) twice to reduce

autofluorescence, and imaged on EMM5S with 20% gelatin pad with 5  $\mu$ M n-propyl-gallate as described (Laporte *et al.*, 2011; Ye *et al.*, 2012). For long movies, cells were washed in YE5S, and resuspended in YE5S with 5  $\mu$ M n-propyl-gallate. 2  $\mu$ l concentrated cells were then spotted onto a coverglass-bottom dish (Delta TPG Dish; Biotechs Inc., Butler, PA) and covered with a layer of YE5S agar before imaged at 23.5°C or in a preheated climate chamber (Stage Top Incubator INUB-PPZI2-F1 equipped with UNIV2-D35 dish holder, Tokai Hit, Shizuoka-ken, Japan) for imaging at the restrictive temperatures for certain mutants.

Microscopy was performed at 23.5-25°C except where noted. To visualize cell morphology, DNA, and septum, Hoechst stained cells were imaged with a 100x/1.4 numerical aperture (NA) Plan-Apo objective lens on a Nikon Eclipse Ti inverted microscope (Nikon, Melville, NY) equipped with a Nikon cooled digital camera DS-Q11 and a DAPI filter. Other experiments were performed using 100 $\times$ /1.4 NA Plan-Apo objective lenses (Nikon, Melville, NY) on a spinning disk confocal microscope (UltraVIEW ERS, Perkin Elmer Life and Analytical Sciences, Waltham, MA) with 440, 568-nm solid state lasers and 488, 514-nm argon ion lasers and an ORCA-AG camera (Hamamatsu, Bridgewater, NJ) with 2  $\times$  2 binning, or on a spinning disk confocal microscope (UltraVIEW Vox CSUX1 system, Perkin Elmer Life and Analytical Sciences, Waltham, MA) with 440-, 488-, 515-, and 561-nm solid state lasers and a back-thinned EMCCD camera (Hamamatsu C9100-13, Bridgewater, NJ) without binning.

Images were analyzed using ImageJ, UltraVIEW, or Volocity software. Fluorescence images shown in figures and movies are maximum projection of images stacks at 0.4-0.6  $\mu$ m spacing except where noted. Nod1 and Gef2 molecules in cells were

counted globally or locally by measuring fluorescence intensity as described (Laporte *et al.*, 2011). Briefly, tagged Nod1 or Gef2 cells were mixed with wt cells, and imaged with 11 z-sections with 0.4  $\mu\text{m}$  spacing on the UltraVIEW ERS confocal system. The offset was subtracted from images that were then corrected for uneven illumination. Mean intensity in whole cells was measured in sum intensity projections and subtracted by that of wt cells as background. Mean intensity in the mature contractile ring was measured using the polygon region of interest (ROI) tool in ImageJ on a sum intensity projection. A  $\geq 3\times$  larger ROI that included the contractile ring was chosen for calculation of background intensity after subtracting ring intensity. For nodes, the fluorescence intensity was measured using a circular ROI with a diameter of 5 pixels that covered the whole node at the best focal plan. The intensity near the plasma membrane outside of the broad band of nodes was used for background subtraction to avoid overlapping with other nodes. The global and local intensity of Nod1 and Gef2 were then normalized to molecule numbers using previous Gef2 data as a reference (Wu and Pollard, 2005; Wu *et al.*, 2008; Ye *et al.*, 2012)

### **2.3.3 FRAP analysis**

FRAP assays were performed using the photokinesis unit on UltraVIEW Vox confocal system, similar to the assays described before (Coffman *et al.*, 2009; Laporte *et al.*, 2011). The best focal plane for bleaching was chosen from z stacks. Selected ROIs were bleached to <50% of the original fluorescence intensity after five pre-bleach images were collected. 100 post-bleach images with 10 s delay were collected. The images were then corrected for background and photobleaching during image acquisition at non-bleached sites. We normalized pre-bleach intensity of the ROI to 100%, the intensity just after

bleaching to 0% and the end of the bleach time as time 0. Intensity of every three consecutive post-bleaching time points was averaged to reduce noise. The data were then plotted and fitted using an exponential equation  $y = m_1 + m_2 \exp(-m_3x)$ , where  $m_3$  is the off-rate (KaleidaGraph; Synergy Software, PA). The half-time of recovery was calculated as  $t_{1/2} = (\ln 2)/m_3$ . p-Values in Chapter 2 were calculated using two-tailed student's *t*-tests.

#### **2.3.4 IP and Western blotting**

IP assay and Western blotting were carried out as previously described (Laporte *et al.*, 2011; Lee and Wu, 2012). Briefly, mECitrine-tagged proteins were pulled down from fission yeast cell extract by protein G covalently-coupled magnetic Dynabeads (100.04D; Invitrogen, Carlsbad, CA) with polyclonal anti-GFP antibodies (NB600-308; Novus Biologicals, Littleton, CO). The bead samples were then boiled in sample buffer after washing 3x. The protein samples were then separated in SDS-PAGE, and Western blotting was performed using monoclonal anti-GFP antibody (Cat: 11814460001; 1:2,000 dilution; Roche, Mannheim, Germany) or monoclonal anti-Myc antibody (9E10; 1:5,000 dilution; Santa Cruz Biotechnology, Santa Cruz, CA). The anti-tubulin monoclonal TAT1 antibody was used at 1:20,000 dilution (Woods *et al.*, 1989). Anti-mouse secondary antibody was used at 1:5000 dilution.

#### **2.3.5 Yeast two-hybrid assays**

$\beta$ -galactosidase activity assays were performed to semi-quantitatively detect protein interactions in yeast two-hybrid assays (Laporte *et al.*, 2011). DNAs or cDNAs of interest were constructed into vectors with either VP16 activation domain or GBT9 DNA-binding domain. The pairs of plasmids were then co-transformed into *S. cerevisiae* strain MAV203 (11281-011; Invitrogen, CA) and plated on solid medium lacking leucine and

tryptophan (SD-L-W). The transformants were selected and used for  $\beta$ -galactosidase activity measurements in the *o*-nitrophenyl  $\beta$ -D-galactopyranoside assay (Sigma-Aldrich). The results were displayed as fold changes over the highest negative control value.

### **2.3.6 Protein purification and the interaction between Gef2 and Rho GTPases**

Pull down assays between recombinant 6His-Gef2 (GEF) and GST-Rho proteins were adapted from a previous study (Iwaki *et al.*, 2003). Expression of 6His-tagged GEF domain of Gef2 (aa 211-600) was induced when ArcticExpress RIL cells (230193; Agilent Technologies, Santa Clara, CA) carrying the plasmid were grown at 10°C for 18 h after adding 1 mM IPTG (Saha and Pollard, 2012b). After sonication (Output 9, 50% duty cycle, 4x 20 pulses) and ultracentrifugation (25,000 rpm for 15 min, then 38,000 rpm for 30 min), 6His-Gef2 (GEF) was purified on Talon Metal Affinity Resin (635501; Clontech, Mountain View, CA) followed by gel filtration with a HiLoad 16x60 Superdex 200 (17-5175-01; GE healthcare, Buckinghamshire, United Kingdom) in phosphate buffer (50 mM sodium phosphate, pH 6.2, 0.3 M NaCl, 1 mM DTT). The purified His-Gef2 (GEF) was then dialyzed into the final binding buffer (25 mM MOPS, pH 7.2, 60 mM  $\beta$ -glycerophosphate, 15 mM *p*-nitrophenyl phosphate, 1 mM DTT, 1% Triton X-100, 1 mM PMSF, and protease inhibitor tablets). GST and GST-Rho1 to Rho5 and Cdc42 were purified from BL21(DE3)pLysS cells (69451; Novagen, EMD Chemicals Inc., Darmstadt, Germany) (induced with 0.5 mM IPTG at 15°C for 6 h) using Glutathione Sepharose beads (17-5132-01; GE healthcare, Buckinghamshire, United Kingdom). The beads with Rho proteins were then incubated at 30°C for 10 min with buffer containing 50 mM Tris (pH 7.5), 1 mM DTT, and 5 mM EDTA to deplete nucleotides. 500  $\mu$ l 0.25

$\mu$ M 6His-Gef2 (GEF) in binding buffer was then added to 30  $\mu$ l beads with each nucleotide-depleted Rho protein and incubated at 4°C for 1 h. After incubation, glutathione beads were washed with 1 ml binding buffer 3x and the bound proteins were detected by Western blotting. Rho GTPases were detected by monoclonal anti-GST antibody (3G10/1B3; 1:5,000 dilution; NB600-446, Novus Biologicals, Littleton, CO) and bound 6His-Gef2 (GEF) was detected by anti-His antibody (631212; 1:10,000 dilution; Clontech, Mountain View, CA). Secondary anti-mouse antibody was used at 1:5,000 dilution.

## **2.4 Results**

### **2.4.1 Nod1 is a Gef2 related protein that localizes to cortical nodes and the contractile ring**

We previously found the putative Rho-GEF Gef2 plays a role in division-site positioning in cooperation with Polo kinase Plo1 (Ye *et al.*, 2012). Concurrently, we identified a novel protein Nod1 (SPAC12B10.10; Jourdain *et al.*, 2013) in the *S. pombe* protein database with sequence similarity to Gef2. Nod1 is annotated as a sequence orphan with 419 amino acids (aa) at <http://www.pombase.org/spombe/result/SPAC12B10.10>.

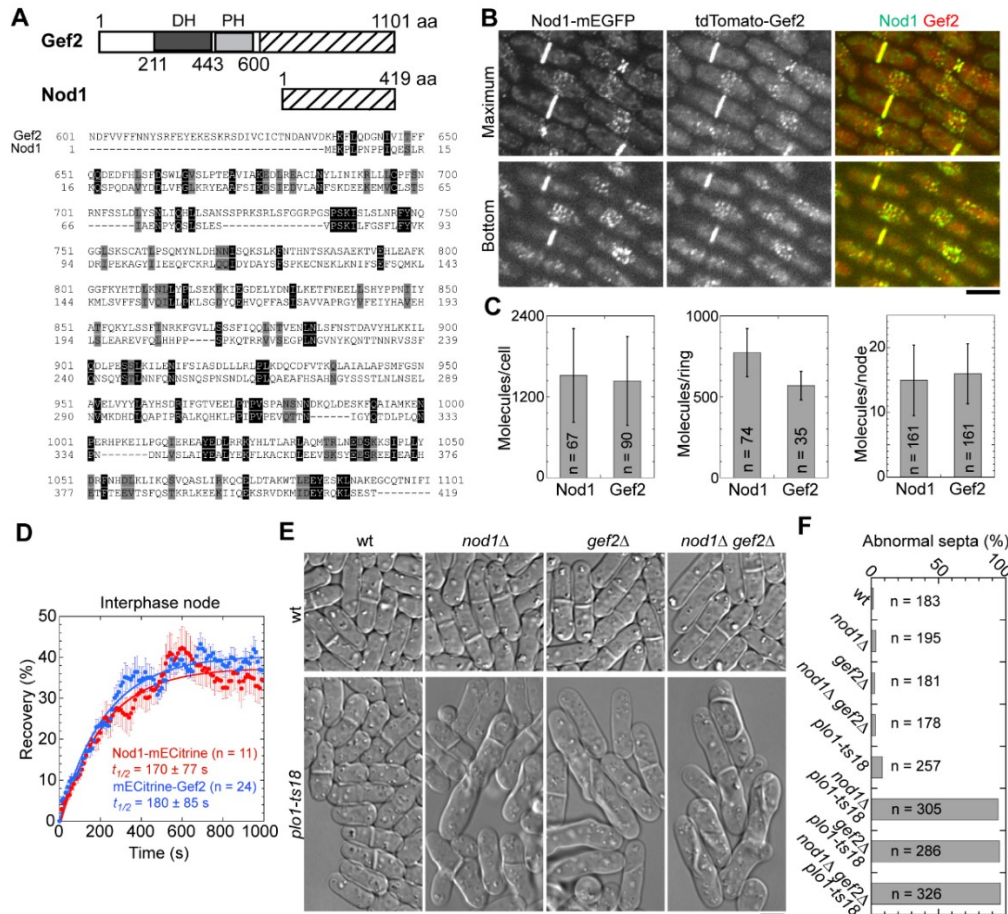
Although it has no GEF domain, Nod1 shares 18% identity and 34% similarity with Gef2 C-terminal aa 636-1101 (Figure 2.1 A). The structure prediction program suggested that Nod1 is a helix-rich protein with no predicted domain (Jones, 1999; Wood *et al.*, 2012).

To determine Nod1's functions, we first tagged Nod1 with mEGFP at its C-terminus and examined its localization. Interestingly, Nod1 colocalized with Gef2 throughout the cell cycle at interphase nodes, cytokinesis nodes, and the contractile ring (Figure 2.1 B). We next counted Nod1 molecule numbers in cells by measuring its global

and local fluorescence intensity (Wu and Pollard, 2005; Laporte *et al.*, 2011). In our previous study, strain *kanMX6-Pgef2-mECitrine-gef2* (JW3825) was used to measure the intensity of Gef2 (Ye *et al.*, 2012). We found that the *kanMX6* cassette in the strain affected Gef2 expression level, similar to N-terminal tagged F-BAR protein Cdc15 (Wu and Pollard, 2005). We therefore used the *kanMX6* looped-out *mECitrine-gef2* strain (JW4912) to re-quantify Gef2 molecules globally and locally. The global Gef2 level was 1/3 in the *kan* sensitive strain (JW4912) while the local Gef2 concentrations at the contractile ring and cortical nodes were similar to the original data (Ye *et al.*, 2012). Compared to Gef2 (1,440 ± 660 molecules/cell, 570 ± 90 molecules at the contractile ring, and 16 ± 5 molecules/interphase node), Nod1 had 1,520 ± 700 molecules/cell, 770 ± 150 molecules at the contractile ring, and 15 ± 5 molecules/interphase node (Figure 2.1 C). Thus, the ratios of Nod1 to Gef2 in interphase nodes and the contractile ring are ~1:1 and 1.35:1, respectively.

We performed fluorescence recovery after photobleaching (FRAP) assays on interphase nodes to determine Nod1 dynamics at the cell cortex. Nod1 fluorescence recovered at a halftime of 170 ± 77 s and the mobile fraction was ~40%, which was similar to Gef2 ( $t_{1/2} = 180 \pm 85$  s, 37% mobile fraction; Figure 2.1 D). This indicates that both Nod1 and Gef2 are relatively stable on the plasma membrane compared to some other cytokinesis proteins (Laporte *et al.*, 2011). Together, these data suggested that Nod1 might play a role in cytokinesis together with the putative Rho-GEF Gef2.

**Figure 2.1 Nod1 colocalizes with Gef2 in cortical nodes and the contractile ring and shares similar function with Gef2 in division-site selection.**



(A) Nod1 shares similarity with Gef2 C-terminus. (Top) Schematics of Gef2 and Nod1 domains or regions. Similar region between Nod1 and Gef2 are marked with the same pattern. DH, DBL-homology; PH, pleckstrin homology. (Bottom) Sequence alignment between Gef2 aa 601-1101 (upper row) and FL Nod1 (lower row) using Vector NTI program. Identical and similar (D/E, I/L/V, K/R, N/Q, and S/T) aa are shaded in black and gray, respectively. (B-F) Cells were grown and imaged at 25°C. (B) Colocalization of Nod1 with Gef2 in cortical nodes and the contractile ring (strain JW4457). Top, maximum intensity projection. Bottom, single slice at cell bottom. (C) Molecule numbers of mECitrine-Gef2 (JW4912) and Nod1-mECitrine (JW4008) globally in whole cells and locally in the contractile ring and interphase nodes. (D) FRAP analysis of Nod1 (JW4008) and Gef2 (JW3825). Cells were bleached at time zero. Mean  $\pm$  SEM is plotted. (E and F) Nod1 has similar function to Gef2 in division-site positioning. (E) Differential interference contrast (DIC) images and (F) the quantification of the division-site positioning. The abnormal septa are defined as septa not placed within the central 20% of the cell or not within 80 to 100° angle to the long axis of the cell. Strains used: wt (JW81), *nod1* $\Delta$  (JW3773), *gef2* $\Delta$  (JW1826), *nod1* $\Delta$  *gef2* $\Delta$  (JW3814), *plot1-ts18* (IH1600), *nod1* $\Delta$  *plot1-ts18* (JW3815), *gef2* $\Delta$  *plot1-ts18* (JW3078), and *nod1* $\Delta$  *gef2* $\Delta$  *plot1-ts18* (JW3873). Bars, 5  $\mu$ m.

### 2.4.2 Nod1 regulates division-site positioning cooperatively with Polo kinase Plo1

Interphase nodes are important for cell-size control and mitotic entry in fission yeast (Martin and Berthelot-Grosjean, 2009; Moseley *et al.*, 2009; Hachet *et al.*, 2011; Deng and Moseley, 2013). As reported (Jourdain *et al.*, 2013), we found that similar to the length of dividing *gef2Δ* cells (Ye *et al.*, 2012), dividing cell *nod1Δ* cells were  $16.2 \pm 1.0$   $\mu\text{m}$  long (n = 148 septating cells), slightly but significantly longer than  $14.4 \pm 0.9$   $\mu\text{m}$  of wild type (wt) cells (n = 117, p < 0.001). Thus, Nod1 and Gef2 play a role in cell-size control.

Gef2 coordinates with Polo kinase Plo1 to recruit anillin-related protein Mid1 to the cortical nodes for division-site specification (Ye *et al.*, 2012). Because of the sequence similarity between Nod1 and the C-terminus of Gef2 and their colocalization (Figure 2.1, A and B), we hypothesized that Nod1 has a function similar to Gef2 at early cytokinesis. To test this hypothesis, we crossed *nod1Δ* to the temperature-sensitive mutant of Polo kinase, *plo1-ts18* (Figure 2.1 E). Similar to *gef2Δ plo1-ts18* (Ye *et al.*, 2012), 95% of *nod1Δ plo1-ts18* cells had abnormal septa at 25°C (Figure 2.1, E and F). Moreover, *nod1Δ* and *gef2Δ* also had the same strong synthetic interactions with mutations known to affect early cytokinesis such as *mid1*, *rng2*, and *cdc4-8* but not with mutations in cell-size control such as *cdr2Δ* and *blt1Δ* (Table 2.1). Thus, Nod1 shares a similar function with Gef2 in division-site specification and contractile-ring assembly (Ye *et al.*, 2012; Jourdain *et al.*, 2013).

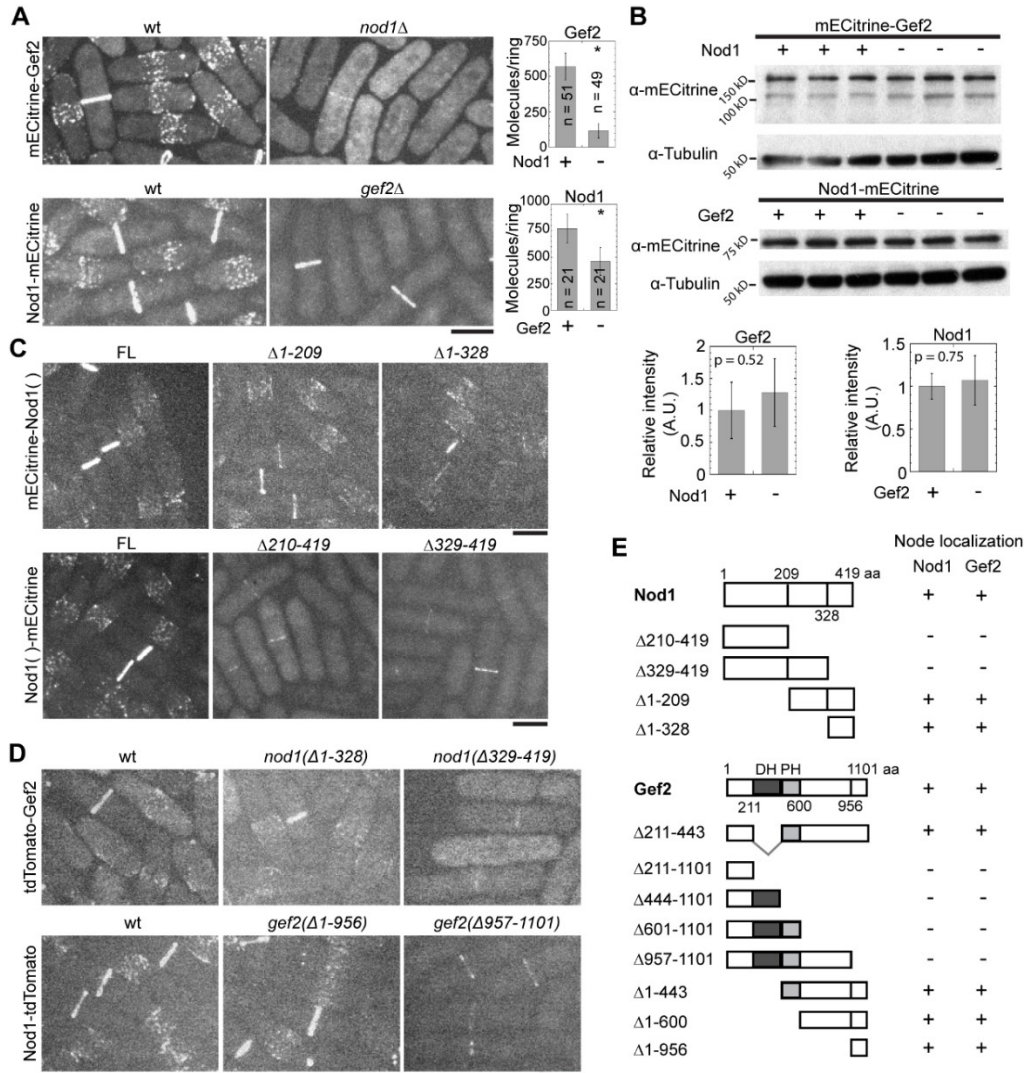
To examine if Nod1 and Gef2 function in the same or parallel genetic pathways, we tested the genetic interactions among *nod1Δ*, *gef2Δ*, *plo1-ts18* (Figure 2.1, E and F). *nod1Δ gef2Δ* double mutant cells resembled the single mutants. The *nod1Δ gef2Δ plo1-*

*ts18* triple mutant was still viable with ~96% cells displaying abnormal septa at 25°C, which is similar to *nod1Δ plo1-ts18* and *gef2Δ plo1-ts18*. These results indicated that Nod1 and Gef2 are in the same genetic pathway.

### **2.4.3 Nod1 and Gef2 are interdependent on their C-termini for localization to cortical nodes**

Because Gef2 and Nod1 are in the same genetic pathway, we tested whether they affect each other's localization. In wt cells, Gef2 localized to cortical nodes and the contractile ring (Figure 2.2 A). However, the node localization was abolished and the contractile ring localization was greatly reduced in *nod1Δ* (Figure 2.2 A). Gef2 was detected at the contractile ring with  $115 \pm 50$  molecules, at ~20% of wt levels, in *nod1Δ* cells ( $p < 0.001$ ). Nod1 also failed to localize to cortical nodes in *gef2Δ* while the localization to the contractile ring was reduced to ~60% of wt level with  $460 \pm 130$  molecules ( $p < 0.001$ ; Figure 2.2 A). The losses of localizations were not due to the global protein concentration since Nod1 and Gef2 protein levels were not significantly affected in the absence of each other (Figure 2.2 B). Thus, Gef2 and Nod1 are interdependent for localization to cortical nodes (Jourdain *et al.*, 2013) and partially interdependent for localization to the contractile ring.

**Figure 2.2 Nod1 and Gef2 are interdependent on their C-termini for cortical node localization and partially interdependent for localization to the contractile ring.**

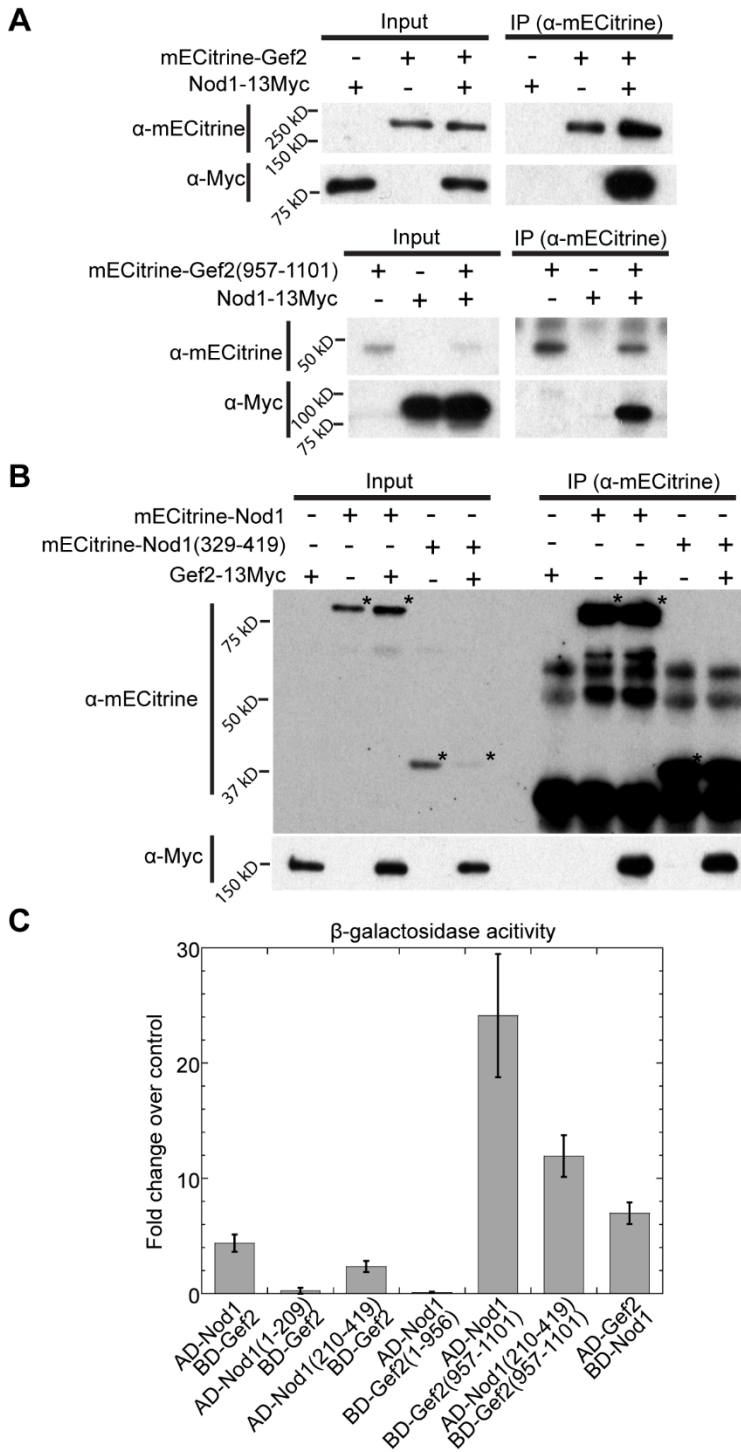


(A) Micrographs of Nod1 and Gef2 localization in wt and deletion mutants (left). Molecules in the contractile ring were counted (right). Cells expressing mECitrine-Gef2 (JW3825 and JW4014) and Nod1-mECitrine (JW4008 and JW4038) were used. (B) Nod1 and Gef2 protein levels in wt and deletion mutants. Cells extracts from the strains used in (A) were loaded in triplicate in Western blotting. Tubulin from the cell extracts was used to normalize the protein concentrations (bottom). (C) Micrographs of Nod1 localization in cells expressing mECitrine-tagged FL Nod1 (JW4750 and JW4008) or Nod1 truncations (JW5065, JW4856, JW4325, and JW4326). (D) Micrographs of localizations of Nod1 and Gef2 (strains JW4226, JW5107, JW4359, JW4010, JW4256, and JW4355). (E) Summary of Nod1 and Gef2 localizations to cortical nodes in different truncation mutants. +, localized to cortical nodes; -, not localized to cortical nodes. Bars, 5  $\mu$ m.

Gef2 C-terminal aa 957-1101 are necessary and sufficient for its cellular localization (Ye *et al.*, 2012). To test which region of Nod1 is important for its localization, we truncated Nod1 at its native chromosomal locus under the control of *nod1* promoter based on the sequence alignment between Gef2(601-1101) and Nod1 (Figures, 2.1 A and 2.2 E). N-terminal truncations of Nod1 still localized to the cortical nodes and contractile ring (Figure 2.2 C, upper panels). However, when the last 91 aa of Nod1 from the C-terminus were truncated, Nod1 failed to localize to cortical nodes, but it still localized to the contractile ring with lower intensity (Figure 2.2 C, lower panels). We conclude that Nod1 C-terminal aa 329-419 are both essential and sufficient for Nod1 node localization.

Next, we studied how the Nod1 and Gef2 truncations affect each other's localization (Figure 2.2, D and E). Gef2 localized to both cortical nodes and the contractile ring in *nod1*( $\Delta 1-328$ ), but only localized to the contractile ring weakly when the last 91 aa of Nod1 were truncated in *nod1*( $\Delta 329-419$ ) (Figure 2.2 D), which is similar to Gef2 localization in *nod1* $\Delta$  (Figure 2.2 A). Similarly, Nod1 localized normally in *gef2*( $\Delta 1-956$ ) but failed to localize to cortical nodes when Gef2 C-terminal aa 957-1101 were truncated (Figure 2.2 D). Together, Nod1 and Gef2 are interdependent on their C-termini for cortical node localization and partially interdependent on their C-termini for localization to the contractile ring (Figure 2.2 E).

**Figure 2.3 Nod1 and Gef2 physically interact through their C-termini.**



(A and B) Antibodies against mECitrine were used in IP. Monoclonal antibodies against mECitrine and Myc were used in Western blotting. (A) Nod1 co-IP with Gef2 C-terminus. IPs were carried out from cell extracts of *nod1-13Myc* (JW4013), *mECitrine-gef2* (JW3825), *mECitrine-gef2 nod1-13Myc* (JW4330), *mECitrine-gef2(957-1101)* (JW3826), and *mECitrine-gef2(957-1101) nod1-13Myc* (JW4331). (B) Gef2 co-IP with Nod1 C-terminus. Strains JW3622, JW4453, JW5093, JW4455, and JW5095 were used. (C) Nod1 and Gef2 interact via their C-termini in yeast two-hybrid assays. β-Galactosidase activities (mean ± SD, n = 2) are shown as fold changes over the highest negative control.

#### **2.4.4 Nod1 physically interacts with Gef2 through their C-termini**

Based on the interdependency between Nod1 and Gef2 for localization, we hypothesized that the two proteins interact with each other. Indeed, mECitrine-Gef2 pulled down Nod1-13Myc in co-immunoprecipitation (IP) assay (Figure 2.3 A). In reciprocal co-IP, mECitrine-Nod1 also pulled down Gef2-13Myc (Figure 2.3 B). Because Nod1 and Gef2 C-termini are important for their localization, we tested if they interact through their C-termini. As expected, Nod1 interacted with Gef2(957-1101) (Figure 2.3 A), and Gef2 with Nod1(329-419) (Figure 2.3 B) in co-IP assays. These data suggested that Nod1 and Gef2 interact with each other in vivo through their C-termini.

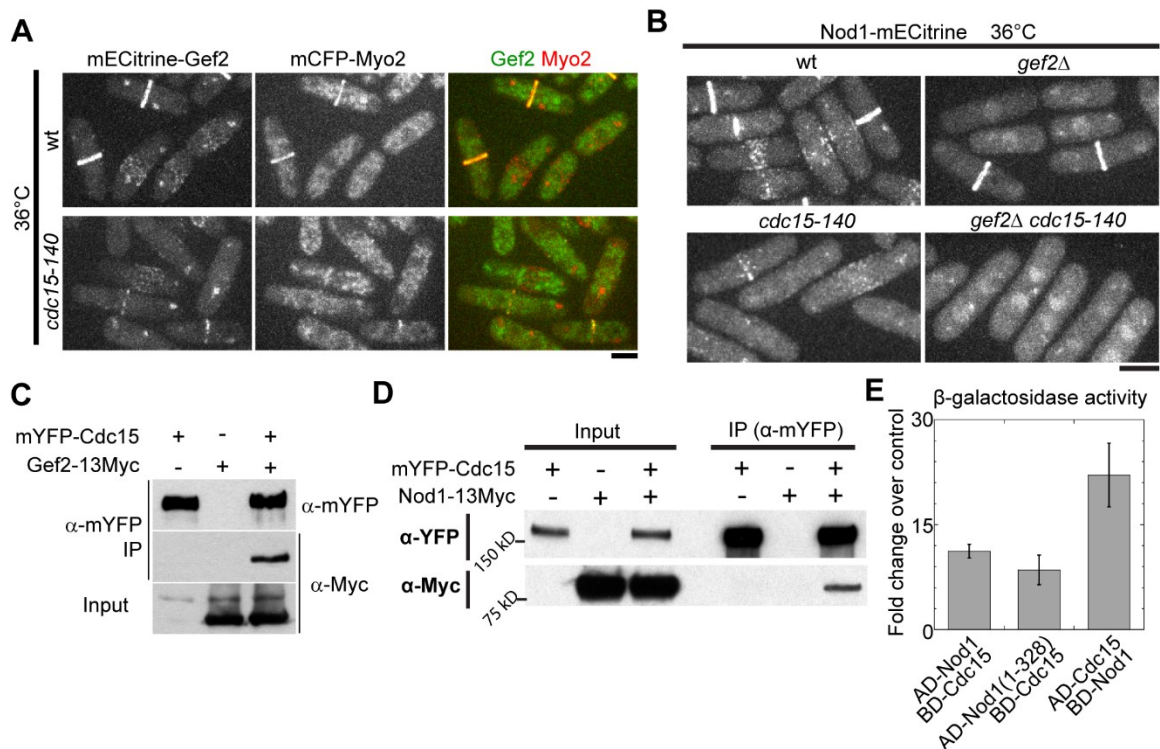
We tested whether the interaction might be direct between Nod1 and Gef2 through yeast two-hybrid assays (Figure 2.3 C). Full length (FL) Nod1 displayed positive interaction with Gef2 and Gef2(957-1101) but not with Gef2(1-956), while FL Gef2 bound to Nod1 and Nod1(210-419) but not to Nod1(1-209). Moreover, Nod1(210-419) interacted with Gef2(957-1101). In summary, Nod1 and Gef2 physically interact with each other through their C-termini and the interaction is critical for their localization.

#### **2.4.5 The F-BAR protein Cdc15 recruits Nod1 and Gef2 to the contractile ring through its interaction with the Nod1 N-terminus**

Gef2 localizes to cytokinesis nodes and the contractile ring in *blt1Δ* although the interphase-node localization is abolished (Ye *et al.*, 2012). The timings of appearance at cytokinesis nodes for Gef2 in *blt1Δ* and the F-BAR protein Cdc15 in wt cells are similar (Laporte *et al.*, 2011; Ye *et al.*, 2012). Thus, we observed Gef2 and Nod1 localization in the temperature-sensitive mutant *cdc15-140* at the restrictive temperature (Figure 2.4, A and B). After 2 h at 36°C, both Gef2 and Nod1 formed some aggregates and signals were

weaker in *cdc15*<sup>+</sup> than at 25°C (Figures, 2.2 A and 2.4, A and B). Gef2 and Nod1 still localized to cortical nodes with low intensity but their contractile-ring localizations were greatly reduced in *cdc15-140* cells (Figure 2.4, A and B). Unlike in *gef2*Δ cells, the contractile-ring localization of Nod1 was completely abolished in *gef2*Δ *cdc15-140* cells (Figure 2.4 B). Together, our data indicate that the contractile-ring localization of Nod1 and Gef2 depends on each other and the F-BAR protein Cdc15.

**Figure 2.4 The F-BAR protein Cdc15 recruits or stabilizes Nod1 and Gef2 localization to the division site by interaction with Nod1 N-terminus.**



(A and B) Nod1 and Gef2 localizations depend on Cdc15. Cells expressing Nod1-mECitrine (A) and Gef2-mECitrine (B) were cultured at 25°C and shifted to 36°C for 2 h before imaging. Myo2 was used to mark the contractile ring in (B). Strains used were JW4008, JW4038, JW5027, JW5028, JW3571, and JW3572.

Figure 2.4: Continued

Figure 2.4: Continued

(C and D) Cdc15 interacts with Nod1 and Gef2 in co-IP (similar to Figure 3A). Strains used were JW1063, JW5120, JW4013, JW3325, and JW3204. (E) Cdc15 interacts with Nod1 N-terminus in yeast two-hybrid assays.  $\beta$ -Galactosidase activities (mean  $\pm$  SD, n = 2) as fold changes over the highest negative control are shown. Bars, 5  $\mu$ m.

We next investigated whether Cdc15 physically interacts with Gef2 and Nod1. mYFP-Cdc15 pulled down both Gef2-13Myc and Nod1-13Myc from cell lysates in co-IP assays (Figure 2.4, C and D), suggesting that the three proteins were in a protein complex. Yeast two-hybrid assays revealed no positive interactions between Cdc15 and Gef2, whereas Cdc15 bound to Nod1 and Nod1(1-328) (Figure 2.4 E). This is consistent with our data that Nod1 N-terminal truncations still localize to the contractile ring (Figure 2.2 C). Thus, we concluded that the F-BAR protein Cdc15 recruits or stabilizes the Nod1/Gef2 complex to the contractile ring through the N-terminus of Nod1 during mitosis.

#### **2.4.6 Nod1 and Gef2 affect the contractile-ring stability during late cytokinesis**

The F-BAR protein Cdc15 is an essential component of the contractile ring that plays multiple roles during early and late cytokinesis (Fankhauser *et al.*, 1995; Roberts-Galbraith *et al.*, 2009, 2010; Laporte *et al.*, 2011). The fact that Cdc15 recruits the Nod1/Gef2 complex to the contractile ring indicated that Nod1 and Gef2 might have additional functions during late cytokinesis besides their role in division-site positioning. Indeed, we found that *nod1* $\Delta$  and *gef2* $\Delta$  had synthetic genetic interactions with *cdc15-140*. The double mutants *nod1* $\Delta$  *cdc15-140* and *gef2* $\Delta$  *cdc15-140* failed to form colonies while *cdc15-140* mutant still grew at 30°C (Figure 2.5 A). At 25°C, both *cdc15-140* single mutant and the double mutants resembled wt (Figure 2.5 B, upper panels). After 6

h at 30°C, cells proliferated with a mean cell length of 11.9 μm for wt, and 17.3 μm for *cdc15-140* cells. In contrast, most *nod1Δ cdc15-140* and *gef2Δ cdc15-140* cells were significantly longer with a mean cell length of 26.5 μm and 28.3 μm, respectively (Figure 2.5, B and C). We next quantified the number of nuclei per cell in these mutants at 30°C (Figure 2.5 D). Wt had ~13% binucleated cells whereas *cdc15-140* had 24% binucleated cells and <1% cells had >2 nuclei. However, the majority of *nod1Δ cdc15-140* and *gef2Δ cdc15-140* mutants were binucleated (62% and 58%, respectively) and ~13% and 7% cells contained >2 nuclei. These results indicated that the synthetic lethality in *nod1Δ cdc15-140* and *gef2Δ cdc15-140* cells was due to defects in cytokinesis.

To further determine the nature of the defects in *nod1Δ cdc15-140* and *gef2Δ cdc15-140* cells, we visualized contractile-ring and septum formation in the mutant cells using markers myosin regulatory light chain Rlc1-tdTomato and (1,3)β-D-glucan synthase GFP-Bgs1 (Figures, 2.5 E and 2.6). At 36°C, most *cdc15-140* mutant cells cannot maintain the contractile ring and form multinucleated cells (Balasubramanian *et al.*, 1998; Wachtler *et al.*, 2006). At a semi-permissive temperature of 30°C, Rlc1 localized to the cytokinesis nodes, which coalesced into the contractile ring in most cells. Then Bgs1 left the growing cell tips and accumulated at the contractile ring. The contractile ring constricted and septum formed (Figure 2.5 E). However, ~30% *cdc15-140* cells were defective in contractile-ring assembly and stability, and the ring eventually collapsed into aggregates (Figure 2.5, F and G). Consequently, Bgs1 dispersed around the cell cortex, and the cells became elongated and swollen. These defects were more pronounced in *nod1Δ cdc15-140* and *gef2Δ cdc15-140* cells, where Rlc1-tdTomato levels at the division site were significantly reduced to ~30% of those in *cdc15-140* single

mutant (Figure 2.5, E and G). ~52% of *nod1Δ cdc15-140* and *gef2Δ cdc15-140* cells failed to maintain the contractile ring (Figures, 2.5 E and F and 2.6). Thus, our data suggest that Nod1 and Gef2 help stabilize the contractile ring.

**Figure 2.5 Nod1 and Gef2 affect contractile-ring stability.**

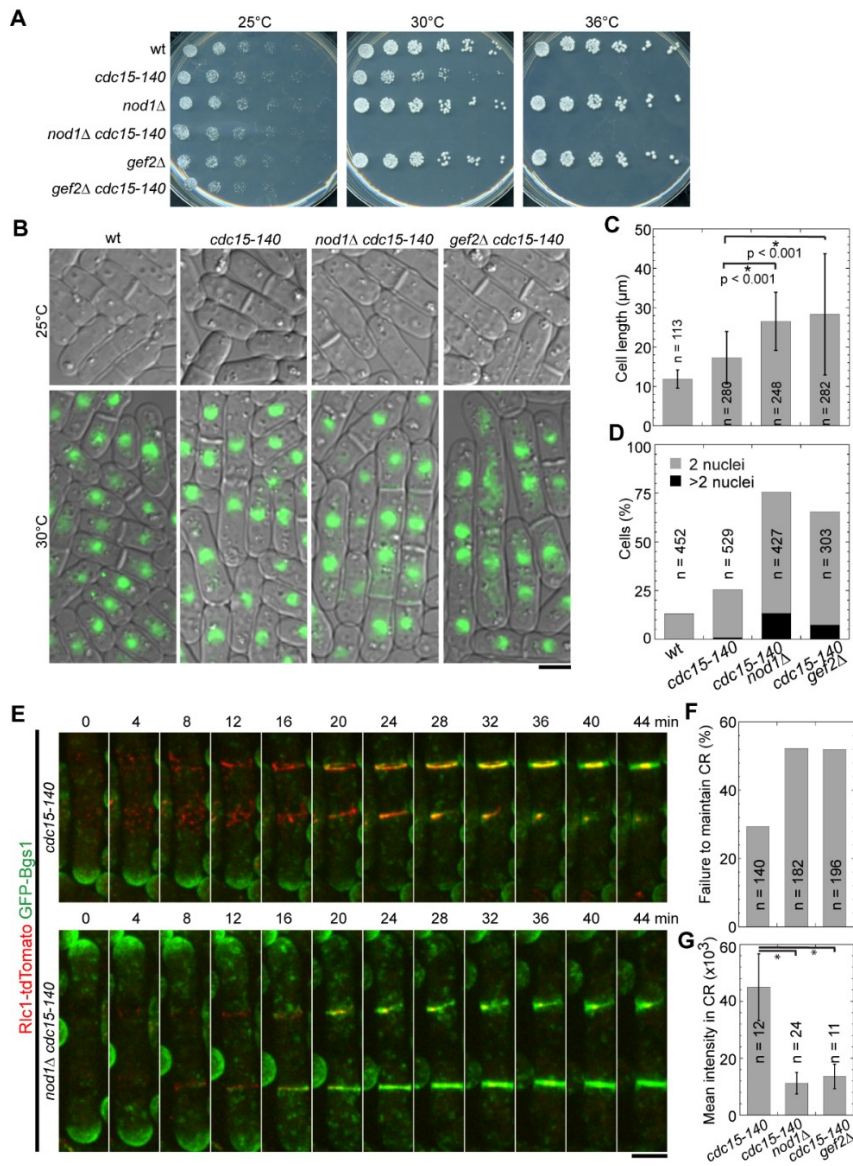
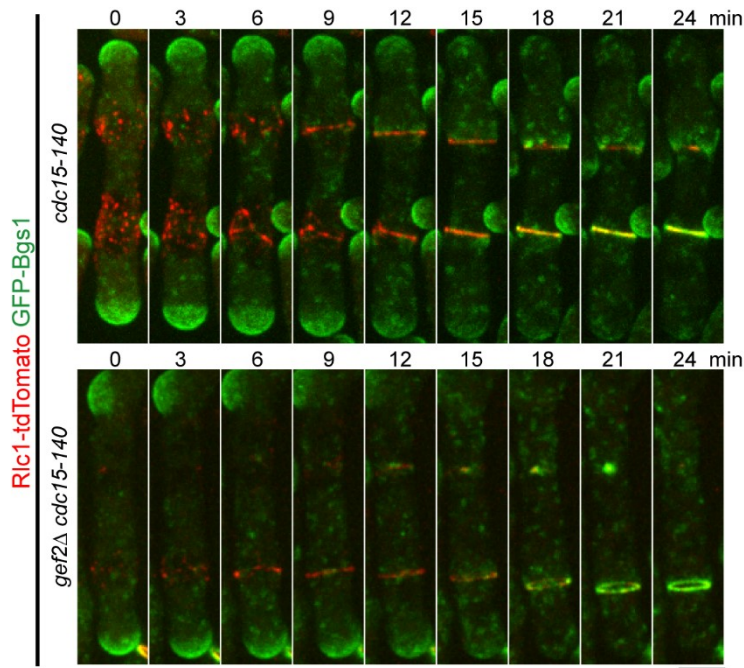


Figure 2.5: Continued

Figure 2.5: Continued

(A) *nod1Δ* and *gef2Δ* display synthetic interaction with *cdc15-140*. Serial dilution (3x) of indicated strains (JW81, JW1743, JW4259, JW4016, JW2854, and JW2937) on YE5S plates at 25, 30, and 36°C, respectively. (B-D) *nod1Δ cdc15-140* and *gef2Δ cdc15-140* cells display typical cytokinesis defects with elongated and multi-nucleated cells. Relevant strains used in (A) were cultured in YE5S liquid at 25°C (upper panel) or 30°C (lower panel) for 6 h before imaging. (B) Before imaging at 30°C, cells were stained with Hoechst for 10 min at 30°C to visualize DNA (green). DIC in grey. (C) Cell length and (D) number of nuclei in cells grown at 30°C for 6 h. (E-G) *Nod1* and *Gef2* affect contractile-ring stability during cytokinesis at 30°C. *Rlc1* and *Bgs1* were used to monitor the contractile ring and septum formation. Cells were grown at 30°C for 6 h before imaging at 30°C. Strains used: JW5357, JW5329, JW5330. (E) Time courses of selected images from a movie with 1 min delay. (F) Quantification of cells that fail to maintain the contractile ring (CR) after ring assembly. (G) Mean intensity of *Rlc1*-tdTomato in the contractile ring (CR). *Rlc1* intensity is significantly reduced in *nod1Δ cdc15-140* ( $p < 0.001$ ) and *gef2Δ cdc15-140* ( $p < 0.001$ ) cells compared to *cdc15-140* cells. Bars, 5 μm.

Figure 2.6 *Gef2* affects contractile-ring stability during cytokinesis.



*Rlc1*-tdTomato and GFP-*Bgs1* were used to monitor the contractile ring and septum formation. Cells (JW5329) were grown at 30°C for 6 h before imaging at 30°C. Time courses of selected images from a movie with 1 min delay. Bars, 5 μm.

#### **2.4.7 Nod1 and Gef2 suppress mutants in the SIN pathway and affect Sid2 kinase localization**

The SIN pathway regulates contractile-ring maturation, stability, and septum formation (Krapp and Simanis, 2008; Roberts-Galbraith and Gould, 2008). We reported that *gef2Δ* suppresses *cdc11-136* and *sid2-250* mutants in the SIN pathway but the mechanism is unknown (Ye *et al.*, 2012). We tested whether *nod1Δ* suppressed SIN mutants using *gef2Δ* as a control. Both *gef2Δ* and *nod1Δ* partially restored cell growth of *cdc7-24* at 30°C (Figure 2.7 A, upper panel) and of *cdc11-136* at both 30°C and 36°C (Figure 2.7 A, middle panel). Surprisingly, unlike *gef2Δ*, *nod1Δ* did not suppress *sid2-250* (Figure 2.7 A, lower panels). To explore the mechanism of the suppression of SIN mutants by *gef2Δ* and *nod1Δ*, we examined cell morphology of SIN single mutants and *SIN gef2Δ* or *SIN nod1Δ* double mutant cells. *cdc7-24* and *sid2-250* displayed cell lysis (Figures 2.7 B and 2.8). Except *nod1Δ sid2-250*, all double mutants partially restored the cell viability by reducing cell lysis. ~60% *gef2Δ sid2-250* cells survived at a semi-permissive temperature of 30°C whereas only ~20% *sid2-250* and *nod1Δ sid2-250* cells were viable (Figure 2.7 C). On the other hand, cells overexpressing Gef2 from *3nmt1* or *41nmt1* promoter under inducing conditions were synthetic lethal with *sid2-250* at 30°C, and synthetic sick with *sid2-1* from 30-36°C (Figure 2.7 D). Taken together, our data suggest that both Nod1 and Gef2 negatively affect the SIN pathway or the process regulated by the pathway.

**Figure 2.7** *nod1* $\Delta$  and *gef2* $\Delta$  suppress SIN mutants by reducing cell lysis.

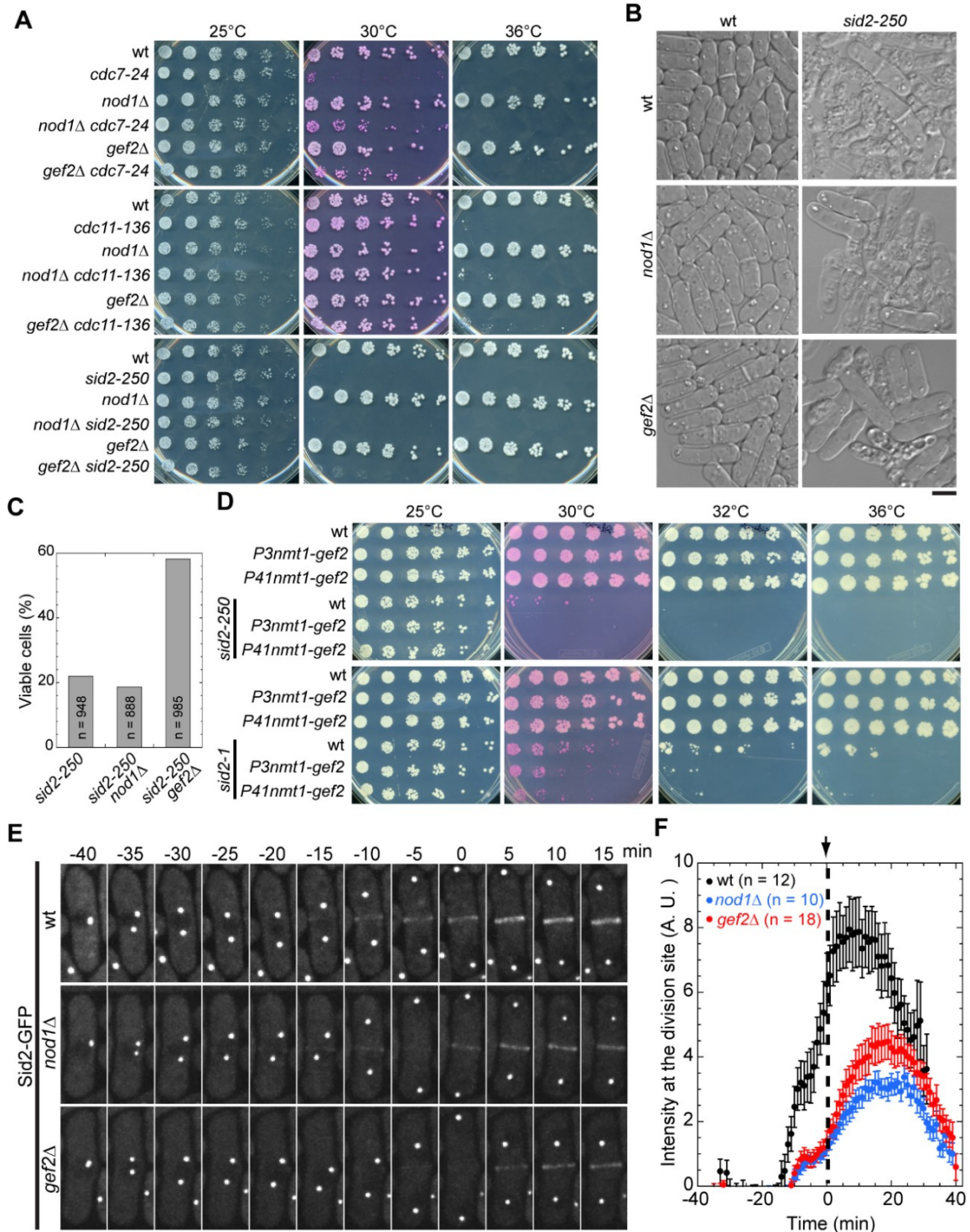
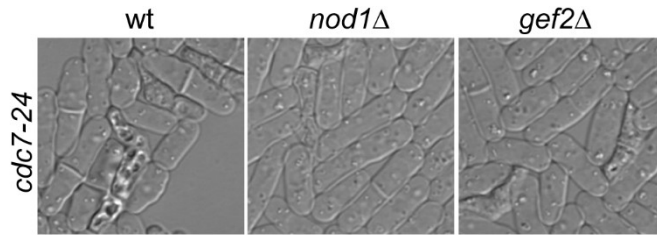


Figure 2.7: Continued

Figure 2.7: Continued

(A) Serial dilution (3x) of indicated strains on YE5S or YE5S + Phloxin B (red dye accumulated in dead cells) plates at 25, 30, and 36°C. Strains used: wt (JW81), *cdc7-24* (TP34), *nod1Δ* (JW4259), *nod1Δ cdc7-24* (JW4304), *gef2Δ* (JW2854), *gef2Δ cdc7-24* (JW3021), *cdc11-136* (TP47), *nod1Δ cdc11-136* (JW4306), *gef2Δ cdc11-136* (JW2972), *sid2-250* (YDM429), *nod1Δ sid2-250* (JW4294), and *gef2Δ sid2-250* (JW3009). (B and C) *gef2Δ* but not *nod1Δ* partially rescued cell lysis in *sid2-250*. Cells were grown in liquid culture at 25°C and then shifted 30°C for 6 h. (B) DIC images of *sid2* mutant strains used in (A). (C) Percentage of viable cells. Dead or lysed cells were identified as those that failed to maintain their cytoplasm. (D) Overexpression of Gef2 is synthetic lethal with *sid2* mutants. Serial dilutions (3x) of indicated strains on YE5S or YE5S + Phloxin B plates at 25, 30, and 36°C. Strains used: JW81, JW3561, JW3562, YDM429, JW5360, JW5361, VS2367, JW5405, and JW5406. (E) Sid2 localization and accumulation at the division site is compromised. Time courses of representative cells expressing Sid2-GFP in wt (YDM415), *gef2Δ* (JW5580) and *nod1Δ* (JW5581). Time 0: SPB separation. (F) Quantification of total intensity of Sid2-GFP at the division site for strains in (E). Black arrow and dashed line mark Time 0 as the end of Anaphase B. Black, wt; Blue, *nod1Δ*; Red, *gef2Δ*. Bars, 5 μm.

**Figure 2.8** *nod1Δ* and *gef2Δ* suppress SIN mutant *cdc7-24* by reducing cell lysis.



DIC images of *cdc7* mutant strains used in Figure 6A were taken after growth at 30°C for 6 h. Bars, 5 μm.

We next tested whether Sid2 localization is affected in *gef2Δ* and *nod1Δ*. Sid2 localizes to the SPB, the contractile ring, and the septum during cytokinesis (Sparks *et al.*, 1999). Sid2 appeared at the contractile ring at the beginning of anaphase B and the level gradually increased until the contractile ring started to constrict (Figure 2.7, E, upper row and F) as reported (Sparks *et al.*, 1999; Tebbs and Pollard, 2013). In *gef2Δ* and *nod1Δ*, Sid2 appeared at the contractile ring at a similar timing as in wt. However, the recruitment of Sid2 to the division site was defective. By the end of anaphase B, Sid2

intensity at the division site in *gef2* $\Delta$  and *nod1* $\Delta$  was only ~20% of that in wt (Figure 2.7, E, middle and lower rows and F;  $p < 0.001$  for both *gef2* $\Delta$  and *nod1* $\Delta$  compared to wt). Moreover, the peak level of Sid2 at the division site in *gef2* $\Delta$  and *nod1* $\Delta$  was reduced to 57% and 46% that of wt (Figure 2.7 F;  $p < 0.005$  for both *gef2* $\Delta$  and *nod1* $\Delta$  compared to wt). We noted that both wt and the mutant cells expressing Sid2-GFP spent more time in mitosis. Because Sid2 regulates proper spindle elongation during anaphase (Mana-Capelli *et al.*, 2012), it seems that Sid2-GFP may not be fully functional. Together, these data suggest that Gef2 and Nod1 play a role in recruiting Sid2 to the contractile ring.

#### **2.4.8 Gef2 interacts with Rho GTPases in vitro and is involved in Rho4 localization**

Rho GTPases regulate contractile-ring formation, septum formation and degradation during cytokinesis (Arellano *et al.*, 1997; Nakano *et al.*, 1997, 2003, 2005; Tolliday *et al.*, 2002; Santos *et al.*, 2003; Tajadura *et al.*, 2004; Mutoh *et al.*, 2005; Yoshida *et al.*, 2006). To further dissect the role of Gef2, we tested the interactions between the GEF domain of Gef2 and all six Rho GTPases from *S. pombe*. The 6His-tagged GEF domain (aa 211-600) of Gef2 consisting of the DH and PH domains was purified from *E. coli*. The purified GEF domain was then pulled down by purified GST-tagged Rho proteins. We found that Gef2 interacted with Rho1, Rho4, and Rho5, but not with Rho2, Rho3, and Cdc42 in the pull-down assays (Figure 2.9, A and B).

**Figure 2.9** Gef2 GEF domain binds to GTPases Rho1, Rho4, and Rho5 in vitro.

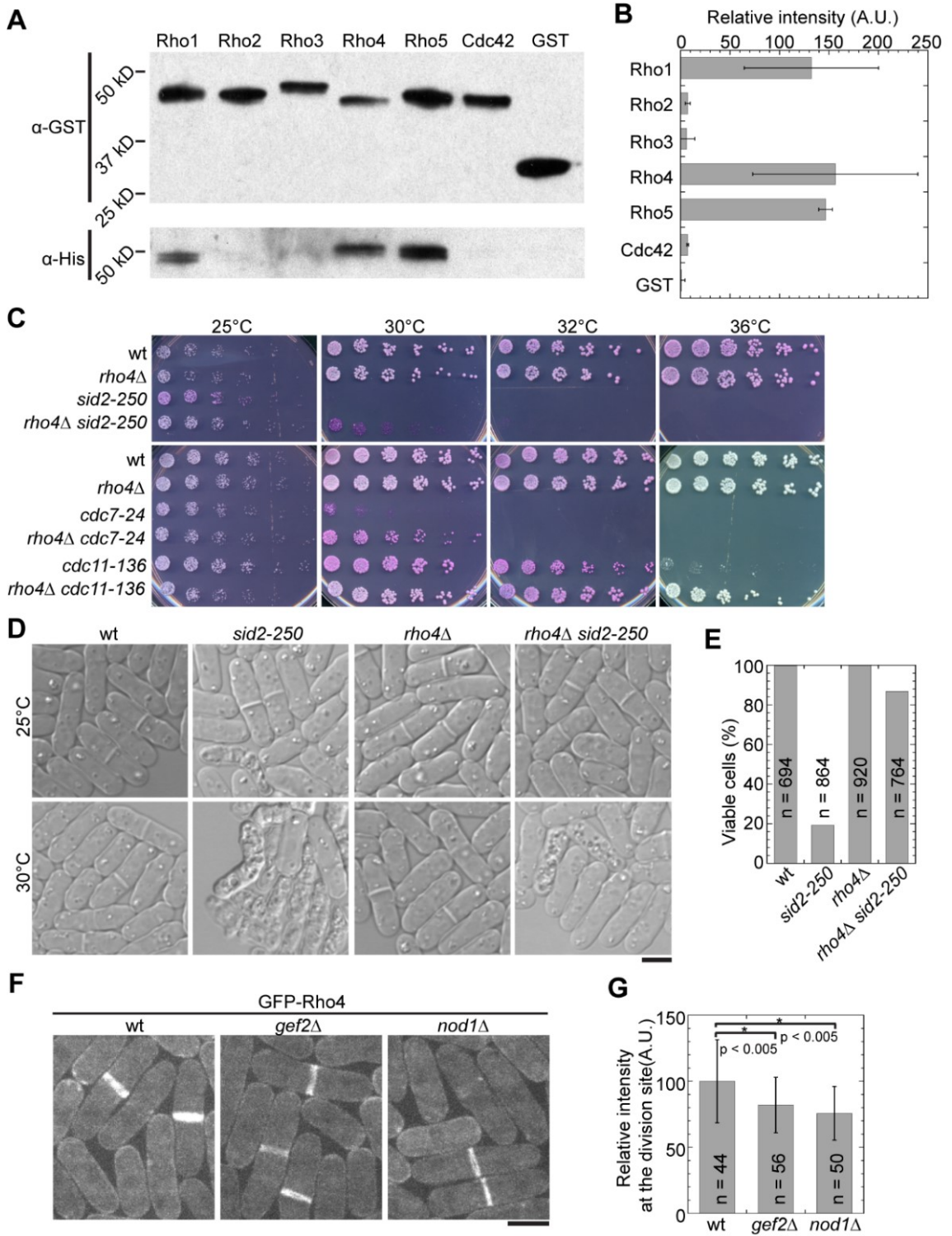


Figure 2.9: Continued

Figure 2.9: Continued

(A and B) Purified GST-Rho GTPases and GST control were bound to the beads and then incubated with purified His-GEF domain (aa 211-600) of Gef2. The amount of pulled down Gef2 was detected by Western blotting (A) and quantified (B). The intensities of His-Gef2(GEF) bands were measured, background subtracted, corrected for Rho GTPase amount, and normalized by setting the intensity of His-Gef2(GEF) in GST control as 1. (C-E) *rho4Δ* suppresses SIN mutants. Strains used: JW81, JW3041, YDM429, JW5505, TP34, JW5503, TP4713, and JW5504. (C) Serial dilution (3x) of indicated strains on YE5S or YE5S + Phloxin B plates at 25, 30, 32 and 36°C for 3 d. (D and E) *rho4Δ* rescues the cell-lysis phenotype of *sid2-250*. (D) DIC images of cells grown in liquid culture at 25°C or after 6 h at 30°C. (E) Quantification of viable (not lysed or dead) cells after 6 h at 30°C. (F) Micrograph of GFP-Rho4 in wt and deletion mutants. Strains used: wt, PPG1580; *gef2Δ*, JW4909; *nod1Δ*, JW4910. (G) Quantification of Sid2 total local intensity at the division site for strains in (F). (H) Micrograph of mECitrine-Rho5 in wt and deletion mutants. Cells were cultured in EMM5S for 12 h before imaging to induce the expression of Rho5. Strains used: wt, JW5596; *gef2Δ*, JW5612; *nod1Δ*, JW5611. Bars, 5 μm.

To investigate if Gef2 might function through a Rho GTPase in vivo, we crossed *rho4Δ* to mutants in the SIN pathway since *rho4Δ*, like *gef2Δ*, has been shown to suppress *sid2-250* (Jin *et al.*, 2006). We found that in addition to rescuing *sid2-250* at both 25 and 30°C, *rho4Δ* also partially rescued *cdc7-24* at 30°C, and *cdc11-136* at 30-36°C (Figure 2.9 C). We next observed the cell morphology of *rho4Δ sid2-250* at 25°C or after 6 h at 30°C (Figure 2.9 D). At 25°C, both *rho4Δ* and *rho4Δ sid2-250* resembled wt whereas *sid2-250* displayed slight cell lysis. At 30°C, only ~20% *sid2-250* cells were viable, whereas ~85% cells survived in *rho4Δ sid2-250* double mutant (Figure 2.9 E). Thus, *rho4Δ* resembled *gef2Δ* (Figure 2.9, A-C) in the suppression of the SIN mutants. Together, these data suggest that Gef2 functions through Rho4 GTPase to regulate late cytokinesis.

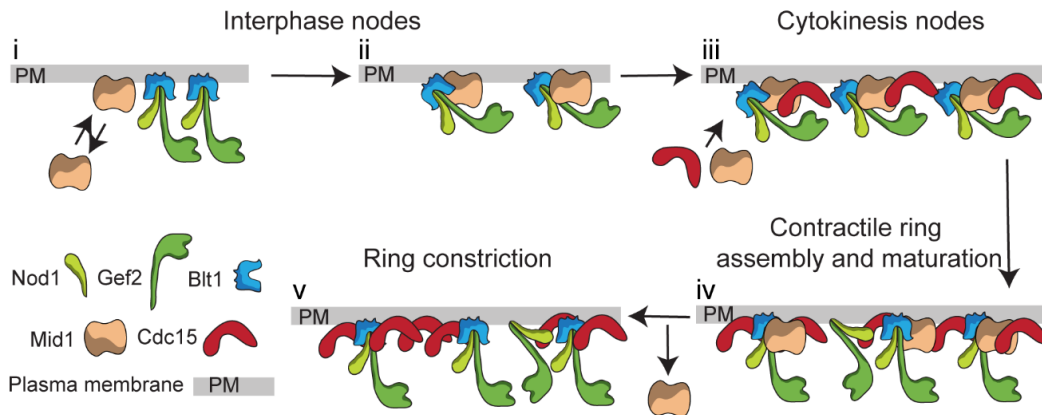
We next determined if Gef2 or Nod1 affect Rho4 localization. GFP-Rho4 localized to the cell-division site as well as cell periphery in wt cells (Nakano *et al.*, 2003; Santos *et al.*, 2003). Although its localization was not abolished, Rho4 intensity at the

division site was reduced to 82% and 75% of wt level in *gef2Δ* and *nod1Δ*, respectively (Figure 2.9, F and G;  $p < 0.005$  for both *gef2Δ* and *nod1Δ* compared to wt). Thus, Gef2 and Nod1 are involved in concentrating Rho4 GTPase to the division site during cytokinesis.

## 2.5 Discussion

In Chapter 2, we found that Nod1, a new player in cytokinesis, regulates division-site positioning and contractile-ring stability together with the putative Rho-GEF Gef2 (Figure 2.10). In addition, we identified the potential Rho GTPase substrates for Gef2, suggesting the possible involvement of Gef2 GEF activity and Rho GTPases in the regulation of cytokinesis.

**Figure 2.10 Model of Nod1 and Gef2 localizations and interactions with other proteins on the cytoplasmic side of the plasma membrane during the cell cycle.**



(i) During interphase, Nod1 and Gef2 localize to interphase nodes via Blt1 or other interphase node components, (ii) where they help recruit and stabilize anillin-related protein Mid1. (iii) The nodes mature into cytokinesis nodes and coalesce into the contractile ring as more Mid1 and other cytokinesis proteins like F-BAR protein Cdc15 arrive at the division site. (iv) Cdc15 continuously recruits or stabilizes Nod1-Gef2 complex during ring maturation, which helps to maintain the contractile-ring integrity and stability. (v) Mid1 disappears from the ring at the onset of its constriction. For clarity, the potential interactions between Gef2 and Rho GTPases are not shown.

### 2.5.1 The roles of Rho GTPases during cytokinesis

Among the seven Rho GEFs in *S. pombe*, Gef2 and Gef3 have no identified Rho substrates. We find that Gef2 interacts with Rho1, Rho4, and Rho5 in vitro (Figure 2.9, A and B). It is unclear whether Gef2 interacts and activates these Rho GTPases in vivo, but these data still provide us insight into Gef2's functions as a potential Rho GEF. In previous study, we reported that deletion of Gef2 DH domain causes defects in division-site positioning in ~50% *plo-ts18* mutant cells at 25°C (Ye *et al.*, 2012). Therefore, it is possible that the GEF activity of Gef2 is involved in division-site placement. Rho1 regulates cell integrity and septum formation during late cytokinesis in fission yeast (Nakano *et al.*, 1997; Mutoh *et al.*, 2005). However, its homologs RhoA or Rho1 in animal cells and budding yeast are active in early cytokinesis for division-site selection and contractile-ring assembly (Imamura *et al.*, 1997; Tolliday *et al.*, 2002; Bement *et al.*, 2005; Piekny *et al.*, 2005; Yoshida *et al.*, 2006; Watanabe *et al.*, 2010). The presence and function of Gef2 in the cortical nodes might suggest a role of Rho1 during early cytokinesis if Gef2 indeed activates Rho1 in vivo. However, one difficulty in studying RhoA or Rho1 is that its native concentration is low, and therefore it is difficult to detect Rho1 at the division site during early cytokinesis by fluorescence microscopy. Whether Rho1 participates in division-site positioning in fission yeast remains to be tested, and we cannot rule out the possibility that other Rho candidates are also involved.

Of the six Rho GTPases in fission yeast, Rho1 and Cdc42 are relatively well studied whereas our knowledge on Rho2-5 is limited. For example, no Rho GEFs have been assigned to Rho2, Rho3, and Rho4. Rho4 affects the localization and activity of  $\beta$ -glucanase Eng1 and  $\alpha$ -glucanase Agn1, which results in cell separation defects (Nakano

*et al.*, 2003; Santos *et al.*, 2003, 2005). Rho5 is a Rho1 paralogue that shares similar functions (Nakano *et al.*, 2005). However, how Rho4 and Rho5 are regulated and localized remains unknown. Our data suggest Gef2 might be a GEF for Rho4 or Rho5, and help recruit Rho4 to the division site. However, Rho4 localization is only partially dependent on Gef2 (Figure 2.9, F and G). More efforts are needed to investigate whether and how Gef2 works with these Rho GTPases in the future.

### **2.5.2 Localization of Nod1 and Gef2 during the cell cycle**

We and others found that Gef2 coordinates with Polo kinase Plo1 to recruit anillin-like protein Mid1 to the cortical nodes during G2/M transition (Ye *et al.*, 2012; Guzman-Vendrell *et al.*, 2013; Jourdain *et al.*, 2013). During the course of that study, we identified Nod1 as a Gef2 related protein and binding partner. We found that Gef2 and Nod1 form a complex, which is important for their cortical node localization and functions. These results are consistent with a recent report on Nod1 (Jourdain *et al.*, 2013). Gef2 and Nod1 are stable in interphase nodes as revealed by FRAP assays. Besides a GEF (DH-PH) domain, Gef2 has no other known structures or motifs (Figure 1A; Iwaki *et al.*, 2003). Blt1 was reported to recruit Gef2 to the interphase nodes (Ye *et al.*, 2012; Guzman-Vendrell *et al.*, 2013; Jourdain *et al.*, 2013). It is likely that Blt1 interacts with Nod1 and Gef2 through their C-termini (Figure 2.10). Both Nod1 and Gef2 have enriched  $\alpha$ -helix structures at C-termini (Jones, 1999). However, Gef2 still localizes to cytokinesis nodes in *blt1* $\Delta$ , so Gef2 must have other binding partner during early mitosis. We previously showed that Gef2 interacts with Mid1(300-350) *in vivo* (Ye *et al.*, 2012). Although we found that Mid1(1-580), which includes the Gef2 binding region, depended on Gef2 C-

terminus for node localization, no positive interactions were observed between Mid1(300-350) and several regions of Gef2 or Nod1 in yeast two hybrid assays (our unpublished data). Thus, the interactions between Gef2 and Mid1 may be indirect.

Although the majority of Gef2 are recruited to the contractile ring through the cortical nodes, our localization dependency data reveal that both Nod1 and Gef2 are capable of localizing to the contractile ring without each other. We find that F-BAR protein Cdc15 physically interacts with Nod1 and recruits Nod1 to the contractile ring (Figures, 2.4 and 2.10). Cdc15 appears at cytokinesis nodes ~5 min before SPB separation and is continuously recruited to the contractile ring during mitosis (Wu and Pollard, 2005; Laporte *et al.*, 2011). Consistently, the contractile ring contains ~40% more molecules of Nod1 than Gef2 (Figure 2.1 C). Nod1 intensity at the contractile ring in *gef2Δ* also increases during ring maturation at late mitosis. Without Nod1, Gef2 can still localize to the division site during later stages of cytokinesis (Figure 2.2 A), although Gef2 does not interact with Cdc15 in yeast two-hybrid assays. It is possible that Gef2 depends on alternative mechanisms to localize. One attractive candidate is a Rho GTPase. We found that Gef2 can interact with Rho1, Rho4, and Rho5, and all of them localize to the division site at late cytokinesis (Nakano *et al.*, 2003, 2005; Santos *et al.*, 2003; Mutoh *et al.*, 2005). In budding yeast, activated Cdc42 recruits the Rho-GEF Cdc24 and scaffold protein Bem1 to activate more Cdc42 and establish cell polarity (Butty *et al.*, 2002; Slaughter *et al.*, 2009; Bi and Park, 2012). It is possible that Gef2 and its Rho substrates are involved in a similar positive feedback loop to regulate cytokinesis.

### **2.5.3 Nod1 and Gef2 coordinate with F-BAR protein Cdc15 to maintain contractile-ring stability**

Cdc15 has multiple functions during cytokinesis. During early cytokinesis, Cdc15 recruits the formin Cdc12 to promote contractile-ring assembly (Carnahan and Gould, 2003; Kovar *et al.*, 2003; Laporte *et al.*, 2011). During ring maturation at anaphase, Cdc15, together with the SIN pathway and the F-BAR protein Imp2, is thought to be important for maintaining contractile-ring stability and integrity (Wachtler *et al.*, 2006; Hachet and Simanis, 2008; Huang *et al.*, 2008; Roberts-Galbraith *et al.*, 2009). However, the exact mechanism remains elusive.

Here we add another layer of complexity to the function of Cdc15 during late cytokinesis. In *nod1Δ cdc15-140* and *gef2Δ cdc15-140*, most cells form a fragile contractile ring and become elongated and multinucleated (Figure 2.5). The severely reduced level of the myosin regulatory light chain Rlc1 suggests loss of proteins from the contractile ring (Figures, 2.5 E-G, and 2.6). One possible explanation could be related to the scaffolding protein Mid1. Mid1 is anchored to the equatorial cortex through the cooperation of its own lipid binding domains and other cytokinesis proteins including Cdr2, Gef2, and Blt1 (Almonacid *et al.*, 2009; Lee and Wu, 2012; Ye *et al.*, 2012; Guzman-Vendrell *et al.*, 2013). Mid1 is more dynamic and mobile at the division site without Gef2 (Ye *et al.*, 2012). As a result, the recruitment and maintenance of the contractile-ring components might be less effective during late mitosis, which aggravates the *cdc15* mutant phenotype. It is also possible that Rho1 and/or Rho5 GTPases are also involved in contractile-ring stability and their activities are compromised in *nod1Δ* and *gef2Δ* cells. Further experiments are needed to distinguish these possibilities.

#### **2.5.4 Nod1 and Gef2 suppress the SIN pathway**

The SIN pathway includes a small GTPase and several protein kinases and their adaptors, which form a kinase cascade on the SPB (Fankhauser and Simanis, 1993, 1994; Furge *et al.*, 1998, 1999; Sparks *et al.*, 1999; Chang and Gould, 2000; Guertin *et al.*, 2000; Hou *et al.*, 2000; Salimova *et al.*, 2000; Tomlin *et al.*, 2002). The activation of SIN pathway leads to contractile-ring constriction and septum formation (Wachtler *et al.*, 2006; Hachet and Simanis, 2008; Krapp and Simanis, 2008; Johnson *et al.*, 2012). This is executed by translocation of kinase Sid2 and its adaptor Mob1 from the SPB to the contractile ring (Sparks *et al.*, 1999; Hou *et al.*, 2000; Chen *et al.*, 2008). Discoveries of suppressors of SIN pathway mutants, especially those of *sid2*, have helped us understand how SIN pathway regulates cytokinesis (Jiang and Hallberg, 2001; Jin and McCollum, 2003; Jin *et al.*, 2006; Goyal and Simanis, 2012). Here we found that *nod1Δ* and *gef2Δ* suppress the SIN mutants by improving cell survival at the semi-permissive temperature whereas single SIN mutant cells lyse when trying to separate with defective septa (Figure 2.7, A-C). We also observed that Sid2 accumulation at the division site is delayed and compromised in *nod1Δ* and *gef2Δ* cells (Figure 2.7, E and F). Similar results were observed in IQGAP *rng2* without the IQ motifs (Tebbs and Pollard, 2013), suggesting a requirement of intact contractile ring for Sid2 stable localization. Therefore, the contractile ring components including Gef2 and Nod1 may regulate the SIN pathway through direct or indirect influence on contractile-ring localization of Sid2. However, it is still possible that the defects caused by *nod1Δ* and *gef2Δ* affect the rates of contractile-ring maturation and constriction, allowing more time for septum synthesis. Consistently, increasing the amount and activity of  $\beta$ -glucan synthase Bgs1 by overexpressing Rho1 GTPase or its GEF Rgf3 can rescue *sid2* mutants (Jin *et al.*, 2006).

However, Rho4 GTPase might be also involved in the suppression of *sid2-250* by *gef2Δ*. We found that Gef2 binds to Rho4 in vitro. Interestingly, deletion of *rho4*, and its effectors *eng1* or *agn1* all partially suppress *sid2-250* (Jin *et al.*, 2006), which is consistent with our results (Figure 2.9, C-E). Thus, it is likely that the suppression of SIN mutants by *gef2Δ* is due to a reduced function of Rho4 and its effectors. Consistently, we found that Rho4 localization to the division site was slightly but significantly reduced in both *nod1Δ* and *gef2Δ* cells (Figure 2.9, F and G). This suggests that Gef2 and Nod1 contribute to Rho4 localization besides the undefined role of Rho4 activation. The cell-separation defect of *rho4Δ* is mild even at 36°C (Santos *et al.*, 2003), suggesting other mechanisms and pathways are involved in septum degradation. Further studies are needed to identify the redundant pathways.

In conclusion, we find that the Nod1/Gef2 complex functions in division-site positioning, contractile-ring maintenance, and septation besides its role in cell-size control. We also discover the potential Rho GTPase substrates for Gef2. In the future, it will be very informative to investigate if Gef2 has GEF activity towards the Rho GTPase candidates, and if Nod1 affects Gef2 activity in addition to its localization.

## **2.6 Acknowledgements**

We thank Iain Hagan, Dannel McCollum, James Moseley, Kurt Runge, Viesturs Simanis, Pilar Pérez, and Thomas Pollard for strains; Masaaki Miyamoto for the Rho plasmids; Valerie Coffman and Matthew Karikomi for the Gef2 plasmid; and the James Hopper, Anita Hopper, and Stephen Osmani laboratories for sharing equipment. We thank Hay-Oak Park, Stephen Osmani, Dmitri Kudryashov, and the members of Wu lab for helpful suggestions and discussion. We appreciate Valerie Coffman, I-Ju Lee, and Ning Wang

for critical reading of the manuscript. This work was supported by National Institutes of Health Grant R01GM086546 and American Cancer Society Grant RSG-13-005-01-CCG to J.-Q.W.

**Table 2.1 Genetic interactions of *nod1*Δ with other mutations affecting cytokinesis and cell-size control**

Strains	Temperature (°C) <sup>a</sup>				<i>gef2</i> Δ <sup>b</sup>
	25	30	32	36	
<i>plol-ts18</i>	+++	++	++	+	same
<i>plol-ts18 nod1</i> Δ	+	+	+	+/-	
<i>mid1-6</i>	+++	+++	+++	++	same
<i>mid1-6 nod1</i> Δ	+++	++	++	++	
<i>mid1-366</i>	+++	+++	+++	++	same
<i>mid1-366 nod1</i> Δ	+	+	+	+	
<i>rng2-D5</i>	+++	++	++	-	same
<i>rng2-D5 nod1</i> Δ	++	+	+	-	
<i>rng2-346</i>	+++	++	++	-	same
<i>rng2-346 nod1</i> Δ	++	+	+	-	
<i>cdc4-8</i>	+++	++	++	-	same
<i>cdc4-8 nod1</i> Δ	+++	+	+	-	
<i>cdc15-140</i>	+++	+	-	-	same
<i>cdc15-140 nod1</i> Δ	+++	-	-	-	
<i>cdr2</i> Δ	+++	+++	+++	+++	same
<i>cdr2</i> Δ <i>nod1</i> Δ	+++	+++	+++	+++	
<i>blt1</i> Δ	+++	+++	+++	+++	same
<i>blt1</i> Δ <i>nod1</i> Δ	+++	+++	+++	+++	

Continued

---

**Table 2.1: Continued**

<i>klp8Δ</i>	+++	+++	+++	+++	
<i>klp8Δ nod1Δ</i>	+++	+++	+++	+++	same
<i>cdc7-24</i>	+++	+	-	-	
<i>cdc7-24 nod1Δ</i>	+++	++	-	-	same
<i>cdc11-136</i>	+++	++	++	-	
<i>cdc11-136 nod1Δ</i>	+++	+++	+++	+/-	same
<i>sid2-250</i>	++	-	-	-	
<i>sid2-250 nod1Δ</i>	++	-	-	-	different
<i>sid2-250 gef2Δ</i>	++	+/-	-	-	

---

<sup>a</sup>Growth and color of colonies on YE5S + phloxin B plates at various temperatures. “+++” similar to wt; “++” mild defects or cell lysis; “+” cell lysis with reduced growth rate; “+/-” severe cell lysis and slow growth “-” inviable. <sup>b</sup>The genetic interactions of *nod1Δ* were compared to those of *gef2Δ* with corresponding mutants.

**Table 2.2 *S. pombe* strains used in Chapter 2**

Strain	Genotype	Source/Reference
JW81	<i>h<sup>-</sup> ade6-210 ura4-D18 leu1-32</i>	Wu <i>et al.</i> , 2003
JW1063	<i>h<sup>+</sup> mYFP-cdc15 ade6-M216 leu1-32 ura4-D18</i>	Wu and Pollard, 2005
JW1636	<i>h<sup>+</sup> mid1-6 ade6-M210 leu1-32 ura4-D18</i>	Coffman <i>et al.</i> , 2013
JW1743	<i>cdc15-140 ade6-M210 leu1-32 ura4-D18</i>	Coffman <i>et al.</i> , 2013
JW1824	<i>h<sup>+</sup> klp8Δ::kanMX4 ade6 leu1-32 ura4-D18</i>	Kim <i>et al.</i> , 2010
JW1825	<i>h<sup>+</sup> blt1Δ::kanMX4 ade6-M216 leu1-32 ura4-D18</i>	Ye <i>et al.</i> , 2012
JW1826	<i>h<sup>+</sup> gef2Δ::kanMX4 ade6 leu1-32 ura4-D18</i>	Ye <i>et al.</i> , 2012
JW2249	<i>rng2-346 ade6-M210 leu1-32 ura4-D18</i>	Chapter 2
JW2255	<i>h<sup>+</sup> mid1-366 ade6-M210 leu1-32 ura4-D18</i>	Ye <i>et al.</i> , 2012
JW2854	<i>h<sup>+</sup> gef2Δ::hphMX6 ade6 leu1-32 ura4-D18</i>	Chapter 2
JW2937	<i>cdc15-140 gef2Δ::kanMX4 ade6 leu1-32 ura4-D18</i>	Chapter 2
JW2972	<i>h<sup>+</sup> cdc11-136 gef2Δ::hphMX6 ade6 leu1-32 ura4-D18</i>	Ye <i>et al.</i> , 2012
JW3009	<i>gef2Δ::hphMX6 sid2-250 ade6 leu1-32 ura4-D18</i>	Ye <i>et al.</i> , 2012
JW3021	<i>gef2Δ::hphMX6 cdc7-24 ade6 leu1-32 ura4-D18</i>	Chapter 2
JW3041	<i>h<sup>+</sup> rho4Δ::kanMX4 ade6 leu1-32 ura4-D18</i>	Kim <i>et al.</i> , 2010
JW3078	<i>h<sup>-</sup> gef2Δ::hphMX6 plo1.ts18::ura4<sup>+</sup> ade6 leu1-32 ura4-D18</i>	Ye <i>et al.</i> , 2012
JW3204	<i>h<sup>-</sup> gef2-13Myc-hphMX6 ade6-M210 leu1-32 ura4-D18</i>	Ye <i>et al.</i> , 2012
JW3325	<i>gef2-13Myc-hphMX6 mYFP-cdc15 ade6-M210 leu1-32 ura4-D18</i>	Chapter 2
JW3561	<i>h<sup>-</sup> kanMX6-3nmt1-gef2 ade6-M216 leu1-32 ura4-D18</i>	Chapter 2

Continued

---

**Table 2.2: Continued**

JW3562	<i>h<sup>-</sup> kanMX6-41nmt1-gef2 ade6-M216 leu1-32 ura4-D18</i>	Chapter 2
JW3622	<i>h<sup>+</sup> gef2-13Myc-hphMX6 ade6-M210 leu1-32 ura4-D18</i>	Chapter 2
JW3773	<i>h<sup>-</sup> nod1Δ::kanMX6 ade6-M210 leu1-32 ura4-D18</i>	Chapter 2
JW3814	<i>h<sup>+</sup> nod1Δ::kanMX6 gef2Δ::kanMX4 ade6 leu1-32 ura4-D18</i>	Chapter 2
JW3815	<i>nod1Δ::kanMX6 plo1.ts18::ura4<sup>+</sup> ade6-M210 ura4-D18 leu1-32</i>	Chapter 2
JW3825	<i>h<sup>-</sup> kanMX6-Pgef2-mECitrine-4Gly-gef2 ade6-M216 leu1-32 ura4-D18</i>	Ye et al., 2012
JW3826	<i>h<sup>-</sup> kanMX6-Pgef2-mECitrine-4Gly-gef2-(957-1101) ade6- M216 leu1-32 ura4-D18</i>	Ye et al., 2012
JW3861	<i>h<sup>+</sup> nod1Δ::kanMX6 mid1-6 ade6-M210 leu1-32 ura4-D18</i>	Chapter 2
JW3873	<i>nod1Δ::kanMX6 gef2Δ::kanMX4 plo1.ts18::ura4<sup>+</sup> ade6 leu1-32 ura4-D18</i>	Chapter 2
JW3875	<i>h<sup>-</sup> nod1Δ::kanMX6 mid1-366 ade6-M210 leu1-32 ura4-D18</i>	Chapter 2
JW4008	<i>h<sup>-</sup> nod1-mECitrine-kanMX6 ade6-M210 leu1-32 ura4-D18</i>	Chapter 2
JW4010	<i>h<sup>-</sup> nod1-tdTomato-hphMX6 ade6-M210 leu1-32 ura4-D18</i>	Chapter 2
JW4013	<i>h<sup>-</sup> nod1-13Myc-hphMX6 ade6-M210 leu1-32 ura4-D18</i>	Chapter 2
JW4014	<i>nod1Δ::kanMX6 kanMX6-Pgef2-mECitrine-4Gly-gef2 ade6 leu1-32 ura4-D18</i>	Chapter 2
JW4015	<i>h<sup>-</sup> nod1Δ::kanMX6 cdc4-8 ade6 leu1-32 ura4-D18</i>	Chapter 2
JW4016	<i>h<sup>-</sup> nod1Δ::kanMX6 cdc15-140 ade6-M210 leu1-32 ura4- D18</i>	Chapter 2

Continued

---

**Table 2.2: Continued**

JW4038	<i>nod1-mECitrine-kanMX6 gef2Δ::hphMX6 ade6 leu1-32 ura4-D18</i>	Chapter 2
JW4042	<i>nod1Δ::kanMX6 rng2-D5 ade6-M210 leu1-32 ura4-D18</i>	Chapter 2
JW4043	<i>h<sup>+</sup> nod1Δ::kanMX6 rng2-346 ade6-M210 leu1-32 ura4-D18</i>	Chapter 2
JW4098	<i>nod1Δ::kanMX6 cdr2Δ::kanMX6 ade6 leu1-32 ura4-D18</i>	Chapter 2
JW4099	<i>h<sup>+</sup> nod1Δ::kanMX6 blt1Δ::kanMX4 ade6 leu1-32 ura4-D18</i>	Chapter 2
JW4226	<i>h<sup>+</sup> kanMX6-Pgef2-tdTomato-4Gly-gef2 ade6-M210 leu1-32 ura4-D18</i>	Ye <i>et al.</i> , 2012
JW4256	<i>nod1-tdTomato-hphMX6 kanMX6-Pgef2-mECitrine-4Gly-gef2-(957-1101) ade6 leu1-32 ura4-D18</i>	Chapter 2
JW4259	<i>h<sup>-</sup> nod1Δ::hphMX6 ade6-M210 leu1-32 ura4-D18</i>	Chapter 2
JW4294	<i>nod1Δ::hphMX6 sid2-250 ade6-M210 leu1-32 ura4-D18</i>	Chapter 2
JW4295	<i>klp8Δ::kanMX4 nod1Δ::hphMX6 ade6 leu1-32 ura4-D18</i>	Chapter 2
JW4304	<i>nod1Δ::hphMX6 cdc7-24 ade6 leu1-32 ura4-D18 his2 or his7</i>	Chapter 2
JW4306	<i>nod1Δ::hphMX6 cdc11-136 ade6-M210 leu1-32 ura4-D18 his2 or his7</i>	Chapter 2
JW4325	<i>h<sup>-</sup> nod1(1-209)-mECitrine-kanMX6 ade6-M210 leu1-32 ura4-D18</i>	Chapter 2
JW4326	<i>h<sup>-</sup> nod1(1-328)-mECitrine-kanMX6 ade6-M210 leu1-32 ura4-D18</i>	Chapter 2

Continued

---

**Table 2.2: Continued**

JW4330	<i>nod1-13Myc-hphMX6 kanMX6-Pgef2-mECitrine-4Gly-gef2</i> <i>ade6 leu1-32 ura4-D18</i>	Chapter 2
JW4331	<i>nod1-13Myc-hphMX6 kanMX6-Pgef2-mECitrine-4Gly-gef2-</i> <i>(957-1101) ade6 leu1-32 ura4-D18</i>	Chapter 2
JW4355	<i>nod1-tdTomato-hphMX6 kanMX6-Pgef2-mECitrine-4Gly-</i> <i>gef2-(1-956)-TADH1-hphMX6 ade6 leu1-32 ura4-D18</i>	Chapter 2
JW4359	<i>h<sup>-</sup> nod1(1-328)-mECitrine-kanMX6 kanMX6-Pgef2-</i> <i>tdTomato-4Gly-gef2 ade6 leu1-32 ura4-D18</i>	Chapter 2
JW4453	<i>h<sup>-</sup> kanMX6-Pnod1-mECitrine-nod1 ade6-M210 leu1-32</i> <i>ura4-D18</i>	Chapter 2
JW4455	<i>h<sup>-</sup> kanMX6-Pnod1-mECitrine-nod1(329-419) ade6-M210</i> <i>leu1-32 ura4-D18</i>	Chapter 2
JW4457	<i>nod1-mEGFP-hphMX6 kanMX6-Pgef2-tdTomato-4Gly-gef2</i> <i>ade6-M210 leu1-32 ura4-D18</i>	Chapter 2
JW4750	<i>Pnod1-mECitrine-Nod1 ade6-M210 leu1-32 ura4-D18</i>	Chapter 2
JW4856	<i>h<sup>+</sup> Pnod1-mECitrine-nod1(329-419) ade6-M210 leu1-32</i> <i>ura4-D18</i>	Chapter 2
JW4909	<i>rho4Δ::kanMX6 leu1::GFP-rho4 gef2Δ::kanMX4 leu1-32</i> <i>ura4-D18 ade6</i>	Chapter 2
JW4910	<i>h<sup>-</sup> rho4Δ::kanMX6 leu1::GFP-rho4 nod1Δ::kanMX6 leu1-</i> <i>32 ura4-D18</i>	Chapter 2
JW4912	<i>Pgef2-mECitrine-4Gly-gef2 ade6 leu1-32 ura4-D18</i>	Chapter 2

Continued

---

**Table 2.2: Continued**

JW5027	<i>cdc15-140 nod1-mECitrine-kanMX6 gef2Δ::hphMX6 ade6 leu1-32 ura4-D18</i>	Chapter 2
JW5028	<i>cdc15-140 nod1-mECitrine-kanMX6 ade6-M210 leu1-32 ura4-D18</i>	Chapter 2
JW5065	<i>h<sup>+</sup> Pnod1-mECitrine-nod1(210-419) ade6-M210 leu1-32 ura4-D18</i>	Chapter 2
JW5093	<i>kanMX6-Pnod1-mECitrine-nod1 gef2-13Myc-hphMX6 ade6-M210 leu1-32 ura4-D18</i>	Chapter 2
JW5095	<i>kanMX6-Pnod1-mECitrine-nod1(329-419) gef2-13Myc-hphMX6 ade6-M210 leu1-32 ura4-D18</i>	Chapter 2
JW5107	<i>kanMX6-Pgef2-tdTomato-4Gly-gef2 kanMX6-Pnod1-mECitrine-nod1(329-419) ade6-M210 leu1-32 ura4-D18</i>	Chapter 2
JW5120	<i>nod1-13Myc-hphMX6 mYFP-cdc15 ade6 leu1-32 ura4-D18</i>	Chapter 2
JW5329	<i>h<sup>+</sup> gef2Δ::kanMX4 cdc15-140 GFP-bgs1-leu1<sup>+</sup> bgs1Δ::ura4<sup>+</sup> rlc1-tdTomato-natMX6 ade6 leu1-32 ura4-D18</i>	Chapter 2
JW5330	<i>nod1Δ::kanMX6 cdc15-140 GFP-bgs1-leu1<sup>+</sup> bgs1Δ::ura4<sup>+</sup> rlc1-tdTomato-natMX6 ade6-M210 leu1-32 ura4-D18</i>	Chapter 2
JW5357	<i>h<sup>-</sup> cdc15-140 GFP-bgs1-leu1<sup>+</sup> bgs1Δ::ura4<sup>+</sup> rlc1-tdTomato-natMX6 ade6-M210 leu1-32 ura4-D18</i>	Chapter 2
JW5360	<i>sid2-250 kanMX6-3nmt1-gef2 ade6 leu1-32 ura4-D18</i>	Chapter 2
JW5361	<i>sid2-250 kanMX6-41nmt1-gef2 ade6 leu1-32 ura4-D18</i>	Chapter 2

Continued

---

**Table 2.2: Continued**

JW5405	<i>sid2-1 kanMX6-3nmt1-gef2 ade6 leu1-32 ura4-D18</i>	Chapter 2
JW5406	<i>sid2-1 kanMX6-41nmt1-gef2 ade6 leu1-32 ura4-D18</i>	Chapter 2
JW5503	<i>rho4Δ::kanMX4 cdc7-24 ade6 leu1-32 ura4-D18 his7-366</i>	Chapter 2
JW5504	<i>rho4Δ::kanMX4 cdc11-136 ade6 leu1-32 ura4-D18</i>	Chapter 2
JW5505	<i>rho4Δ::kanMX4 sid2-250 ade6 leu1-32 ura4-D18</i>	Chapter 2
JW5580	<i>gef2Δ::kanMX4 sid2-GFP-ura4<sup>+</sup> ade6-M210 leu1-32 ura4-D18</i>	Chapter 2
JW5581	<i>nod1Δ::kanMX6 sid2-GFP-ura4<sup>+</sup> ade6-M210 leu1-32 ura4-D18</i>	Chapter 2
JW5582	<i>Pgef2-mECitrine-4Gly-gef2 Pmyo2-mCFP-myosin2 ade6 leu1-32 ura4-D18</i>	Chapter 2
JW5583	<i>cdc15-140 Pgef2- mECitrine-4Gly-gef2 Pmyo2-mCFP-myosin2 ade6 leu1-32 ura4-D18</i>	Chapter 2
IH1600	<i>h<sup>+</sup> plo1.ts18::ura4<sup>+</sup> ura4-D18 leu1-32 ade6-M210 his2</i>	MacIver <i>et al.</i> , 2003
JM578	<i>h<sup>+</sup> cdr2Δ::kanMX6 ade6 leu1-32 ura4-D18</i>	Moseley <i>et al.</i> , 2009
PPG1580	<i>h<sup>-</sup> rho4Δ::kanMX6 leu1::GFP-rho4 leu1-32 ura4-D18</i>	Santos <i>et al.</i> , 2003
TP7	<i>h<sup>-</sup> cdc4-8 his7-366 leu1-32 ura4-D18 ade6-M216</i>	Thomas Pollard
TP34	<i>h<sup>-</sup> cdc7-24 his7-366 leu1-32 ade6-M216 ura4-D18</i>	Thomas Pollard
TP47	<i>h<sup>-</sup> cdc11-136 ura4-D18 leu1-32 his7-366</i>	Bezanilla <i>et al.</i> , 1997
VS2367	<i>h<sup>+</sup> sid2-1 ade6-M210 leu1-32 ura4-D18</i>	Salimova <i>et al.</i> , 2000

Continued

---

**Table 2.2: Continued**

YDM26	<i>h<sup>-</sup> rng2-D5 ade6-210 ura4-D18 leu1-32</i>	Eng <i>et al.</i> , 1998
YDM415	<i>h<sup>-</sup> sid2-GFP-ura4<sup>+</sup> ade6-M210 leu1-32 ura4-D18</i>	Sparks <i>et al.</i> , 1999
YDM429	<i>h<sup>+</sup> sid2-250 ade6-M210 leu1-32 ura4-D18</i>	Sparks <i>et al.</i> , 1999

---

## **Chapter 3: Involvement of the UNC-13/Munc13 Protein Ync13 in Endocytosis during Fission Yeast Cytokinesis**

### **3.1 Abstract**

Cytokinesis is a complicated yet conserved step of the cell-division cycle that requires the coordination of multiple proteins and cellular processes. Here we describe a previously uncharacterized protein Ync13 and its roles during fission yeast cytokinesis. Ync13 is a member of the UNC-13/Munc13 protein family, whose animal homologs are essential priming factors for the SNARE complex assembly during exocytosis in various cell types. We find that Ync13 localizes to the plasma membrane at the division site during cytokinesis. The deletion of Ync13 leads to defective cell wall formation, high levels of cell lysis during cell separation, and uneven distribution of the cell wall enzymes along the division site. We further show that loss of Ync13 compromises both the TRAPP-II mediated exocytosis and the clathrin mediated endocytosis at the division site.

Collectively, we find that Ync13 has a novel function in coordinating the spatial distribution of membrane trafficking events and cell-wall integrity during fission yeast cytokinesis.

### **3.2 Introduction**

Cytokinesis is an essential step in the cell cycle that partitions a mother cell into two daughter cells. From yeast to mammalian cells, cytokinesis starts with the assembly of an

actomyosin contractile ring at the specified division site. The ring then constricts and guides the plasma membrane invagination and the extracellular matrix formation/remodeling (Pollard and Wu, 2010; Lee *et al.*, 2012; D'Avino *et al.*, 2015; Meitinger and Palani, 2016; Rincon and Paoletti, 2016). To ensure proper cell separation and integrity, cytokinesis requires the coordination of multiple pathways, including the contractile ring machinery, the Rho GTPase dependent cell integrity pathway, exocytosis, and endocytosis (Arellano *et al.*, 1999; Albertson *et al.*, 2005; Joo *et al.*, 2005; Sipiczki, 2007; Montagnac *et al.*, 2008; Wu *et al.*, 2010; Sanchez-Mir *et al.*, 2014; Simanis, 2015). However, the mechanisms and coordination of these events remain poorly understood.

Rho GTPases are small molecular switches that regulate multiple cellular processes including cytokinesis (Hall, 2012). Of the six Rho GTPases (Rho1-5 and Cdc42) in fission yeast, Rho1 and Rho2 play crucial roles in maintaining the cell integrity during cytokinesis (Arellano *et al.*, 1999; Calonge *et al.*, 2000; Garcia *et al.*, 2006; Perez and Rincon, 2010; Sanchez-Mir *et al.*, 2014). Activated mainly by Rho GEF Rgf3 and its adapter arrestin Art1, the GTP-bound Rho1 activates the  $\beta$ -glucan synthases Bgs1 and Bgs4, and triggers the Mitogen Activated Protein Kinase (MAPK) signaling pathway via the protein kinase C Pck1 and Pck2 (Arellano *et al.*, 1996; Arellano *et al.*, 1999; Tajadura *et al.*, 2004; Morrell-Falvey *et al.*, 2005; Mutoh *et al.*, 2005; Sanchez-Mir *et al.*, 2014; Davidson *et al.*, 2015; Ren *et al.*, 2015). Similarly, Rho2 GTPase functions in the cell integrity pathway and activates the  $\alpha$ -glucan synthase Ags1 for septum formation (Calonge *et al.*, 2000; Sanchez-Mir *et al.*, 2014). The transmembrane cell wall synthases Bgs1, Bgs4, and Ags1 are essential for septum formation during cytokinesis and

maintained at the proper levels on the plasma membrane via membrane trafficking (Ishiguro *et al.*, 1997; Katayama *et al.*, 1999; Liu *et al.*, 1999).

Membrane trafficking during cytokinesis relies on the balance between exocytosis and endocytosis to expand the plasma membrane and remodel the extracellular matrix at the division site. Exocytosis delivers and fuses secretory vesicles to the plasma membrane (Albertson *et al.*, 2005; Echard, 2008). Exocytosis starts with the budding of the secretory vesicles from trans-Golgi or late endosomes. Once vesicles are delivered to the target site, they are kept in proximity to the plasma membrane by the tethering complexes during the “docking” stage (Guo *et al.*, 1999b; Donovan and Bretscher, 2012; James and Martin, 2013). The SNARE proteins on the vesicles and the plasma membrane are converted to an open conformation during the “priming” stage by UNC-13/Munc13 and Munc18 proteins (Rizo and Sudhof, 2012; James and Martin, 2013; Rizo and Xu, 2015). Then tight SNARE complex assembles to bring the membrane layers close enough and provide the energy for membrane fusion (James and Martin, 2013; Feyder *et al.*, 2015; Martin, 2015). The blockage of vesicle secretion impairs cytokinesis from yeast to human cells (Skop *et al.*, 2001; Liu *et al.*, 2002; Gromley *et al.*, 2005; Giansanti *et al.*, 2015). It was thought that most vesicles dock at or within a narrow zone adjacent to the leading edge of the cleavage furrow via the exocyst, an octomeric tethering complex, during cytokinesis (TerBush *et al.*, 1996; Guo *et al.*, 1999b; Shuster and Burgess, 2002; Danilchik *et al.*, 2003; VerPlank and Li, 2005; He and Guo, 2009; Neto *et al.*, 2013). Surprisingly, we recently found that the exocytic vesicles are delivered all over the division plane in the fission yeast *S. pombe*, upon which the Transport Particle Protein II

(TRAPP-II) complex and the exocyst work together to tether the vesicles (Wang *et al.*, 2016).

Endocytosis is also essential for cytokinesis, and mutations in the endocytic pathway often lead to cytokinesis failure (McCollum *et al.*, 1996; Wienke *et al.*, 1999; Gerald *et al.*, 2001; Feng *et al.*, 2002; Schweitzer *et al.*, 2005; Baluska *et al.*, 2006; Wu *et al.*, 2006; Boucrot and Kirchhausen, 2007; Montagnac *et al.*, 2008; de Leon *et al.*, 2013). The clathrin mediated endocytosis (CME) is the best characterized and the main endocytic pathway, which occurs in a stepwise fashion (Berro *et al.*, 2010; Feyder *et al.*, 2015; Goode *et al.*, 2015; Lu *et al.*, 2016). The early (Ede1, F-BAR Syp1, AP-2, and clathrin), middle (Sla2, Epsins, and YAP1801), and late (Sla1, Pan1, End3, and WASP) coat complexes are recruited to the endocytic site sequentially; and they trigger the actin polymerization, membrane bending, and vesicle scission (Berro *et al.*, 2010; Weinberg and Drubin, 2012; Idrissi and Geli, 2014; Mishra *et al.*, 2014; Goode *et al.*, 2015; Lu *et al.*, 2016). The internalized vesicles are released from the clathrin coats and are sorted to vacuoles/lysosomes for degradation or recycled back to the plasma membrane with the help of Rab11 GTPase (Grant and Donaldson, 2009; Neto *et al.*, 2013; Feyder *et al.*, 2015; Goode *et al.*, 2015). In addition to the CME, the clathrin independent endocytosis (CIE) mediated by Rho GTPases has also been found in yeast and animal cells (Prosser *et al.*, 2011; Prosser and Wendland, 2012). The exact role of endocytosis during cytokinesis remains poorly understood. Nevertheless, the temporal and spatial balance between endocytosis and exocytosis is critical for proper cellular functions (Wu *et al.*, 2014). In budding yeast, the Sec4 Rab GTPase couples exocytosis with endocytosis to maintain the polarized Cdc42 GTPase for bud growth (Layton *et al.*, 2011; McCusker *et al.*, 2012;

Johansen *et al.*, 2016). During mating, the focused pheromone secretion and shmoo formation can be explained in a mathematical model with exocytosis corralled by endocytosis (Chou *et al.*, 2012). In neuronal cells, the inhibition of exocytosis abolishes endocytosis (Xie *et al.*, 2017). In fission yeast, the balanced membrane trafficking is vital for regulating the antibiotic tolerance and antibiotic sensitive sterol-rich domains on the plasma membrane (Nishimura *et al.*, 2014). We recently found that endocytosis happens preferentially at the rim of the division plane while the exocytic vesicles are deposited evenly along the cleavage furrow during fission yeast cytokinesis, raising the question how the temporal and spatial regulation of membrane trafficking affects cytokinesis (Wang *et al.*, 2016).

In Chapter 3, we explored the roles of Ync13, an uncharacterized protein from the UNC-13/Munc13 protein family, during cytokinesis in fission yeast. The UNC-13/Munc13 proteins are usually large proteins with a characteristic MUN domain and various C1 and C2 domains (Pei *et al.*, 2009; Li *et al.*, 2011). The MUN domain forms an elongated arch-shape  $\alpha$ -helix structure with a hydrophobic pocket in the middle and resembles some vesicle tethering factors such as the exocyst subunit Sec6 (Yang *et al.*, 2015; Xu *et al.*, 2017). It opens the closed conformation of the syntaxin-Munc18 complex and promotes the SNARE complex formation in a  $\text{Ca}^{2+}$ -dependent manner during the priming stage of fast neurotransmitter release (Guan *et al.*, 2008; Ma *et al.*, 2011; James and Martin, 2013; Rizo and Xu, 2015; Yang *et al.*, 2015). The C1 and C2 domains help tether the vesicles to the plasma membrane by interacting with lipids,  $\text{Ca}^{2+}$ , or other binding partners (Shen *et al.*, 2005; Lu *et al.*, 2006; Dimova *et al.*, 2009; Shin *et al.*, 2010; Herbst *et al.*, 2014; Liu *et al.*, 2016a; Xu *et al.*, 2017). The *C. elegans* UNC-13, the

founding member of the family, is recruited by RHO-1 to the presynaptic active zone and is crucial for the priming of both fast and slow transmitter release in neuronal cells (Maruyama *et al.*, 2001; Madison *et al.*, 2005; McMullan *et al.*, 2006; Hu *et al.*, 2013; Zhou *et al.*, 2013). Besides their vital roles in neuronal cells, the mammalian Munc13s also contribute to regulated exocytosis in other cell types (Brose *et al.*, 1995; Betz *et al.*, 1996; Ma *et al.*, 2011; James and Martin, 2013; Yang *et al.*, 2015). Munc13-1 mediates the priming for secretory amyloid precursor protein processing in brain and insulin secretion in pancreatic cells (Sheu *et al.*, 2003; Rossner *et al.*, 2004; Kwan *et al.*, 2007; Hartlage-Rubsamen *et al.*, 2013). Munc13-3 is expressed in the visual cortex for neuronal plasticity during the critical period in addition to its function in the cerebellum (Yang *et al.*, 2002; Yang *et al.*, 2007; Netrakanti *et al.*, 2015). Munc13-4, an effector of Rab27 GTPase, promotes the exocytosis of lytic granule in cytotoxic T cells and neutrophils, secretory lysosomes in hematopoietic cells, and dense granules in platelets (Brzezinska *et al.*, 2008; Chang *et al.*, 2011; Elstak *et al.*, 2011; Johnson *et al.*, 2011; Dudenhoffer-Pfeifer *et al.*, 2013; Chicka *et al.*, 2016). Recently, Munc13-4 has been found to affect late endosome maturation, and interact with Rab11 for recycling endosome delivery (He *et al.*, 2016; Johnson *et al.*, 2016). However, there was previously no evidence that the UNC-13/Munc13 family is involved in cytokinesis. The fungal members of the protein family are rarely studied. Intriguingly, the MUN domains in fungal UNC-13/Munc13 proteins are separated into two domains (MHD1 and MHD2) by a C2 domain (Pei *et al.*, 2009). *S. pombe* has two UNC-13/Munc13 homologs, Git1 and Ync13. Git1 is a critical component for glucose sensing in cAMP signaling pathway (Kao *et al.*, 2006). Despite

the sequence homology, Ync13 does not share the same function as Git1 (Kao *et al.*, 2006).

Here we find that Ync13 is an essential protein functioning during late stages of cytokinesis in fission yeast. Ync13 localizes to the growing plasma membrane including the division site. Surprisingly, purified Ync13 cannot promote vesicle clustering and fusion. The deletion of Ync13 causes massive cell lysis during cell division due to a defective septum. Ync13 plays overlapping roles with the exocyst and the TRAPP-II complex during cytokinesis. Ync13 is important for the endocytic site selection to ensure the normal localizations and dynamics of the cell wall enzymes and the cell integrity pathway regulators. Septin deletion and Rho1 overexpression can partially rescue the cell lysis and endocytic defects in *ync13* mutants. Collectively, our study reveals that a fungal UNC-13/Munc13 protein plays essential and novel roles in cytokinesis.

### **3.3 Materials and methods**

#### **3.3.1 Strains, genetic, molecular, and cellular methods**

Strains used in Chapter 3 are listed in Table 3.2. We constructed strains using PCR-based gene targeting and standard yeast genetic methods (Moreno *et al.*, 1991; Bahler *et al.*, 1998). All tagged or truncated Ync13 are expressed from the native chromosomal loci and regulated under endogenous promoters. The strains with Ync13 truncations were grown and selected on medium with 1.2 M sorbitol. Ync13 C-terminal truncations were constructed as previously described (Bahler *et al.*, 1998). For N-terminal truncations, we cloned -305 to +6 bp of *ync13* into pFA6a-kanMX6-P3nmt1-mECitrine at *Bgl*III and *Pac*I sites to replace the *3nmt1* promoter. The resulting plasmid (JQW745) was used as the template for PCR amplification and gene targeting. To delete the C2 domain, a DNA

fragment encoding *ync13(aa922-1237)-tdTomato-natMX6* was amplified from strain JW5722 (*ync13-tdTomato-natMX6*) and cloned into a TOPO vector (Invitrogen). The resulting plasmid (JQW806) was then used as a template for gene targeting and the PCR product was transformed into strain JW5896 (*ync13[aa1-804]-mECitrine-kanMX6*) to replace *mECitrine-kanMX6*. We performed PCR to verify the insertions in the *nat<sup>R</sup> kan<sup>S</sup>* colonies. The C terminal tagged full length Ync13 was fully functional, revealed by growth tests on YE5S + Phloxin B (PB) plates at various temperatures.

To delete *ync13*, a diploid strain *rlc1-tdTomato-natMX6/rlc1-tdTomato-natMX6 ade6-210/ade6-216 leu1-32/leu1-32 ura4-18/ura4-18* was made by *ade6* intragenic complementation (Kohli *et al.*, 1977; Moreno *et al.*, 1991). One copy of *ync13* was then replaced by *kanMX6* using JQW1 as PCR template and primers immediate upstream and downstream of *ync13* ORF (Bahler *et al.*, 1998). The resulting diploid strain *ync13Δ::kanMX6/ync13<sup>+</sup> rlc1-tdTomato-natMX6/rlc1-tdTomato-natMX6 ade6-210/ade6-216 leu1-32/leu1-32 ura4-18/ura4-18* was sporulated on SPA5S plate, and the tetrads were dissected onto YE5S rich medium or YE5S + 1.2 M sorbitol for spore germination or microscopy. The colonies grown on sorbitol medium were replica plated to the selection medium YE5S + G418 + 1.2 M sorbitol to verify the *ync13Δ* genotype. For crosses involving *ync13Δ* strains, the parent strains were mixed on SPA5S + 1.2 M sorbitol, and the formed tetrads were dissected and germinated on YE5S + 1.2 M sorbitol.

To construct *ync13* temperature sensitive alleles, we used marker reconstitution mutagenesis method (Tang *et al.*, 2011; Lee *et al.*, 2014). A *his5<sup>ΔC</sup>-kanMX6* construct was inserted after the 3'UTR of *ync13* to obtain strain JW5750. The *ync13* full length gene with its 3'UTR was cloned onto pHis5<sup>C</sup>, which was then served as the template for

error-prone PCR using Taq Polymerase (NEB), 0.2 mM dNTPs, and mutagenesis cocktail (8 mM dTTP, 8 mM dCTP, 48 mM MgCl<sub>2</sub>, and 5 mM MnCl<sub>2</sub>). The PCR products were purified and transformed into JW5750. The transformants were selected on EMM5S – histidine plate, and then examined for temperature sensitive growth (on YE5S + phloxin B) and phenotype at 36°C. The selected mutants were sequenced. The mutations in *ync13-4* are E365G, I373T, K581E, M593L, L744S, I1013T, I1031V, and V1081E, and an “A” deletion 99 bp downstream of the stop codon; the mutations in *ync13-19* are L916H and W1048C.

For Calcofluor staining, 1 ml cell culture was washed with 1 ml EMM5S and 1 ml EMM5S + 5 μM n-propyl-gallate, and concentrated to 100 μl. 1 μl of 1 mg/ml calcofluor stock solution was added, and the samples were incubated in dark for 1 min before imaging. For MBC treatment, 1 ml cells were incubated with 5 μl 5 mg/ml MBC or DMSO for 15 min before mounted on the gelatin with same concentration of MBC or DMSO for imaging. For other drug treatment, cells were mounted on bare slide for imaging. Conditions: LatA, 100 μM; BFA, 50 μg/ml for 5 min; CK666, 100 μM for 5 min. Corresponding drug solvent DMSO or ethanol were used for controls.

### **3.3.2 Confocal microscopy and image analysis**

We grew cells from -80°C stock on YE5S plates at 25°C for about two days, and then cultured them in YE5S liquid medium at log phase for ~48 h at 25°C before imaging except where noted. For strains with *ync13Δ* and *ync13* truncations, 1.2 M sorbitol was included in the growth medium and was washed out 2 h before imaging except where

noted. Alternatively, some *ync13Δ* strains were grown in EMM5S medium without sorbitol for 48 h before imaging.

Microscopy samples were prepared as described (Zhu *et al.*, 2013; Davidson *et al.*, 2016). Briefly, 1 ml cells were centrifuged at 3,000 to 5,000 rpm for 30 s, and washed once with 1 ml EMM5S and once with 1 ml EMM5S + 5  $\mu$ M n-propyl-gallate before mounted on an EMM5S + 20% gelatin pad with 5  $\mu$ M n-propyl-gallate. For long movies, cells were washed and resuspended in 50  $\mu$ l YE5S + 5  $\mu$ M n-propyl-gallate before spotted onto a coverglass-bottom dish (Delta TPG Dish; Biotechs Inc., Butler, PA). Then an agar pad cut from a YE5S plate was placed onto cells to immobilize the cells and provide nutrients. For Tetrad Fluorescence Microscopy (Coffman *et al.*, 2013; Lee *et al.*, 2014), spores from tetrads were dissected onto a YE5S plate at 2.5 mm apart and were incubated at 25°C for 12 to 18 h. The YE5S agar containing cells from germinated spores was then incised from the plate, and placed upside down onto a coverglass-bottom dish or a 24 x 60 mm coverglass. The agar was then covered by a piece of coverslip to slow drying. Air bubbles were removed by gently pressing on the coverslip before microscopy.

Cells were imaged at 23°C or at restrictive temperatures in a climate chamber (Stage Top Incubator INUB-PPZI2-F1 equipped with UNIV2-D35 dish holder, Tokai Hit, Shizuoka-ken, Japan) with 100x/1.4 numerical aperture (NA) Plan-Apo objectives. For observing cell morphology only, samples were imaged on a Nikon Eclipse Ti inverted microscope (Nikon, Melville, NY) equipped with a Nikon cooled digital camera DS-Q11. For fluorescence imaging, cells were observed on a spinning disk confocal microscope (UltraVIEW ERS, Perkin Elmer Life and Analytical Sciences, Waltham, MA) with 440, 568-nm solid state lasers and 488, 514-nm argon ion lasers and an ORCA-AG camera

(Hamamatsu, Bridgewater, NJ) with  $2 \times 2$  binning, or on a spinning disk confocal microscope (UltraVIEW Vox CSUX1 system, Perkin Elmer Life and Analytical Sciences, Waltham, MA) with 440-, 488-, 515-, and 561-nm solid state lasers and a back-thinned EMCCD camera (Hamamatsu C9100-13, Bridgewater, NJ) without binning.

Images and data were collected and analyzed using Volocity (Perkin Elmer), UltraVIEW, and ImageJ software. For measuring the levels of the cell wall synthases across the division plane, the cells with mature septa were chosen and rotated so that the septa were horizontal. An  $85 \times 20$  pixel box was drawn to cover the whole septum area, and the plot profile of the box was recorded. For Figure 3.11 B, a 2x ROI of the previous ROI (elongated along the cell's long axis) was used for calculating and subtracting background (Wu and Pollard, 2005; Zhu *et al.*, 2013; Coffman and Wu, 2014). We tracked vesicles similarly as before (Wang *et al.*, 2016). The Syb1 or Ypt3 labeled exocytic vesicle delivery and Fim1 labeled endocytic patch initiation sites were tracked manually using ImageJ plugin mTrackJ. The locations of endocytic patch initiation sites were recorded after they reached maximum intensity and started to move. The coordinates of data were then transformed by Matlab software so that the septa were horizontal. The cell width was normalized to  $4 \mu\text{m}$  before plotting.

To count protein molecules of Ync13 and its truncations, strains tagged with mECitrine were mixed with wt cells without fluorescence before imaging (Davidson *et al.*, 2016). Cells were imaged at  $0.5 \mu\text{m}$  spacing for 13 slices. The global mean intensity from the sum projection was measured and subtracted by that of wt cells as background. For local intensity, an ROI was drawn to measure the mean intensity at the division site. A 2x ROI same as Figure 3.11 B was used for calculating and subtracting the background

(Wu and Pollard, 2005; Zhu *et al.*, 2013; Coffman and Wu, 2014). To obtain molecule numbers, the mean intensities of Ync13 and truncations were plotted on the standard curve generated with proteins with known molecule numbers (Gef2, Nod1, Rng8, and Rng9) (Zhu *et al.*, 2013; Wang *et al.*, 2014).

The error bars in figures are 1 SDs. The statistical analyses were done using two-tailed student's *t* test.

### **3.3.3 Photobleaching, FRAP, and FLIP analysis**

To monitor the vesicle delivery, we bleached Syb1 signals at the division site before taking a 2-minute continuous movie with a speed of 5 frame per second (fps) on a single focal plane as described previously (Wang *et al.*, 2016). We performed the FRAP assays using the Photokinesis unit on UltraVIEW Vox confocal system as described (Coffman *et al.*, 2009; Laporte *et al.*, 2011; Zhu *et al.*, 2013). Briefly, a single focal plane was chosen to perform FRAP. Selected ROIs were bleached to <50% of the original fluorescence intensity after 4-5 pre-bleach images were collected. 100 post-bleach images with 1 s delay were collected. After correcting images for background and photobleaching during image acquisition at non-bleached sites, we normalized pre-bleach intensity of the ROI to 100%, the intensity just after bleaching to 0%. Rolling average of every three consecutive post-bleaching time points was used to plot and fit using an exponential equation  $y = m_1 + m_2 \exp(-m_3x)$ , where  $m_3$  is the off-rate (KaleidaGraph; Synergy Software, PA). The half-time of recovery was calculated as  $\tau_{1/2} = (\ln 2)/m_3$ .

The FLIP experiments were performed on Photokinesis units of UltraVIEW Vox CSUX1 system (Davidson *et al.*, 2016; Liu *et al.*, 2016b). Briefly, we selected cells

bearing mEGFP and Rlc1-tdTomato at the final stage of ring constriction for FLIP. A 2 x 2 pixel ROI was photobleached in one of the daughter cells using the 488 nm laser every 30 s. Recovery images were taken immediately before the next round of photobleaching. Ring closure was defined as when Rlc1 reached highest pixel intensity as a dot at the middle of the cleavage furrow; and plasma membrane closure was defined as when the cytoplasmic mEGFP stopped exchange in the two daughter cells. The time between the ring closure and the membrane closure was quantified.

### **3.3.4 Superresolution microscopy**

The superresolution microscopy was performed on an inverted microscopy (IX71; Olympus, Tokyo, Japan) with a 100×/1.49 NA oil immersion total internal reflection fluorescence objective and an EMCCD camera (iXon Ultra 897; Andor Technologies, Belfast, United Kingdom) with the EM gain of 255 and the exposure time of 0.02 s (Liu *et al.*, 2016b). We used 405 and 488-nm diode lasers (Vortran Laser Technology, Sacramento, CA) and a 561-nm diode-pumped solid-state laser (CrystaLaser, Reno, NV) for photoactivation and imaging. Sample preparation was the same as previously described (Liu *et al.*, 2016b). After we selected an ROI by GFP channel, Ync13-mMaple3 was photoactivated by the 405-nm laser with increasing power for optimization of the fluorophore activation efficiency, and images were taken using the 561-nm laser with a 593/40 nm filter. DIC images were taken to monitor focus drift. We took 4500–8000 images for each field. Superresolution images were reconstructed using Mempo-STORM (Huang *et al.*, 2015).

### **3.3.5 Electron microscopy**

The electron microscopy was performed at Campus Microscopy and Imaging facility at The Ohio State University or the Boulder Electron Microscopy Services at University of Colorado (Davidson *et al.*, 2015; Liu *et al.*, 2016b; Wang *et al.*, 2016). For Figure 3.5 G, we grew wt and *ync13Δ* cells in YE5S with 1.2M sorbitol at log phase for 48 h. Cells were washed into YE5S 2 h before fixation with 2.5% glutaraldehyde and 0.1 M sucrose in 0.1 M sodium phosphate, pH 7.4. The samples were then submitted to the imaging facility at OSU for further processing and imaging. For Fig 3.10 A, wt (strain JW81), *sec8-1*, and *ync13Δ* cells were grown in EMM5S at log phase for 48 h. Cells were then prepared and imaged (Giddings *et al.*, 2001; Lee *et al.*, 2014).

### **3.3.6 Plasmid construction and protein purification**

The Ync13 cDNA sequence or corresponding fragments amplified from a cDNA library were cloned into the pQE80L plasmid with *Bam*HI and *Sal*I restriction sites. The plasmids were then transformed into BL21 (DE3)pLysS cells. The protein expression was induced with 1 mM IPTG at 25°C for 6 h.

To purify full-length Ync13, frozen cells from every liter cell culture was homogenized in 50 ml Tris extraction buffer (20 mM Tris, 150 mM NaCl, 10% glycerol, 0.5% NP-40, 10 mM imidazole, 1 mM PMSF, 10 mM β-ME, and protease inhibitor tablet (Roche), pH 9), and sonicated for four times at output 9, 50% duty cycle, and 20 pulses. The cell lysate was then centrifuged at 25,000 rpm for 15 min and 38,000 rpm for 30 min, before incubated with Talon Metal Affinity Resin (635501; Clontech, Mountain View, CA) at 4°C for 1 h. The mixture was then packed in a column and washed with 50 ml washing buffer (20 mM Tris, 150 mM NaCl, 10% glycerol, 0.5% NP-40, 20 mM imidazole, 1 mM PMSF and 10 mM β-ME, pH 9) per liter cell culture, and eluted with

elution buffer (20 mM Tris, 150 mM NaCl, 10% glycerol, 0.1% NP-40, 200 mM imidazole, 1 mM PMSF, and 10 mM  $\beta$ -ME, pH 9). The obtained sample was dialyzed against HEPES (25 mM HEPES, 150 mM NaCl or KCl, 10% glycerol, pH 7.4) or TBS buffer (20 mM Tris-HCl, 150 mM NaCl, pH 7.5) for future experiments and imidazole removal.

The purification of Ync13 MHD1C2MHD2 (aa590-1130) and C2 (aa805-921) fragments were similar to described before (Zhu *et al.*, 2013). The phosphate buffer (50 mM sodium phosphate, 300 mM NaCl, 1 mM PMSF, 10 mM  $\beta$ -ME, and protease inhibitor (Roche), pH 8) with various concentration of imidazole (10 mM for extraction, 20 mM for washing, and 200 mM for elution) was used for purification. After purification, the C2 domain fragment was dialyzed in low salt buffer (50 mM sodium phosphate, 25 mM NaCl, 1 mM DTT, and 0.01% NaN<sub>3</sub>, pH 6.4) and further purified through MonoS 5/50 GL cation exchange column on AKTA Explorer 10 system (GE Healthcare). MHD1C2MHD2 domain was dialyzed in low salt buffer (50 mM sodium phosphate, 100 mM NaCl, 1 mM DTT, and 0.01% NaN<sub>3</sub>, pH 7.5) and loaded onto a MonoQ 5/50 GL anion exchange column on the same AKTA system. Both Ync13 fragments were then dialyzed against the TBS or HEPES buffer for experiments.

### **3.3.7 Protein-lipid overlay assays**

The protein-lipid overlay assay was performed as described previously (Lee and Wu, 2012). Briefly, the PIP membrane strips (Invitrogen, cat. no. P23751) were first blocked by TBS (20 mM Tris-HCl, 150 mM NaCl, pH 7.5) with 3% fatty-acid-free BSA (Sigma, cat. no. A7030) at 23°C for one hour with shaking. The purified proteins were added to the strips with a final concentration of 50 nM at 23°C for one hour or at 4°C overnight.

The strips were then washed with TBST (20 mM Tris-HCl, 150 mM NaCl, 0.1% Tween 20, pH 7.5) to remove the unbound protein. Lipid bindings were examined by immunoblot with anti-His antibody (Clontech, cat. no. 631212; 1:20,000 dilution) as primary antibody, and anti-mouse IgG as secondary antibody (1:5000 dilution) in TBS + 3% fatty-acid-free BSA.

### **3.3.8 Liposome cofloatation, clustering, and copelleting assays**

Lipids from Avanti Lipids (Alabaster, Alabama) were used to make liposomes of single lipids, or to make T liposomes by mixing POPC 38%, DOPS 18%, POPE 20%, PIP<sub>2</sub> 2%, DAG 2%, cholesterol 20% (Liu *et al.*, 2016a). Rhodamine-PE was used to visualize the lipids. We dried the lipids in glass tubes by nitrogen gas and vacuum, and resuspended the lipids in the HEPES buffer (25 mM HEPES, 150 mM NaCl or KCl, 10% glycerol, pH 7.4) to make a final lipid concentration of 5 mM. The suspension was then frozen/thawed in liquid nitrogen and 42°C water bath five times, and extruded 19 times through a 0.1 µm filter. All protein samples were dialyzed into the HEPES buffer before experiments.

For cofloatation assays, 1 mM T liposomes and 1 µM final concentration of Munc13-1 C1C2BMUNC2C, Ync13 C2, or Ync13 MHD1C2MHD2 were mixed in HEPES buffer to a total volume of 165 µl, and incubated at 23°C for 1 h. The samples were then mixed with an equal volume of 80% histodenz and added to the ultracentrifuge tube. A layer of 150 µl 35% and 150 µl 30% histodenz were then carefully loaded to the top of the samples to form a histodenz gradient (30%:35%:40%). 50 µl HEPES buffer was then added to the top of the ultracentrifuge tubes and centrifuged at 48,000 rpm for 4 h at 4°C. The floating liposome samples were taken from the top of the gradient after

ultracentrifuge, and used to run SDS-PAGE gel with 1 µg of protein samples as reference.

For clustering assays, 1 µl of T liposomes or T liposomes mixed with 0.5 µM of Ync13 C2 or MHD1C2MHD2 fragments were loaded to a DynaPro instrument to measure dynamic light scattering (DLS) at 30°C (Liu *et al.*, 2016a).

For copelleting assays, 5 µM of Ync13 C2 fragment was mixed and incubated with a range of concentrations of PS, PIP<sub>2</sub>, or PC 80%/PE 20% liposomes to a total volume of 100 µl at 23°C for 1 h before centrifugation at 90,000 rpm for 30 min or 1 h at 4°C (Sun *et al.*, 2015). For PS and PIP<sub>2</sub>, supernatants (S) were carefully removed, and the pellets (P) were resuspended with the HEPES buffer with the same reaction volume. For PC/PE, the sample below the floating lipid layer was taken as soluble fraction (S), and the lipid (L) layer was resuspended. Samples from lipid and non-lipid fractions were run on SDS-PAGE gel and compared with the total input protein. The intensities of the C2 protein in the supernatant (S) samples were used to calculate the bound C2 and generate curves for determining the  $K_d$ .  $y = m1x/(x+m2)$ , where  $m2$  is  $K_d$ .

### **3.3.9 Simultaneous lipid mixing and content mixing assays**

The assays were performed similarly as previously described (Liu *et al.*, 2016a). Lipid mixture for T and V liposomes was resuspended in the HEPES buffer by vortex and sonication. Purified syntaxin and SNAP25 proteins were added to the T liposomes, and synaptobrevin was mixed with the V liposomes in the presence of 1% β-OG to make T and V proteoliposomes. The detergent was then removed by dialysis in the HEPES buffer, and the proteoliposomes were purified by lipid floatation using a histodenz gradient (0%:25%:35%).

For lipid mixing and content mixing assays, 100  $\mu$ l 0.25 mM T proteoliposomes were mixed with 100  $\mu$ l 0.125 mM V proteoliposomes, and Munc18-1,  $\alpha$ -SNAP, and NSF were added unless indicated elsewhere. Munc13-1 C1C2BMUNC2C, Ync13 C2, or Ync13 MHD1C2MHD2 were added to examine their ability to promote lipid mixing and content mixing. The experiments were performed at 30°C, and 0.5 mM final concentration of CaCl<sub>2</sub> were added 5 min after the experiment starts. We measured lipid mixing by the dequenching of Marina Blue labeled V liposomes at excitation 370 nm and emission 465 nm, and content mixing by the FRET between the PhycoE-Biotin wrapped in T liposomes and Cy5-Streptavidin wrapped in V liposomes at excitation 565 nm and emission 670 nm. 1% w/v  $\beta$ -OG was added to solubilize all liposomes and obtain the maximum lipid mixing signal as reference.

### **3.4 Results**

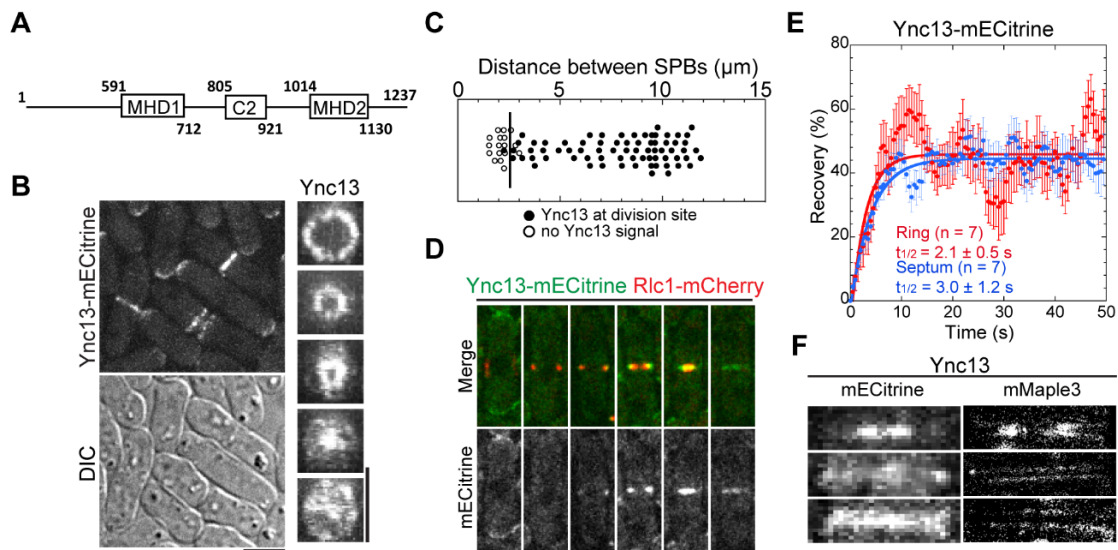
#### **3.4.1 Ync13 localizes to the division site during cytokinesis**

We identified Ync13 (yeast UNC-13/Munc13; SPAC11E03.02c) from existing genome-wide localization and deletion phenotype studies (Matsuyama *et al.*, 2006; Hayles *et al.*, 2013). Most members of the UNC-13/Munc13 family in animals contain several C2 domains and a characteristic MUN domain (Pei *et al.*, 2009) (Figure 3.2 A). As a fungi member, Ync13 has only one C2 domain, which separates the MUN domain into two Munc13 homology domains MHD1 and MHD2 (Figure 3.1 A).

We first examined the cellular localization of Ync13 expressed at the endogenous level. Ync13-mECitrine localized to the cell tips during interphase, and to the cell-division site at early anaphase B, when the spindle pole bodies were  $\sim$ 2.6  $\mu$ m apart (Figure 3.1, B and C). Ync13 partially colocalized with the myosin-II light chain Rlc1

labeled contractile ring and followed the ring constriction before distributing along the division plane (Figure 3.1, B and D). Ync13 was highly dynamic at the division site as it recovered with a halftime of  $2.1 \pm 0.5$  s and  $3.0 \pm 1.2$  s at the contractile ring and mature septum, respectively, in fluorescence recovery after photobleaching (FRAP) assays (Figure 3.1 E).

**Figure 3.1 Ync13 localizes to the division site.**



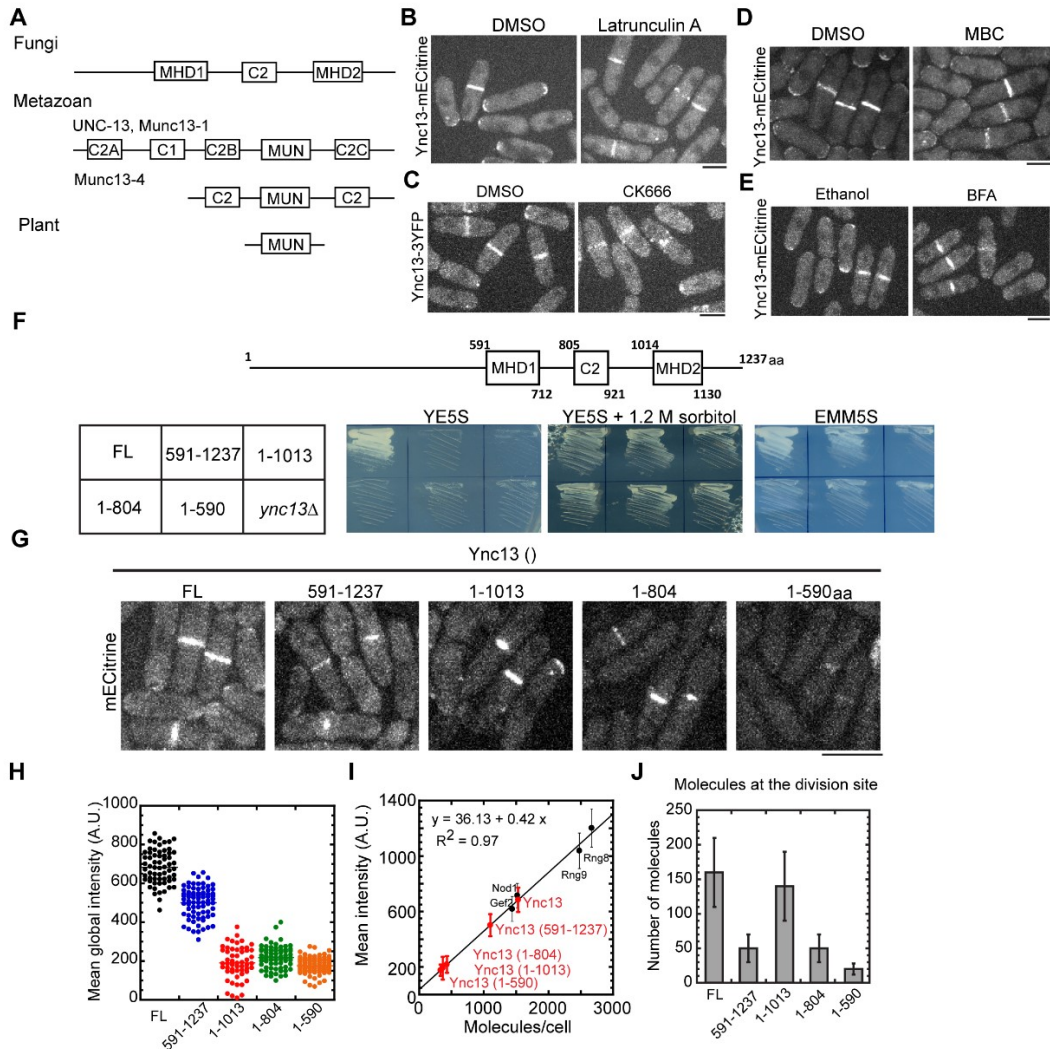
(A) The schematics of Ync13. (B) Localization of Ync13. Left, mECitrine and differential interference contrast (DIC) images of Ync13-mECitrine. Right, vertical views of division-site localization of Ync13 at different stages of cytokinesis. (C) Timing of Ync13 appearance at the division site (marked by the vertical line) relative to the distance between two spindle pole bodies (SPBs). (D) Micrographs of Ync13 (green) localization relative to the contractile ring (red) during cytokinesis. (E) Dynamics of Ync13-mECitrine at the contractile ring (red) and septum (blue) in FRAP assays. (F) Comparison of Ync13 localization in confocal microscopy (left) and super-resolution PALM (right) at the division site during ring constriction (top) and complete septum stages (middle and bottom panels). Bars, 5  $\mu\text{m}$ .

To dissect Ync13 localization with higher spatial resolution, we tagged it with mMaple3 for the photoactivated localization microscopy (PALM). Ync13-mMaple3 localized all over the cleavage furrow with a higher concentration at the leading edge during ring constriction and displayed a double layer structures after furrow ingression (Figure 3.1 F). These data suggested that Ync13 localized to the plasma membrane and concentrated at the leading edge of the cleavage furrow during cytokinesis.

### **3.4.2 Ync13 depends on the contractile ring for localization and interacts with the membrane lipids**

To figure out how Ync13 localized to the division site, we examined its localization in various mutants or under drug treatments. Ync13 did not require actin filaments, microtubules, or membrane trafficking for localization (Figure 3.2, B-E). However, it failed to localize to the division site in *cdc15-140* mutant at the restrictive temperature (Figure 3.3 A), where cells fail to maintain an intact contractile ring (Wachtler *et al.*, 2006; Arasada and Pollard, 2014). Cdc15 binds to the plasma membrane using its F-BAR domain and is one of the key components that bridge the contractile ring and the membrane and organize a sterol-rich membrane domain (Takeda *et al.*, 2004; McDonald *et al.*, 2015; Ren *et al.*, 2015). Moreover, Ync13 localization to the plasma membrane was greatly reduced in the PI4P-5-kinase *its3* mutant *its3-1* (Zhang *et al.*, 2000; Deng *et al.*, 2005), suggesting that Ync13 interacts with lipids for its division site localization (Figure 3.3 B, arrow).

**Figure 3.2 Localization dependence and domain analyses of Ync13.**



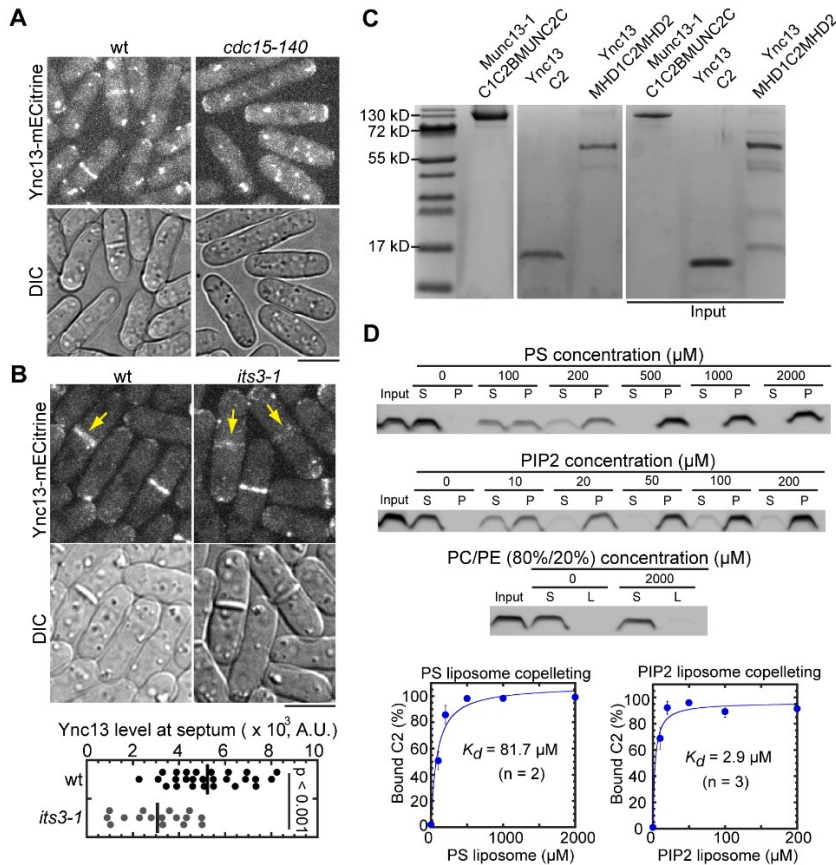
(A) Comparisons of domain organizations of UNC-13/Munc13 family proteins. (B-E) Ync13 localization is independent of actin, microtubule, or membrane trafficking. Cells were treated with Latrunculin A (B), Arp2/3 complex inhibitor CK666 (C), MBC (D), or BFA (E) before imaging. (F) Schematics of Ync13 and growth test of strains expressing Ync13 truncations. Ync13 truncations constructed are lethal on YE5S, but viable on EMM5S medium. Growth test of Ync13 strains on YE5S for 2 d or EMM5S for 3 d at 25°C. (G) Localization of Ync13 truncations. (H and I) Global mean intensity of Ync13 full length (FL) or truncations were quantified (H) and compared to proteins with known molecule numbers (I). (J) Local molecule numbers of Ync13 and truncations at the division site obtained using the standard curve in (I). Bars, 5  $\mu$ m.

We used truncation analysis to dissect Ync13 domains for localization (Figure 3.2, F-J). Unexpectedly, cells with any of the four truncations we made were inviable on rich medium YE5S, but viable on minimal medium EMM5S (Figure 3.2 F). Interestingly, Ync13 with the truncated C terminal (Ync13[1-1013], [1-804], and [1-590]) or N terminal (Ync13[591-1237]) still localized to the division site, although with varied intensity (Figure 3.2, G-I). Moreover, after the ring constriction, the truncated Ync13 was more concentrated at the center of the division plane compared to the full length Ync13 (Figure 3.2 G). The MHD2 domain (and aa 1131-1237) was critical for Ync13 stability or expression level as all C terminal truncations led to significant reduction in Ync13 global level (Figure 3.2, H and I). The C2 domain was important for Ync13 localization as we found only ~50 Ync13(1-804) molecules at the division site compared to ~140 Ync13[1-1013] (Figure 3.2 J) although their global levels were similar (Figure 3.2 H). While truncating the N terminus of Ync13 did not strongly affect its global level (Figure 3.2, H and I), there were only ~50 Ync13(591-1237) molecules at the division site (Figure 3.2 J). Thus, the MHD2 domain contributes to Ync13 stability or expression level, while the C2 domain and the N terminal 1-590 aa are important for Ync13 localization to the division site.

The C2 domains in UNC-13/Munc13 proteins interact with lipids or protein partners (Lu *et al.*, 2006; Shin *et al.*, 2010). Consistently, purified Ync13 C2 and MHD1C2MHD2 (Figure 3.4 A) interacted with lipids. In lipid cofloatation assays, both fragments cofloated with T-liposome after density gradient centrifugations (Figure 3.3 C). Specifically, Ync13 interacted with PS and PIP<sub>2</sub> ( $K_d$  of 82  $\mu$ M and 3  $\mu$ M, respectively) but not with PC and PE in the liposome copelleting and protein-lipid

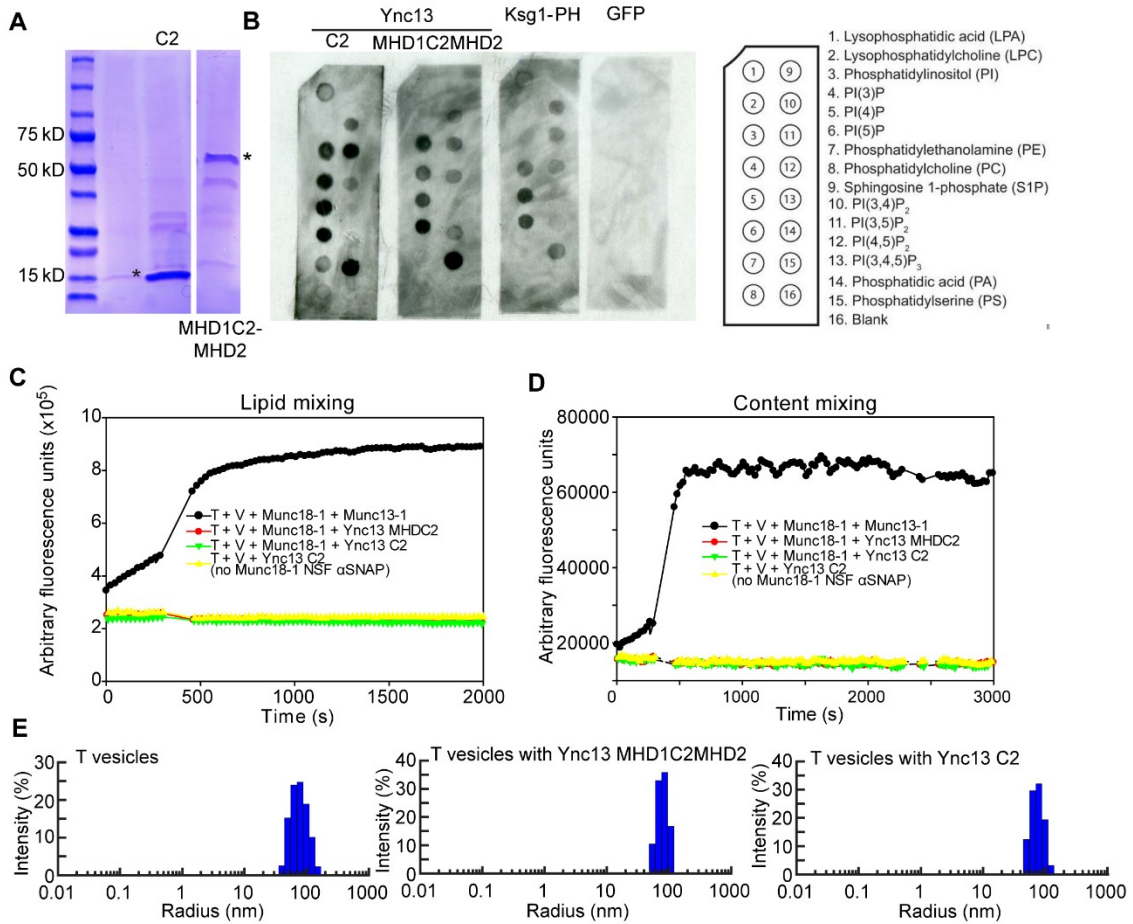
overlay assays (Figures, 3.3 D and 3.4 B). Thus, the C2 domain may contribute to Ync13 localization by its interaction with the plasma membrane.

**Figure 3.3 Ync13 depends on the contractile ring for localization and interacts with the membrane lipids.**



(A and B) Localization of Ync13 depends on Cdc15 (A) and Its3 (B). Cells were grown and imaged at 25°C (B) or grown 2 h at 36°C and imaged at 36°C (A). Yellow arrows in B mark Ync13 localization in cells with complete septa, which is quantified. Bars, 5  $\mu\text{m}$ . (C) Ync13 C2 and MHD1C2MHD2 domains co-float with T-liposomes. Lipid bound fraction after ultracentrifugation and 1  $\mu\text{g}$  of each input protein were loaded. Munc13-1 is a positive control. (D) Ync13 C2 domain interacts with various concentrations of PS and PIP<sub>2</sub> but not PC/PE in liposome copelleting assays (See 3.3.8). The  $K_d$  of C2 domain to PIP<sub>2</sub> and PS liposomes is shown.

**Figure 3.4 Ync13 interacts with lipids but does not promote vesicle fusion.**



(A) Coomassie blue staining of purified 6His tagged Ync13 C2 domain and MHD1C2MHD2 domain. (B) Protein-lipid overlay assays for purified 6His-Ync13(C2) and 6His-Ync13(MHD1C2MHD2). 6His-Ksg1(PH) is positive control and 6His-GFP is negative control. Lipids on the membrane are listed on the right. (C and D) Lipid mixing (C) and content mixing (D) assays with Ync13 domains. T liposomes (T) and V liposomes (V) were incubated with indicated proteins. (E) Ync13 C2 and MHD1C2MHD2 domains do not cluster membrane in dynamic light scattering assays.

### 3.4.3 Ync13 MHD and C2 domains do not promote lipid mixing or lipid clustering

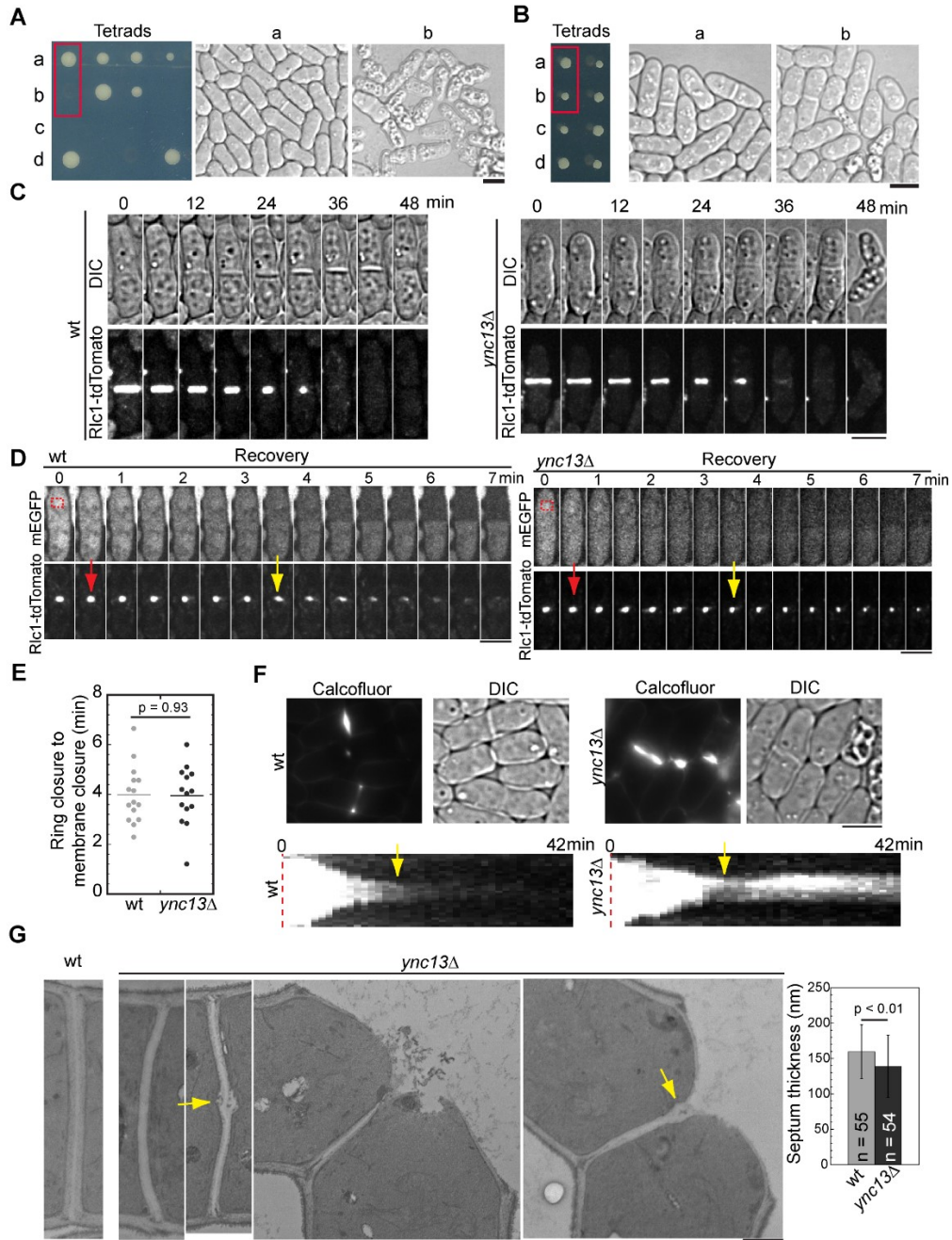
The major function of the UNC-13/Munc13 proteins is to help the SNARE complex assembly and promote vesicle fusion (Rizo and Xu, 2015; Yang *et al.*, 2015; Liu *et al.*, 2016a; Xu *et al.*, 2017). We thus tested if Ync13 promotes lipid and content mixing. The

positive control, the C1C2BMUNC2C domains of Munc13-1, promoted both lipid and content mixing between the T- and V-proteoliposomes upon calcium stimulation (Figure 3.4, C and D). In contrast, neither C2 nor MHD1C2MHD2 of Ync13 did, even without the SNARE disassembly factors NSF and  $\alpha$ -SNAP, and SM protein Munc18-1. We next tested if Ync13 tethered the liposomes. Although both Ync13 C2 and MHD1C2MHD2 domains interacted with T-liposomes (Figure 3.3 C), neither of them promoted liposome clustering to increase the particle size in dynamic light scattering (DLS) assays (Figure 3.4 E), which differs from Munc13-1 C1C2BMUNC2C (Liu *et al.*, 2016a). Thus, Ync13 MHD and C2 domains do not facilitate SNARE complex assembly or tether vesicles in vitro.

#### **3.4.4 Ync13 is essential for the cell integrity**

To explore Ync13 function, we examined the *ync13* $\Delta$  phenotype. *ync13* is an essential gene (Hayles *et al.*, 2013), so we deleted one copy of *ync13* gene from a diploid strain. Germinating spores on YE5S medium confirmed that *ync13* is indeed essential for cell survival (Figure 3.5 A, left). *ync13* $\Delta$  cells could grow and divide for  $\sim 7$  cell cycles ( $n = 37$ ) before most, if not all, cells lysed (Figure 3.5 A). Interestingly, sorbitol rescued *ync13* $\Delta$  cells for growth and the colony formation with drastically reduced cell lysis (Figure 3.5 B). Moreover, *ync13* $\Delta$  cells were also viable on EMM5S medium with  $\sim 33\%$  cell lysis ( $n > 500$  cells; Figure 3.2 F). Despite cell lysis, the morphology (including cell shape, length, and width) of *ync13* $\Delta$  cells was similar to wt cells in both rich and minimal medium. Thus, we cultured *ync13* $\Delta$  cells using YE5S medium with sorbitol or EMM5S for the rest of the experiments and microscopy.

**Figure 3.5** *ync13Δ* is lethal due to cell lysis.



(A and B) Tetrad analyses of *ync13Δ/ync13<sup>+</sup>* diploid cells, which were sporulated and dissected to spots a, b, c, and d on YE5S medium (A) or YE5S + 1.2 M sorbitol (B). DIC images of wt (a) and *ync13Δ* (b) cells from the boxed region are shown on the right. (C) *ync13Δ* cells lyse during cell separation. Time courses of wt (left) and *ync13Δ* (right) cells labeled with Rlc1-tdTomato during cytokinesis. Cells were kept in log phase in YE5S + 1.2 M sorbitol, and washed into YE5S 2 h before imaging, as described in 3.3.2. Time 0 is the start of ring constriction.

Figure 3.5: Continued

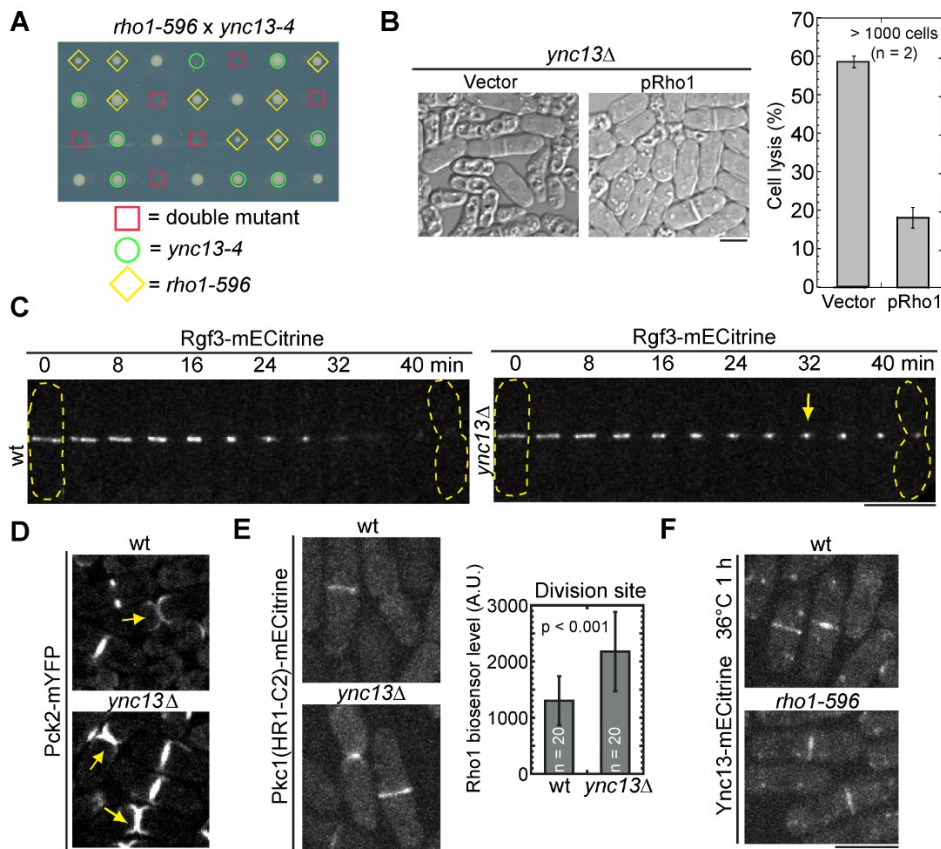
Figure 3.5: Continued

(D and E) Plasma membrane closure is normal in *ync13Δ* cells during cytokinesis in FLIP assays. The red boxes show bleached ROI (D). Time from ring closure (red arrows) to membrane closure (yellow arrows) is shown in (E). (F) Calcofluor staining of *ync13Δ* cells. Kymographs of the division site are shown and the arrows mark the cell separation. (G) *ync13Δ* cells have defective septa. Left, EM images of the division site of wt and *ync13Δ* cells. The arrows point out the bulges on the septa. Right, quantification of septum thickness. Bars, 5 μm for A-F, 0.5 μm for G.

To elucidate how *ync13Δ* causes cell death, we examined the contractile ring and cell separation in live wt and *ync13Δ* cells. It took a similar amount of time for the contractile ring to assemble, mature, constrict, disappear, and for the cells to separate (Figure 3.5 C and 3.7 A). However, ~50% of *ync13Δ* cells lysed during cell separation under the growth condition (Figure 3.5 C), which could result from defects in the membrane closure or septation. It took both wt and *ync13Δ* cells (expressing diffusible mEGFP) ~4 min to close the plasma membrane (yellow arrows) after the end of contractile ring constriction (red arrows) in fluorescence loss in photobleaching (FLIP) assays (Figure 3.5, D and E). Thus, the membrane closure appears normal. We next compared the primary septum in wt and *ync13Δ* cells by Calcofluor staining (Figure 3.5 F). Interestingly, while the cell wall materials from the primary septum disappeared quickly after cell separation in wt (Figure 3.5 F, left), we observed strong accumulations of Calcofluor signal at the division site in *ync13Δ* cells (Figure 3.5 F, right). Under EM, *ync13Δ* cells formed significantly thinner septa ( $139 \pm 44$  nm) than wt cells ( $160 \pm 38$  nm;  $p < 0.01$ ; Figure 3.5 G), and cell wall breakage at or near the center of the septum was often observed (Figure 3.5 G). In addition, we occasionally observed a bulge at the center of the septum in *ync13Δ* cells (Figure 3.5 G, arrows), which could correspond to

the Calcofluor staining (Figure 3.5 F). Thus, *ync13Δ* causes uneven or defective septum formation or septum digestion, which leads to cell lysis during cell separation.

**Figure 3.6 Ync13 coordinates with Rho1 GTPase dependent cell integrity pathway during cytokinesis.**

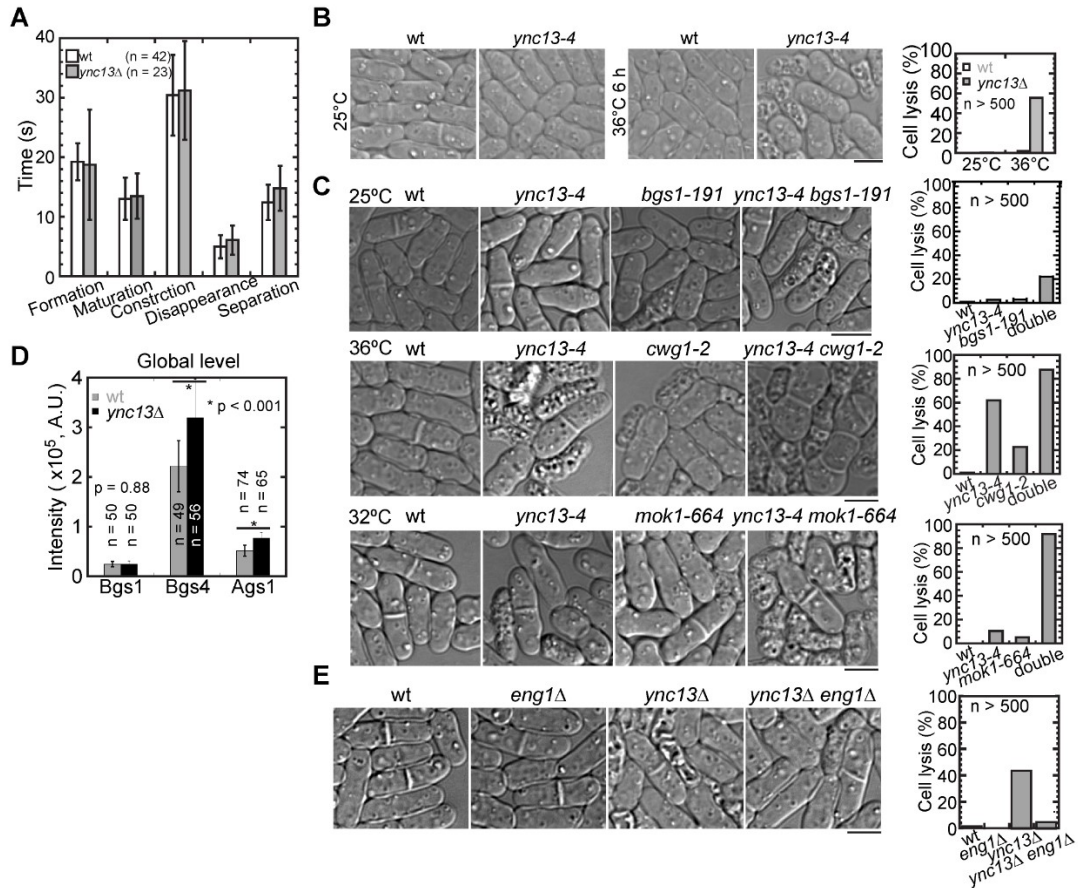


(A) Synthetic lethality between *ync13-4* and *rho1-596*. The four spores from each tetrad were plated in the same column on YE5S plate. The genotype of each colony is indicated. (B) Rho1 overexpression rescues cell lysis in *ync13Δ* cells. *ync13Δ* cells with pUR19-Rho1 or pUR19 empty vector were grown in EMM5S - uracil and then washed into YE5S 4 h before imaging. (C and D) Rgf3 and Pck2 localization in *ync13Δ*. The dashed lines mark cell boundary and arrows mark the accumulated Rgf3 or Pck2. (C) Montages of wt and *ync13Δ* cells with time 0 as the start of ring constriction. (E) Localization and level of Rho1 biosensor in *ync13Δ* cells. Cells were grown in YE5S + 1.2 M sorbitol and washed into YE5S 2 h before imaging. (F) Ync13 localization in *rho1-596*. Cells were imaged after incubation at 36°C for 1 h. Bars, 5 μm.

The cell wall integrity pathway (CIP) in yeasts regulates the cell wall formation and integrity (Levin *et al.*, 1994; Garcia *et al.*, 2006; Levin, 2011; Sanchez-Mir *et al.*, 2014). Rho1 GTPase and its downstream effectors, protein kinase C, recruit and activate the cell wall synthases for septum synthesis (Levin *et al.*, 1994; Nonaka *et al.*, 1995; Tajadura *et al.*, 2004; Sanchez-Mir *et al.*, 2014). We thus explored the relationship between Ync13 and the Rho1 dependent CIP. A temperature sensitive (ts) mutant *ync13-4* caused ~2% cell lysis at 25°C but ~55% at 36°C for 6 h (Figure 3.7 B). We found *ync13-4* was synthetic lethal with Rho1 temperature sensitive mutant *rho1-596* (Figure 3.6 A). In addition, *ync13-4* had strong or lethal genetic interactions with mutations in other components of the CIP including arrestin Art1 (Davidson *et al.*, 2015), protein kinase C Pck1 (Arellano *et al.*, 1999), and GTPase activating protein Rga7 (Martin-Garcia *et al.*, 2014) (Table 3.1). These data supported that Ync13 has a role in cell integrity and plays a redundant role with CIP. Consistently, overexpression of Rho1 dramatically reduced cell lysis in *ync13Δ* (Figure 3.6 B).

To test how Ync13 affects the CIP, we examined the localizations of CIP components in *ync13Δ* cells. Interestingly, both Rho1 activator Rho GEF Rgf3 and effector protein kinase C Pck2 were more concentrated at the center of division site in *ync13Δ* cells, similar to the cell wall synthases (Figure 3.6, C and D). In addition, the active Rho1 level was elevated in *ync13Δ* cells as visualized by the Rho1 biosensor (budding yeast Pkc1[HR1-C2] domain; Figure 3.6 E) (Denis and Cyert, 2005; Davidson *et al.*, 2015). In contrast, the localization of Ync13 was not obviously affected in *rho1* mutant (Figure 3.6 F). Together, our data suggest that Ync13 is essential for cell integrity and controls the proper distribution of CIP components during cytokinesis.

**Figure 3.7 Synthetic interactions between mutations in *ync13* and cell wall enzymes.**



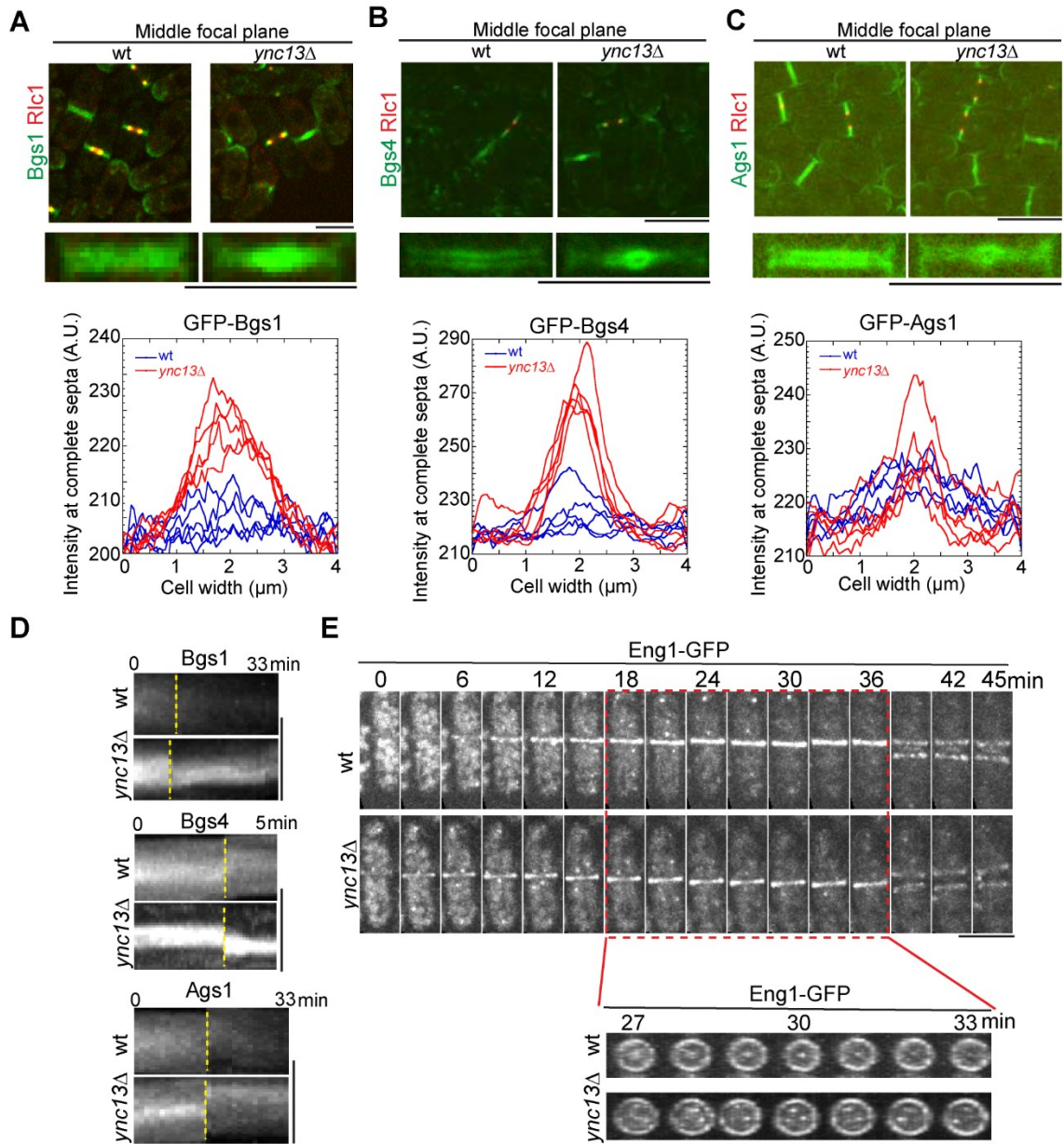
(A) Time needed for each stage of cytokinesis is quantified in *ync13Δ* cells. Formation, from node appearance to formation of a compact ring; Maturation, from the appearance of a compact ring to just before ring constriction; Constriction, the start of ring constriction to Rlc1 reaching highest intensity as a dot; Disappearance, from the end of ring constriction to the disappearance of Rlc1 signal at the division site; Separation, from Rlc1 disappearance to cell separation. (B) DIC images and quantification of cell lysis in *ync13-4* cells at 25°C or after 6 h at 36°C. (C) DIC images and quantification of cell lysis to show synthetic interactions between *ync13-4* and *bgs1-191* (at 25°C), *cwg1-2* (at 36°C for 4 h), and *mok1-664* (at 25°C for 4 h). (D) The global of Bgs1, Bgs4, and Ags1 in wt and *ync13Δ* cells. (E) DIC images and quantification of cell lysis to show synthetic interactions between *ync13Δ* and *eng1Δ*. Bars, 5 μm.

### 3.4.5 Roles of Ync13 in the localizations of the cell wall enzymes glucan synthases and glucanase

Because *ync13* $\Delta$  cells have septum defects and Ync13 is important for the cell integrity, we studied how Ync13 affected the septum formation and degradation. The septum is a three layer structure composed of mainly  $\beta$ - and  $\alpha$ -glucan synthesized by the glucan synthases Bgs1, Bgs4(Cwg1), and Ags1(Mok1) during cytokinesis (Ribas *et al.*, 1991; Ishiguro *et al.*, 1997; Katayama *et al.*, 1999; Liu *et al.*, 1999; Cortes *et al.*, 2005; Cortes *et al.*, 2016; Perez *et al.*, 2016). We first tested the genetic interactions between *ync13* and the cell wall synthase mutants (Table 3.1). *ync13-4* showed strongest synthetic interactions with  $\alpha$ -glucan synthase *ags1* mutant *mok1-664*, and moderate interactions with  $\beta$ -glucan synthase mutants *bgs1-191* and *cwg1(bgs4)-2* (Figure 3.7 C). These data suggest that Ync13 works together with the glucan synthases for cell wall synthesis.

We next examined the expression and localizations of glucan synthases Bgs1, Bgs4, and Ags1 in *ync13* $\Delta$  cells. Bgs4 and Ags1 had higher global protein levels in *ync13* $\Delta$  cells while the Bgs1 level was similar to wt (Figure 3.7 D, top). We further investigated the localization of the synthases at the division site. In wt cells, all three enzymes distributed almost evenly along the division plane after ring constriction (Figure 3.8, A-C). In *ync13* $\Delta$  cells, however, they were more concentrated at the center of the septum and sometimes formed a bubbled structure (Figure 3.8, A-C). These abnormal accumulations persisted even after cell separation (Figure 3.8 D, yellow dashed lines). Interestingly, the overexpression of cell wall enzymes could not rescue cell lysis caused by *ync13* $\Delta$ . Together, *ync13* $\Delta$  caused the concentration of the glucan synthases at the center of the division plane after ring constriction.

**Figure 3.8 Ync13 affects the distribution of cell wall enzymes on the division plane.**



(A-C) Glucan synthases Bgs1 (A), Bgs4 (B), and Ags1 (C) are mislocalized in *ync13Δ* cells. Top, the middle focal plane of merged images; middle, enlarged images of localizations of glucan synthases on complete septa; bottom, area scans of Bgs1, Bgs4, and Ags1 intensity along the complete septa in 5 wt or *ync13Δ* cells. (D) Kymographs of glucan synthases distribution along the division plane (vertical) before and after cell separation (dashlines). (E) Localization and distribution of glucanase Eng1 in *ync13Δ* cells. Top, time courses with time 0 as Eng1 ring appearance; bottom, vertical views of the cell from late stage of ring constriction to just before cell separation (red box). Bars, 5μm.

The glucanases Eng1 and Agn1 digest the primary septum and some adjacent cell wall on cell sides to trigger cell separation (Martin-Cuadrado *et al.*, 2003; Dekker *et al.*, 2004; Cortes *et al.*, 2016; Perez *et al.*, 2016). The deletion of  $\beta$ -glucanase *eng1* significantly rescued *ync13 $\Delta$*  cells (Table 3.1). The *ync13 $\Delta$  eng1 $\Delta$*  cells survived in YE5S medium with only 6% cell lysis compared to 54% in *ync13 $\Delta$*  cells (Figure 3.7 E). By contrast, the deletion of  $\alpha$ -glucanase *agn1* failed to rescue *ync13 $\Delta$*  cells. We previously found that Eng1 localized to a non-constricting ring at the rim and a dot at the center of the division plane (Wang *et al.*, 2015; Wang *et al.*, 2016). In *ync13 $\Delta$*  cells, the dot localization of Eng1 was abolished and Eng1 was more disbursed along the division plane while the rim localization was normal (Figure 3.8 E). Together, Ync13 plays a role in normal distribution of the glucan synthases and glucanase along the division plane.

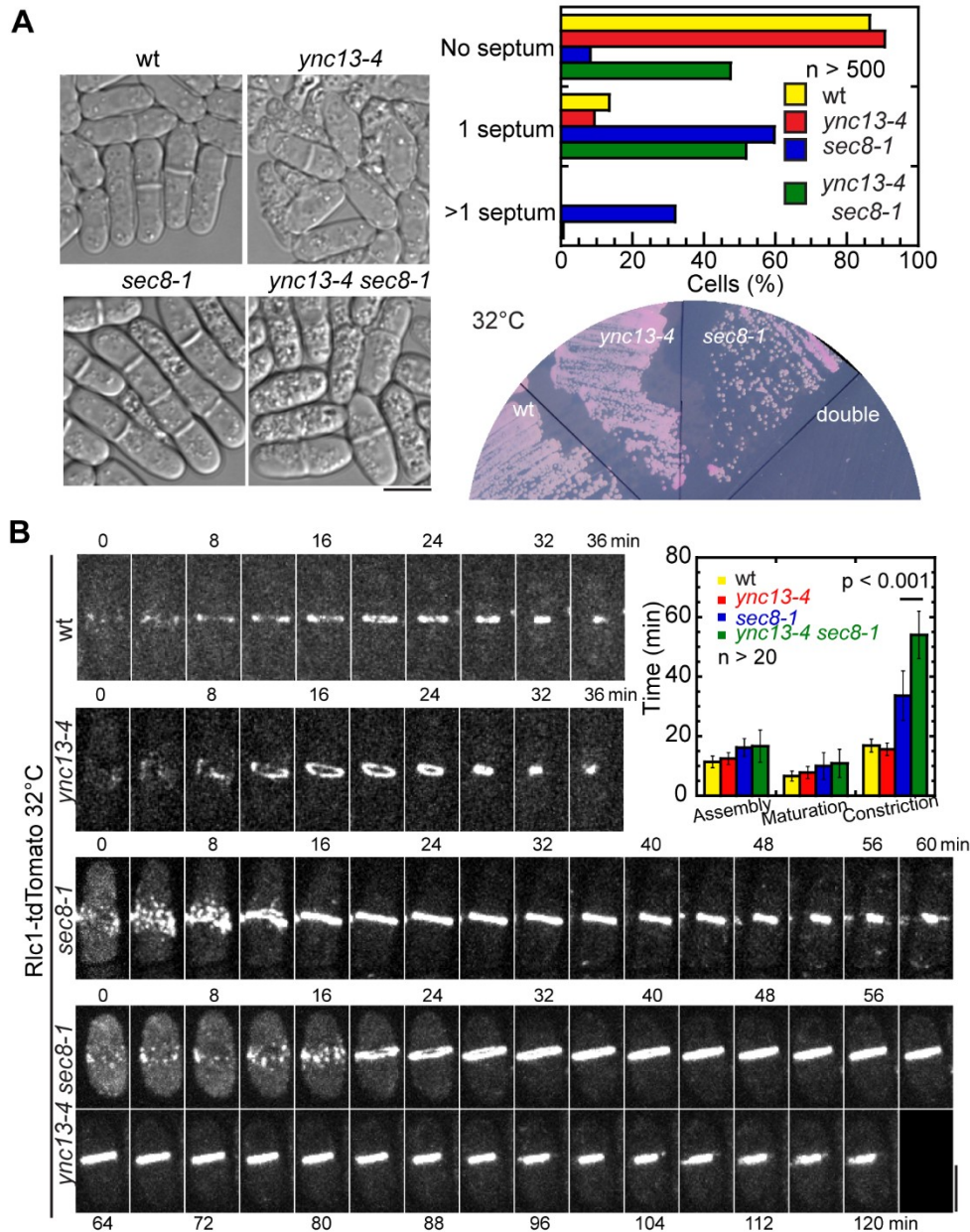
#### **3.4.6 Ync13 collaborates with the exocyst complex to mediate exocytosis at the division site**

Exocytosis delivers cell wall enzymes to the division site to assist septum formation and cell separation (Albertson *et al.*, 2005; Wang *et al.*, 2016). The exocyst is an octameric complex that tethers vesicles to the plasma membrane at the division site during cytokinesis (He and Guo, 2009; Giansanti *et al.*, 2015). Failure in exocytosis or a defective exocyst causes significant vesicle accumulation and delayed cytokinesis (Wang *et al.*, 2002; Wang *et al.*, 2016). We asked whether Ync13 regulates the septum and cell wall integrity through exocyst mediated exocytosis. Unlike exocyst mutants and Ync13 animal homologs (Richmond *et al.*, 1999), *ync13 $\Delta$*  did not cause vesicle accumulation or delay in cytokinesis (Figures, 3.7 A and 3.10 A), which was consistent with our in vitro reconstitution experiments (Figure 3.4, D-F). However, *ync13-4* mutation showed strong

synthetic interactions with mutations in exocyst subunits Sec8, Sec3, and Exo70 (Figures, 3.9 A and 3.10 B, Table 3.1). At 36°C, *sec8-1* died as elongated and multiseptated cells while *ync13-4* displayed cell lysis phenotype. Instead, *ync13-4 sec8-1* cells seemed to halt during the cell division or growth, as 52% of cells had one septa and <1% cells were multiseptated (Figure 3.9 A). Consistently, the contractile ring constricted significantly slower in *ync13-4 sec8-1* cells while the ring assembly and maturation were similar to *sec8-1* (Figure 3.9 B).

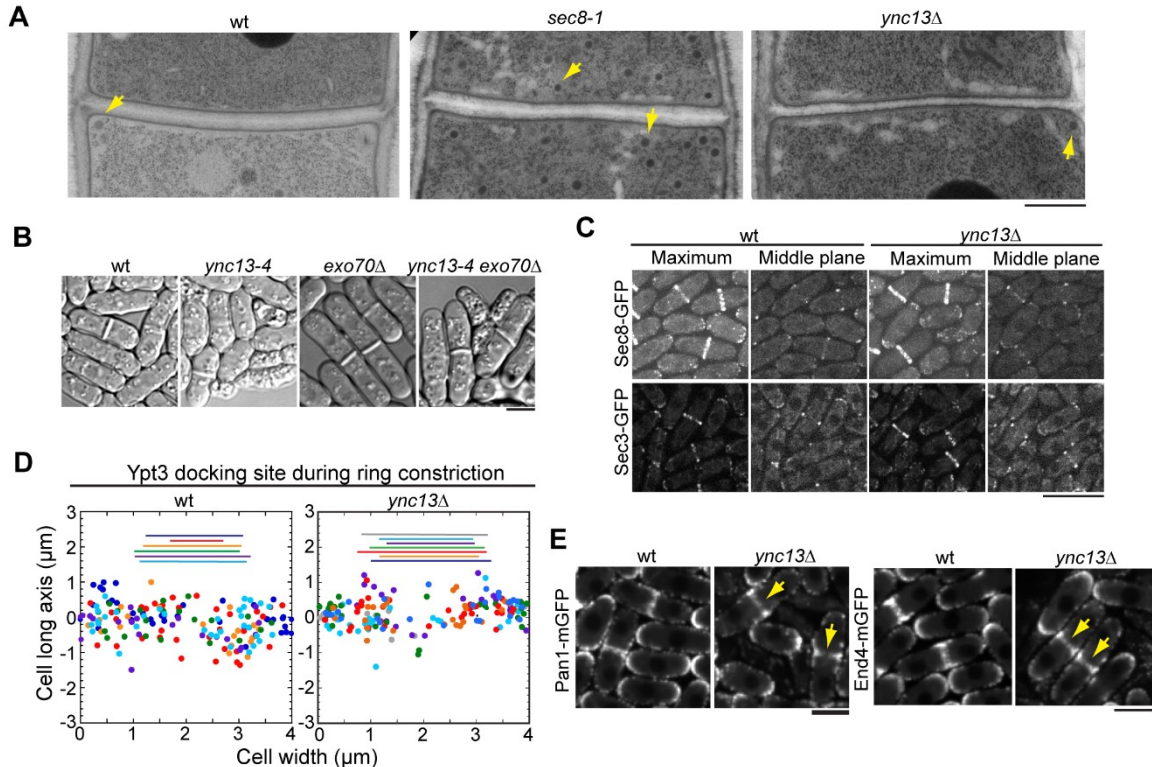
Normal ring constriction and plasma membrane invagination depends on exocytosis (Wang *et al.*, 2016). We investigated whether the defects in *ync13 sec8-1* cells were due to impaired exocytosis. We tracked vesicle delivery using v-SNARE synaptobrevin Syb1 as marker in temperature sensitive mutant *ync13-19*, which had similar synthetic interactions with *sec8-1* but had fewer mutations than *ync13-4* (Table 3.1). *ync13-19 sec8-1* cells resembled *ync13-4 sec8-1* in morphology (Figure 3.9, A and C). Syb1 accumulated close to the division site and cell tips in both *sec8-1* and *ync13-19 sec8-1* cells (Figure 3.9 C). In addition, trackable exocytic vesicles delivered to the division site decreased in *ync13-19 sec8-1* cells compared to the single mutants (Figure 3.9 D). Thus, exocytosis was impaired during cytokinesis in *ync13-19 sec8-1* cells, indicating a role of Ync13 in vesicle delivery to the division site. However, Ync13 did not affect the exocyst localization (Figure 3.10 C), suggesting that Ync13 and the exocyst complex function in parallel pathways to mediate exocytosis during cytokinesis.

**Figure 3.9 Cooperation between Ync13 and the exocyst during cytokinesis.**



(A) Synthetic interaction between Ync13 and the exocyst protein Sec8. DIC images (left) and septation index (top right) of cells grown for 4 h at 36°C; bottom right, growth test on YE5S + phloxin B at 32°C for 2 d. (B) Contractile ring constriction is delayed in *ync13-4 sec8-1* cells. Time courses and quantification of cells imaged at 32°C after shifting cells to 32°C for 2 h. (C and D) Vesicle deposition to the division site is reduced in *sec8-1 ync13-19* cells with complete septa and labeled with GFP-Syb1. Micrographs (C) and tracking of vesicle deposition sites in color coded cells (D).  $y = 0$  is the division plane for this and other vesicle tracking graphs. Bars, 5  $\mu$ m.

**Figure 3.10 The involvement of Ync13 in exocytosis and endocytosis.**



(A) *ync13Δ* cells, unlike *sec8-1*, have no vesicle accumulation at the division site. The arrows mark examples of vesicles in EM images. (B) *ync13-4* has synthetic genetic interaction with *exo70Δ*. DIC images of cells grown at 36°C for 6 h. (C) Localizations of exocyst subunits Sec8 and Sec3 are not affected by *ync13Δ*. Images of maximum projection and middle focal plane are shown. (D) Ypt3 vesicle delivery to the division site during ring constriction. The lines indicate the diameters of the constricting ring for each color-coded cell. (E) Mislocalization of endocytic proteins Pan1 and End4 in *ync13Δ* cells. The sum images of 2 min continuous movies are shown. The arrows mark reduced localization of Pan1 and End4 at the division site. Bars, 0.5  $\mu\text{m}$  for (A); others, 5  $\mu\text{m}$ .

### 3.4.7 Does Ync13 regulate exocytosis mediated by the TRAPP-II complex?

We recently reported that the TRAPP-II complex and the exocyst tether vesicles to different locations at the division site during fission yeast cytokinesis, where the exocyst predominantly tethers vesicles at the rim and the TRAPP-II complex at the interior of the division site (Wang *et al.*, 2016). We thus investigated how Ync13 affected the TRAPP-II mediated exocytosis. As reported (Wang *et al.*, 2016), the TRAPP-II component Trs120

dynamically localizes to the division site during and after ring constriction (Figure 3.11 A). In *ync13Δ*, however, Trs120 concentrated at the center of the division plane after ring constriction (Figure 3.11 A). Syb1 and Rab11 GTPase Ypt3, two proteins that work with the TRAPP-II complex (Wang *et al.*, 2016), had similar accumulations in *ync13Δ* and *ync13-19* cells with mature septa (Figures, 3.9 C and 3.11, B-D).

**Figure 3.11 Ync13 affects the localizations and dynamics of the TRAPP-II complex and Rab11 GTPase Ypt3 at the division plane during cytokinesis.**

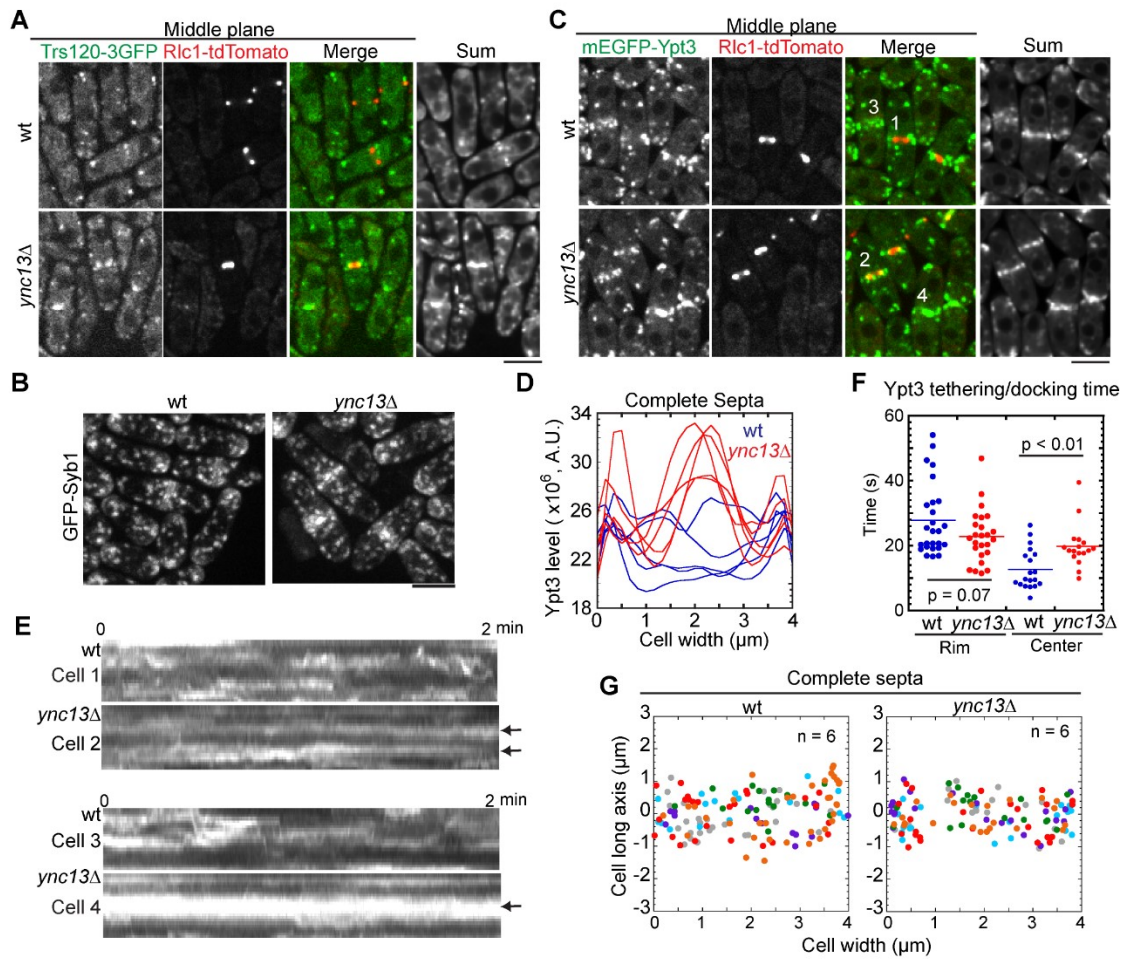


Figure 3.11: Continued

Figure 3.11: Continued

(A) Trs120 accumulates at the center of division plane in *ync13Δ* cells. The middle focal planes are shown with the sum projection of a 2 min continuous movie on the right. (B) Syb1 accumulates at the center of division plane in *ync13Δ* cells. (C-G) *ync13Δ* affects Ypt3 distribution (C and D), dynamics (E), tethering/docking time (F), and the final deposition site in cells with complete septa (G). (C) The sum projection (right) is from a 2 min continuous movie. (D) Area scans of Ypt3 distribution at the complete septa in the sum projection. (E) Kymographs of the division site of the numbered cells in (C) during ring constriction (cells 1 and cell 2) or complete septa (cells 3 and cell 4). The arrows mark stable Ypt3 at the leading edge (cell 2) or the center of septum (cell 4). (F) Ypt3 tethering/docking time at the center of division plane is delayed in *ync13Δ*. The division plane is divided to the center half and rim half. Bars, 5 μm.

We thus used Ypt3 as a marker to track the delivery and docking of vesicles to the division plane (Wang *et al.*, 2016). In wt cells, Ypt3 was highly dynamic both during and after ring constriction at the division site (Figure 3.11 E, cells 1 and 3). In *ync13Δ* cells, however, Ypt3 signal was stable at the leading edge of the cleavage furrow (Figure 3.11 E, cell 2) or at the center of division site after ring constriction (Figure 3.11 E, cell 4). Consistently, the docking/tethering time was significantly longer at the center of the division plane in *ync13Δ* (19 s) than in wt (12 s) (Figure 3.11 F). In contrast, the docking/tethering time of Ypt3 vesicles at the rim of the division plane was insignificantly different between wt (27 s) and *ync13Δ* (22 s) cells (Figure 3.11 F), and close to the reported tethering time of the exocyst (Wang *et al.*, 2016). The uneven distribution of Trs120 and Ypt3 at the division site suggested that *ync13Δ* might affect the TRAPP-II mediated exocytosis at the interior of the division. Surprisingly, the delivery and docking sites of Ypt3 vesicles were not dramatically affected in cells with forming or mature septa (Figures, 3.11 G and 3.10 D). Together with the data on the exocyst, Ync13 plays a minor or redundant role in exocytosis in *S. pombe*.

### **3.4.8 Ync13 is important for selecting endocytic site at the division plane**

The balance between exocytosis and endocytosis is critical for plasma membrane dynamics and expansion (Johansen *et al.*, 2016; Xie *et al.*, 2017). The CME is the major pathway for retrieving lipids and proteins from the plasma membrane (Schweitzer *et al.*, 2005; Weinberg and Drubin, 2012; Goode *et al.*, 2015). We previously reported that endocytosis occurs along the division plane albeit with a preference at the rim (Wang *et al.*, 2016). Ync13 may affect protein distribution at the division site through regulating endocytosis. Thus, we asked whether endocytic sites are altered in *ync13Δ* cells.

**Figure 3.12 Sites of endocytosis at the division plane is compromised in *ync13Δ* cells.**

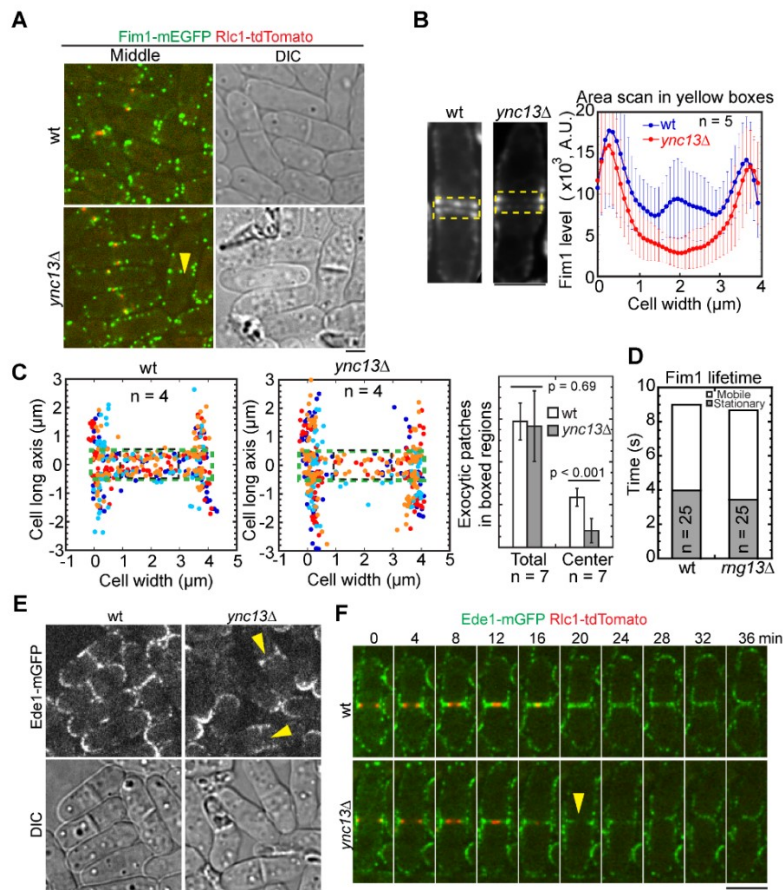


Figure 3.12: Continued

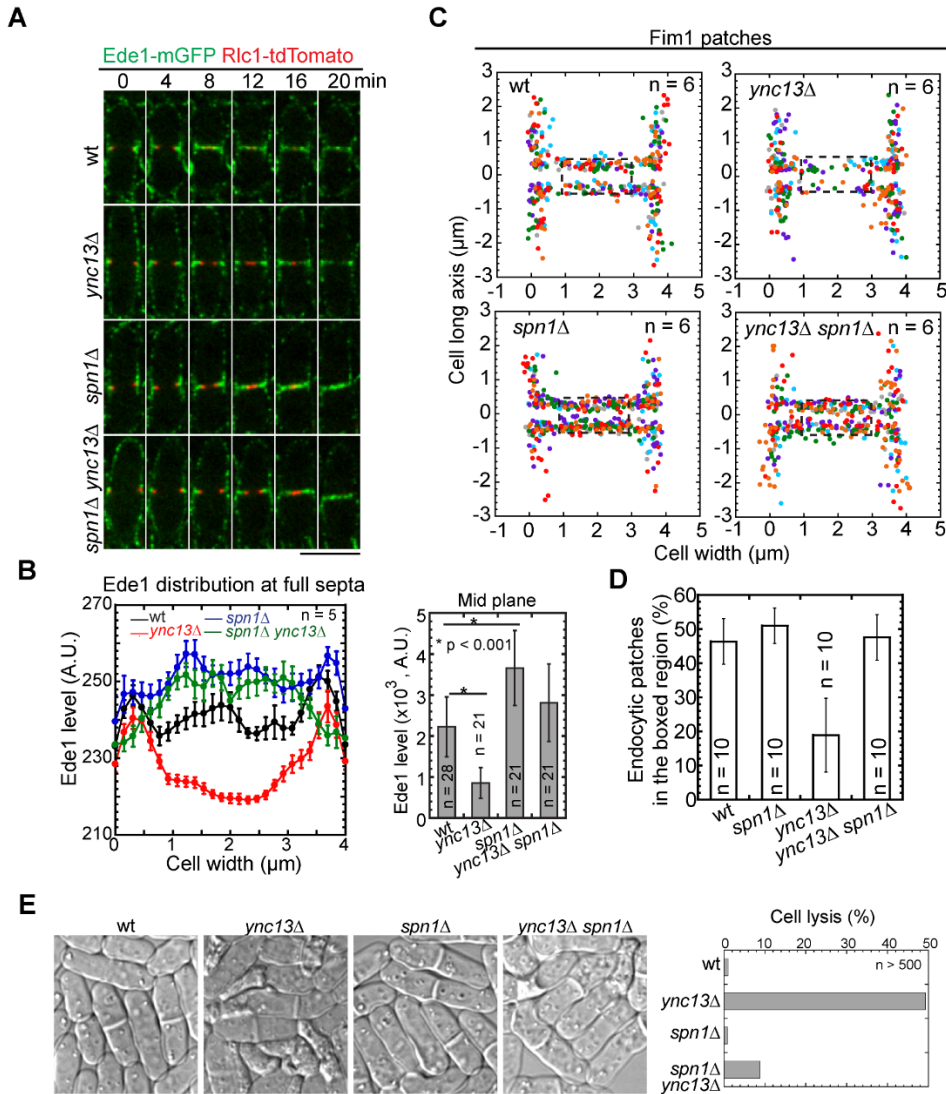
Figure 3.12: Continued

(A-D) Localization (A), intensity (B), tracking of initiation sites (C), and lifetimes (D) of fimbrin Fim1 at the division site in wt and *ync13Δ* cells. (A) The arrowhead indicates the loss of Fim1 at the center of division site in the middle focal plane. (B) Sum projections of middle-focal images from 2 min continuous movies of representative cells with complete septa. Fim1 intensity level in the boxed regions are measured by area scan. (C) Initiation sites of endocytic patches along the division plane (left) and quantification of the numbers of Fim1 patches in the boxed (green, total; black, center) regions (right). (D) Lifetime of Fim1 patches. (E and F) Micrographs (E) and time courses (F) of Ede1 localization in *ync13Δ* cells. The arrowheads mark the loss of Ede1 at the center of division site in *ync13Δ* cells. Bars, 5 μm.

We tracked the initiation sites of endocytic patches using the actin crosslinker fimbrin Fim1 (Figure 3.12, A-D) (Berro *et al.*, 2010). As reported (Wang *et al.*, 2016), the endocytic patches formed predominantly on the plasma membrane at the rim of the division plane and adjacent cortex, with some patches along the division plane in wt cells. In contrast, the patches at the center of the division plane reduced significantly in *ync13Δ* cells although the amount of patches measured across the entire division site and patch life times were similar (Figure 3.12, A-D). Then we asked if locations of proteins involved in the endocytic site selection are affected. The Eps15 protein Ede1 is one of the first coat proteins localizing to the endocytic sites in the CME pathway (Weinberg and Drubin, 2012; Lu and Drubin, 2017). As expected, Ede1 localized to active growth sites such as the cell tips, division site, and its adjacent cortex in wt cells (Figure 3.12 E). During cytokinesis, Ede1 followed the constricting ring and distributed evenly across the division plane (Figure 3.12 F). However, Ede1 barely localized to the center of the division site after ring constriction in *ync13Δ* cells (Figure 3.12, E and F, arrowheads), suggesting that Ync13 plays a role in endocytic site selection. Consistently, the middle coat protein End4 and the late coat protein Pan1 displayed the same defects in *ync13Δ*

cells (Figure 3.10 E). Thus, Ync13 regulates the selection of endocytic sites and protein accumulation across the division plane during cytokinesis.

**Figure 3.13 Deletion of septin partially rescues *ync13Δ*.**



(A and B) Time courses of Ede1 localization (A) and Ede1 distribution and levels at the division sites (B) in wt, *ync13Δ*, *spn1Δ*, and *spn1Δ ync13Δ* cells. (C and D) *spn1Δ* rescues endocytosis in *ync13Δ* cells. (C) Patches (labeled with Fim1-mEGFP) distribution along the division site and (D) percentage within the central 50% of the division site in 2 min continuous movies. (E) *spn1Δ* partially rescues cell lysis in *ync13Δ* cells grown for 2 h in YE5S. Left, DIC images; right, quantification of cell lysis. Bars, 5  $\mu$ m.

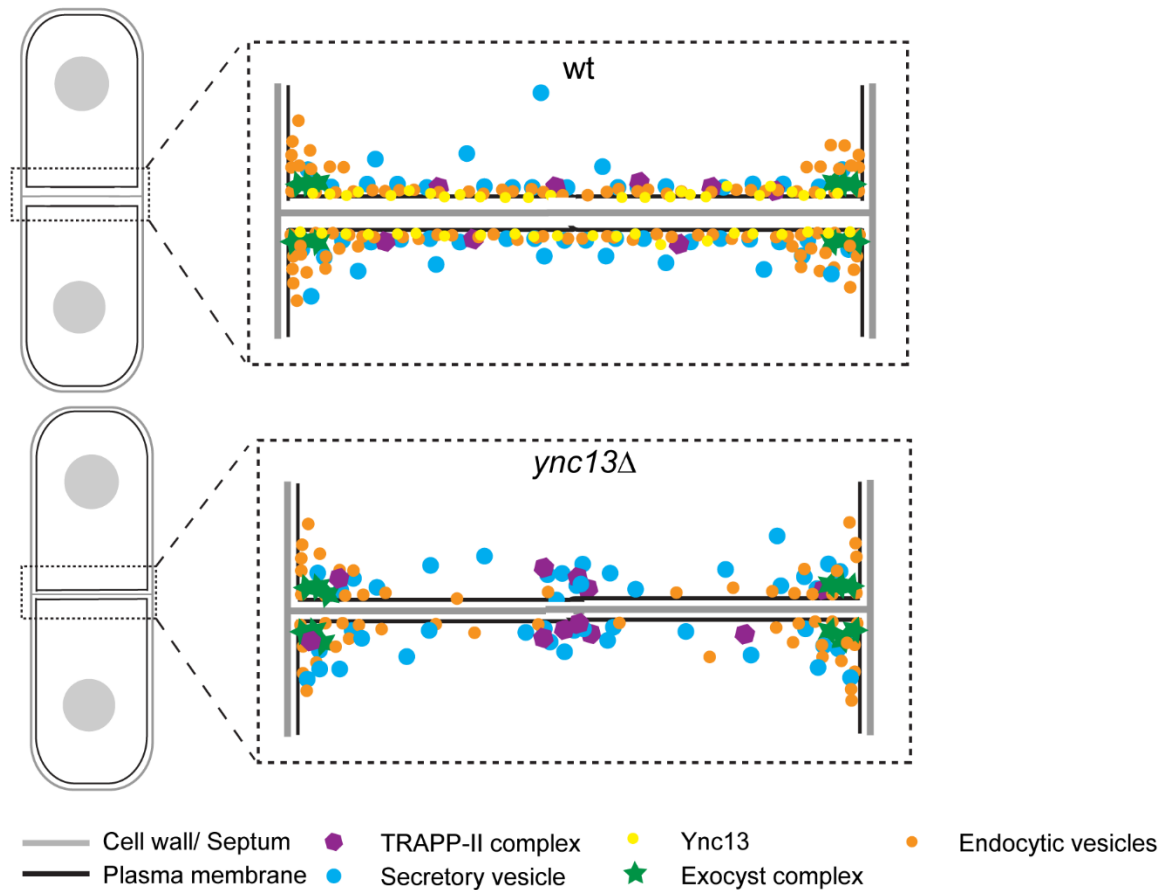
### 3.4.9 Septin deletion partially rescues *ync13Δ* cells

Our results indicated that Ync13 plays an important role in normal protein distribution and accumulation at the division site by defining the sites for endocytosis. Next we asked whether restoration of endocytosis at the center of the division site rescues *ync13Δ* cells. Dynamin, the GTPase responsible for endocytosis in eukaryote cells, is found to be co-immunoprecipitated with septin in brain extract (Maimaitiyiming *et al.*, 2013). A recent mass spectrometry study reported the budding yeast septins interact with a group of endocytic protein including the clathrin coat protein End4/Sla2 and F-BAR protein Syp1 (Renz *et al.*, 2016; Song *et al.*, 2016). Moreover, septin deletions are known to affect the endocytic sites during mating in fission yeast (Onishi *et al.*, 2010). Thus, we tested if septin mutant *spn1Δ* can restore the sites of endocytosis in *ync13Δ* cells (Figure 3.13, A-D). Interestingly, the Ede1 level at cell middle was restored to wt level in *ync13Δ spn1Δ* cells (Figure 3.13, A and B). In addition, numbers of actin patches were also restored to wt levels in *ync13Δ spn1Δ* cells (Figure 3.13, C and D). Moreover, we found that *spn1Δ* partially suppressed the *ync13Δ* cell lysis phenotype (Figure 3.13 E). Together, these data suggest that cell lysis in *ync13Δ* cells results from defective endocytic site selection.

### 3.5 Discussion

In Chapter 3, we identified the UNC-13/Munc13 protein Ync13 as a novel regulator of membrane trafficking during cytokinesis (Figure 3.14). Ync13 guides even distribution of the TRAPP-II mediated exocytosis and the endocytic events at the division site, which indirectly regulates the localizations and dynamics of the cell wall enzymes and the CIP components to ensure the cell integrity during cytokinesis.

**Figure 3.14 Roles of Ync13 in cytokinesis.**



Ync13 ensures proper distribution of cell wall enzymes at the division site. In *ync13Δ* cells, TRAPP-II mediated exocytosis is mistargeted and leads to slightly biased vesicle delivery to the center of the division plane. Importantly, the endocytosis at the center of the division plane is drastically reduced without Ync13. As a result vesicle cargos, glucan synthases and glucanases, are mislocalized. These lead to impaired septum synthesis, cell separation, and cell lysis.

### 3.5.1 A novel role of UNC-13/Munc13 protein family in cytokinesis

The main function of UNC-13/Munc13 proteins is to facilitate the SNARE complex assembly by opening the closed syntaxin-Munc18 conformation through their MUN domains during vesicle priming (Betz *et al.*, 1996; Aravamudan *et al.*, 1999; Yang *et al.*, 2015). However, recent in vitro reconstitution and crystal structure have suggested that

Munc13-1 can bridge T and V liposomes (Liu *et al.*, 2016a; Xu *et al.*, 2017). Such tethering brings vesicles and the target membrane in close proximity and helps MUN domain function. However, no roles of the protein family in cytokinesis have been reported.

The fungi subfamily distinguishes from the rest of UNC-13/Munc13 proteins where the MUN domain is separated into MHD1 and MHD2 domains by a C2 domain (Pei *et al.*, 2009). The MHD1C2MHD2 of Ync13 cannot promote the SNARE complex assembly or liposome bridging in vitro (Figure 3.4). However, whether the FL Ync13 assists the SNARE complex assembly is unknown. Nevertheless, *ync13Δ* cells do not accumulate vesicles at the division site during cytokinesis (Figure 3.10 A), which is commonly seen in the exocyst or TRAPP-II mutants in yeasts or Munc13 deficient neurons (TerBush *et al.*, 1996; Aravamudan *et al.*, 1999; Guo *et al.*, 1999a; Zhou *et al.*, 2013; Wang *et al.*, 2016). What is the exact role of Ync13 in membrane trafficking in fission yeast? In mammalian cells, SNARE proteins are usually restricted to specific cellular locations to fulfill their functions, as predicted by the SNARE hypothesis (Chen and Scheller, 2001). In *S. pombe*, SNARE proteins are only known to be involved in the forespore formation during meiosis (Nakamura *et al.*, 2005; Maeda *et al.*, 2009; Yamaoka *et al.*, 2013). The plasma membrane targeting syntaxin, Psyl, localizes all over the cell cortex (Maeda *et al.*, 2009; Kashiwazaki *et al.*, 2011), and the other t-SNARE SNAP-25 Sec9 is not studied in detail. To direct vesicle delivery to active growth sites like the cell tips and division site, additional proteins like Ync13 and septins may serve as receptors or landmarks. Future work is needed to explore the relationship between Ync13 and the SNARE complex. In addition, we found Ync13 affects the localization and dynamics of

Rab11 Ypt3 (Figure 3.11). The animal Munc13-4 binds to Rab11 and Rab27 GTPases to regulate vesicle trafficking and docking in neutrophil cells and lysosome secretion in hematopoietic cells (Neeft *et al.*, 2005; Johnson *et al.*, 2016). It is possible that Ync13 serves as an effector of Rab GTPases to spatially regulate membrane trafficking.

### **3.5.2 Roles of Ync13 in spatial regulation of the cell wall enzymes and membrane trafficking during cytokinesis**

Exocytosis and endocytosis are essential for cytokinesis as the disruptions of membrane trafficking by mutants or inhibitory drugs like Brefeldin A (BFA) caused slowed furrow ingression, furrow regression, and cytokinesis failure (Neto *et al.*, 2013; Giansanti *et al.*, 2015; Wang *et al.*, 2016). In this study, we showed that the spatial regulation of membrane trafficking is vital to ensure successful cytokinesis. In *ync13Δ* cells, we observed abnormal accumulation of regulators and enzymes of cell wall synthesis that leads to defective septum formation and occasional bulge appearance in the EM images. We showed that the mislocalizations of cell wall enzymes are caused by reduced endocytosis and defects in the TRAPP-II mediated vesicle delivery. The Rho GTPase dependent CIP can recruit and activate cell wall synthases, and the extra activity may compensate for the loss of cell wall synthases in the overexpression strains (Arellano *et al.*, 1996; Arellano *et al.*, 1999). In addition, Rho1/RhoA also coordinates actin filament nucleation, vesicle trafficking by exocyst complex, and clathrin independent endocytosis in budding yeast and animals (Imamura *et al.*, 1997; Guo *et al.*, 2001; Prosser *et al.*, 2011; Jordan and Canman, 2012; Prosser and Wendland, 2012). All these processes can regulate membrane dynamics and make up for the loss of membrane dynamics at the division site, although these Rho1 functions have not yet been validated in fission yeast.

What is the mechanism that recruits TRAPP-II mediated exocytosis and its cargos to the leading edge of the cleavage furrow in *ync13Δ*? First, the myosin V and the actin meshwork surrounding the division site may provide tracks for cargo delivery (Donovan and Bretscher, 2012). Second, the F-BAR proteins at the contractile ring including Cdc15, Imp2, and Rga7 can recruit the cell wall synthases and Rho1 activators Rgf3 and its binding partner Art1 (Martin-Garcia *et al.*, 2014; Ren *et al.*, 2015). We previously reported that the TRAPP-II complex and exocyst complex mediate vesicle delivery independently (Wang *et al.*, 2016). Our study on Ync13 supports this hypothesis since the deletion of Ync13 only mislocalizes the TRAPP-II components, but not exocyst (Figures, 3.10 C and 3.11).

The reduced endocytosis at the division site in *ync13Δ* cells is intriguing. The processes of the CME and CIE in fission yeast are not as systematically studied as their counterparts in budding yeast, let alone their exact roles during cytokinesis (Goode *et al.*, 2015). It was reported that the deletion of the clathrin light chain Clc1 blocks the delivery of Bgs1 to the cortex in *pombe*, which provides a direct link between endocytosis and cell wall synthesis (de Leon *et al.*, 2013). Why are endocytic sites mislocalized in *ync13Δ*? Ync13 may not directly recruit CME as we did not detect interactions between Ync13 and the early coat protein Edel1 in immunoprecipitation (IP) assays or ectopic targeting assays using GFP binding protein (GBP). Alternatively, exocytosis and endocytosis are often tightly coupled. In neuronal cells, endocytosis is blocked upon the deletion of the SNARE complex or the treatment of botulinum neurotoxins that abolishes exocytosis (Xie *et al.*, 2017). In budding yeast, the polarized exocytosis and endocytosis is coupled by Rab GTPase Sec4 (Johansen *et al.*, 2016). Thus, the defects in endocytosis could

instead be a response to the uneven distribution of exocytosis in *ync13Δ*. However, we favor a model that Ync13 plays an active role in endocytosis.

### **3.5.3 Roles of Ync13 domains for localization and functions**

The MHD2 domain and the rest of C terminal sequence in Ync13 was vital for its functions (Figure 3.2, F and G). This domain corresponds to MUN-CD region in Munc13-1, which contains multiple helix structures that share structural homology with the exocyst complex subunit Sec6 (Pei *et al.*, 2009; Li *et al.*, 2011). Together with C1, C2B and MUN-AB, it forms an elongated rod domain composed of mostly  $\alpha$ -helical bundles, which interacts with both SNARE complexes and lipids (Xu *et al.*, 2017). Solving the structures of MHD domains will be helpful to understand Ync13 functions.

We showed that the Ync13 C2 domain interacts with lipids, and is important for Ync13 localization (Figures, 3.2 and 3.3). The N terminal aa 1-590 of Ync13, is equally critical for Ync13 localization and function. The N termini of UNC-13/Munc13 family proteins interact with various binding partners for localization (Lu *et al.*, 2006; Kawabe *et al.*, 2017). Munc13-1 interacts with itself through its C2A domain at its N terminus in an autoinhibitory status (Lu *et al.*, 2006). Despite no predicted domain in the first 590 aa of Ync13, it still localizes to the division site (Figure 3.2 G). It is of great interest to identify Ync13's binding partners besides lipids, especially through its N terminus.

### **3.5.4 Septins as possible regulators of endocytosis**

Septins form highly ordered structures to serve as barriers and scaffolds at the cell cortex (Joo *et al.*, 2005; Bridges and Gladfelter, 2015). In fission yeast, the septins form a non-constricting ring during cytokinesis, and recruit the exocyst complex and glucanase Eng1 (Martin-Cuadrado *et al.*, 2005). In this and previous studies, we showed that ~60% of the

endocytic events occur near the rim at the division plane (Figure 3.12 C) (Wang *et al.*, 2016). Deletion of septins restore the Ede1 level across the division plane in *ync13Δ* (Figure 3.13), suggesting septins may also serve as a barrier for endocytosis.

Consistently, a recent study showed that septins are associated with endocytosis related proteins in budding yeast (Renz *et al.*, 2016). Thus, the septins could be an important factor for the balance of membrane trafficking during cytokinesis. We reason that the suppression does not result from the mislocalization of Eng1 caused by *spn1Δ*, because Eng1 is also mislocalized in a similar way in exocyst mutants, which display strong genetic interactions with Ync13 mutants (Figure 3.9 A) (Martin-Cuadrado *et al.*, 2005). Thus, the suppression of *spn1Δ* may result from the release of the exocyst complex and the restoration of endocytosis along the division plane.

In conclusion, we identified fission yeast UNC-13/Munc13 protein Ync13 as an essential regulator of cytokinesis. Instead of promoting SNARE complex assembly and vesicle fusion, Ync13 regulates the TRAPP-II mediated exocytosis and CME to ensure the proper distribution of the cell wall enzymes and cytokinesis regulators at the division site. It will be interesting to explore if other UNC-13/Munc13 proteins are also involved in endocytosis.

### **3.6 Acknowledgement**

We thank Drs. Juan Carlos, Vladimir Sirotkin, and Takashi Toda for yeast strains; Drs. Jianjie Ma and Mingzhai Sun for PALM; Campus Microscopy and Imaging facility at OSU and the Boulder Electron Microscopy Services at University of Colorado for help with EM; Anita Hopper, Dmitri Kudryashov, and Stephen Osmani laboratories for equipment; Victoria Esser in Rizo lab for helping with liposome co-floatation assays; the

current and former members of the Wu lab and rotation student Vedud Purde for helpful suggestions and assistances. Work in Chapter 3 was supported by a Pelotonia graduate fellowship to Y.-H. Zhu, a Pelotonia undergraduate fellowship to J. Hyun , and the National Institutes of Health grant R01 GM118746 to J.-Q. Wu.

**Table 3.1 Genetic interactions between *ync13* mutants and other mutants affecting cytokinesis and membrane trafficking<sup>a</sup>**

	25°C	30°C	32°C	36°C
<i>ync13-4</i>	+++ <sup>b</sup>	+++	++ <sup>c</sup>	+ <sup>d</sup>
<b>Contractile ring</b>				
<i>myo2-E1</i>	+++	++	+	+
<i>myo2-E ync13-4</i>	++	+	- <sup>e</sup>	-
<i>cdc15-140</i>	+++	+	-	-
<i>cdc15-140 ync13-4</i>	+++	+	-	-
<i>imp2Δ</i>	+	/ <sup>f</sup>	/	/
<i>imp2Δ ync13-4</i>	-	/	/	/
<i>fic1Δ</i>	+++	+++	++	++
<i>fic1Δ ync13-4</i>	+++	+++	++	+
<i>pxl1Δ</i>	+++	+++	+++	++
<i>pxl1Δ ync13-4</i>	+++	++	+	+
<b>Glucan synthases and glucanases</b>				
<i>bgs1-191</i>	+++	+++	++	-
<i>bgs1-191 ync13-4</i>	++	++	-	-
<i>cwgl-2</i>	+++	+++	++	+
<i>cwgl-2 ync13-4</i>	+++	++	+	-
<i>mok1-664</i>	+++	+++	+	-
<i>mok1-664 ync13-4</i>	+++	+++	-	-
<i>eng1Δ</i>	+++	+++	+++	+++
<i>eng1Δ ync13-4</i>	+++	+++	++	++
<i>agn1Δ</i>	+++	+++	+++	+++
<i>agn1Δ ync13-4</i>	+++	+++	++	+
<b>Rho GTPase dependent cell integrity pathway</b>				
<i>rho1-596</i>	+++	/	/	/
<i>rho1-596 ync13-4</i>	-	/	/	/
<i>rho2Δ</i>	+++	+++	+++	+++
<i>rho2Δ ync13-4</i>	+++	+++	++	+
<i>art1Δ</i>	++	/	/	/
<i>art1Δ ync13-4</i>	-	/	/	/
<i>rga7Δ</i>	+	/	/	/
<i>rga7Δ ync13-4</i>	-	/	/	/
<i>pck1Δ</i>	+++	+++	+++	++
<i>pck1Δ ync13-4</i>	+	-	-	-
<i>pck2Δ</i>	+++	+++	++	++
<i>pck2Δ ync13-4</i>	+++	+++	+	+

Continued

**Table 3.1: Continued**

<b>Exocytosis</b>				
<i>sec8-1</i>	+++	++	++	-
<i>sec8-1 ync13-4</i>	++	+	-	-
<i>sec8-1 ync13-19</i>	++	+	-	-
<i>exo70Δ</i>	+++	+++	+++	++
<i>exo70Δ ync13-4</i>	+++	+++	++	-
<i>sec3-913</i>	+++	+++	++	+
<i>sec3-913 ync13-4</i>	+++	+++	+	-
<i>sec3-916</i>	+++	+++	++	-
<i>sec3-916 ync13-4</i>	+	-	-	-
<i>myo52Δ</i>	+++	++	++	+
<i>myo52Δ ync13-4</i>	+++	++	+	+
<i>rho3Δ</i>	+++	+++	+++	+++
<i>rho3Δ ync13-4</i>	+++	+++	+	+
<i>trs120-ts1</i>	+++	+++	+++	-
<i>trs120-ts1 ync13-4</i>	+++	+++	++	-
<b>Endocytosis</b>				
<i>end4Δ</i>	+	-	-	-
<i>end4Δ ync13-4</i>	+	-	-	-
<i>pan1ΔACV</i>	+++	+++	+++	+++
<i>pan1ΔACV ync13-4</i>	+++	+++	++	+
<i>fim1Δ</i>	+++	+++	+++	++
<i>fim1Δ ync13-4</i>	+++	+++	++	+
<i>arp2-1</i>	+++	+++	++	+
<i>arp2-1 ync13-4</i>	+++	+++	++	+
<i>acp2Δ</i>	+++	+++	+++	+++
<i>acp2Δ ync13-4</i>	+++	+++	++	+
<i>wsp1Δ</i>	+++	+++	+++	+++
<i>wsp1Δ ync13-4</i>	+++	+++	++	++
<b>Other mutants</b>				
<i>its3-1</i>	+++	++	+	-
<i>its3-1 ync13-4</i>	+++	++	+	-
<i>spn1Δ</i>	+++	+++	+++	+++
<i>spn1Δ ync13-4</i>	+++	+++	++	+
<i>cdc42-1625</i>	+++	/	/	/
<i>cdc42-1625 ync13-4</i>	-	/	/	/
<i>rho4Δ</i>	+++	+++	+++	+++
<i>rho4Δ ync13-4</i>	+++	+++	+++	++

Continued

<b>Table 3.1: Continued</b>				
<b><i>ync13Δ</i> on EMM5S</b>	25°C	30°C	32°C	36°C
<i>ync13Δ</i>	++	++	++	++
<i>lad1-1(rgf3)</i>	+++	+++	++	++
<i>lad1-1(rgf3) ync13Δ</i>	++	+	-	-
<b><i>ync13Δ</i> on YE5S</b>	25°C	30°C	32°C	36°C
<i>ync13Δ</i>	-	/	/	/
<i>eng1Δ</i>	+++	/	/	/
<i>eng1Δ ync13Δ</i>	++	/	/	/
<i>agn1Δ</i>	+++	/	/	/
<i>agn1Δ ync13Δ</i>	-	/	/	/
<i>spn1Δ</i>	+++	/	/	/
<i>spn1Δ ync13Δ</i>	++	/	/	/

<sup>a</sup>Growth and color of colonies on YE5S with phloxin B plates at various temperatures

<sup>b</sup>+++, similar to wt; <sup>c</sup>++, some cell lysis or cytokinesis defects; <sup>d</sup>+, massive cell lysis,

severe cytokinesis defects with reduced growth; <sup>e</sup>-, inviable; <sup>f</sup>/, not tested

**Table 3.2 Strains used in Chapter 3**

Strain	Genotype	Source
JW5664	<i>h<sup>-</sup> ync13-mECitrine-kanMX6 ade6-210 ura4-D18 leu1-32</i>	Chapter 3
JW5969	<i>sad1-mCherry-natMX6 ync13-mECitrine-kanMX6 ade6-M210 leu1-32 ura4-D18</i>	Chapter 3
JW6657	<i>ync13-mECitrine-kanMX6 rlc1-mCherry-natMX6 ade6-210 leu1-32 ura4-D18</i>	Chapter 3
JW5814	<i>h<sup>-</sup> ync13-mMaple3-kanMX6 ade6-210 leu1-32 ura4-D18</i>	Chapter 3
JW5689	<i>ync13-mECitrine-kanMX6 cdc15-140 ade6-210 leu1-32 ura4-D18</i>	Chapter 3
JW5967	<i>its3-1 ync13-mECitrine-kanMX6 ade6-210 leu1-32 ura4-D18</i>	Chapter 3
JW5984	<i>h<sup>-</sup> kanMX6-Pync13-mECitrine-ync13(591-1237) ade6-M216 leu1-32 ura4-D18</i>	Chapter 3
JW5985	<i>h<sup>-</sup> ync13(1-1013)-mECitrine-kanMX6 ade6-M216 leu1-32 ura4-D18</i>	Chapter 3
JW5986	<i>h<sup>-</sup> ync13(1-804)-mECitrine-kanMX6 ade6-M216 leu1-32 ura4-D18</i>	Chapter 3
JW5987	<i>h<sup>-</sup> ync13(1-590)-mECitrine-kanMX6 ade6-M216 leu1-32 ura4-D18</i>	Chapter 3
JW5861	<i>ync13Δ::kanMX6 rlc1-tdTomato-natMX6 ade6 leu1-32 ura4-D18</i>	Chapter 3
JW4008	<i>h<sup>-</sup> nod1-mECitrine-kanMX6 ade6-M210 leu1-32 ura4-D18</i>	Zhu <i>et al.</i> , 2013
JW4912	<i>Pgef2-mECitrine-4Gly-gef2 ade6 leu1-32 ura4-D18</i>	Zhu <i>et al.</i> , 2013
JW3952	<i>h<sup>-</sup> rng8-mECitrine-kanMX6 ade6-M210 leu1-32 ura4-D18</i>	Wang <i>et al.</i> , 2014
JW4946	<i>h<sup>-</sup> rng9-mECitrine-kanMX6 ade6-M210 leu1-32 ura4-D18</i>	Wang <i>et al.</i> , 2014
JW81	<i>h<sup>-</sup> ade6-210 ura4-D18 leu1-32</i>	Lab stock
YZ3-2	<i>ync13<sup>+</sup>/ync13Δ::kanMX6 rlc1-tdTomato/rlc1-tdTomato ade6-210/ade6-216 leu1-32/leu1-32 ura4-D18/ura4-D18</i>	Chapter 3
JW1341	<i>h<sup>-</sup> rlc1-tdTomato-natMX6 ade6-M210 leu1-32 ura4-D18</i>	Lab stock
JW3313	<i>h<sup>-</sup> kanMX6-3nmt1-mEGFP rlc1-tdTomato-natMX6 ade6-M210 leu1-32 ura4-D18</i>	Chapter 3

Continued

**Table 3.2: Continued**

---

JW5983	<i>ync13Δ::kanMX6 rlc1-tdTomato-natMX6 kanMX6-3nmt1-mEGFP ade6 leu1-32 ura4-D18</i>	Chapter 3
JW5862	<i>ync13-4-his5-kanMX6 ade6-M210 leu1-32 ura4</i>	Chapter 3
JW5895	<i>h<sup>-</sup> rho1-596-natMX6 leu1-32 ura4D-18</i>	Viana <i>et al.</i> , 2013
JW5971	<i>ync13Δ::kanMX6 rlc1-tdTomato-natMX6 ade6 leu1-32 ura4-D18+ pUR19-Rho1</i>	Chapter 3
JW5972	<i>ync13Δ::kanMX6 rlc1-tdTomato-natMX6 ade6 leu1-32 ura4-D18+ pUR19</i>	Chapter 3
JW2245	<i>h<sup>+</sup> rgf3-mECitrine-kanMX6 ade6-M210 leu1-32 ura4-D18</i>	Davidson <i>et al.</i> , 2015
JW6544	<i>h<sup>-</sup> rgf3-mECitrine-kanMX6 ync13Δ::kanMX6 ade6 leu1-32 ura4-D18</i>	Chapter 3
JW1170	<i>h<sup>+</sup> pck2-mYFP-kanMX6 ade6-M210 leu1-32 ura4-D18</i>	Chapter 3
JW6065	<i>ync13Δ::kanMX6 pck2-mYFP-kanMX6 ade6 leu1-32 ura4-D18</i>	Chapter 3
JW5593	<i>h<sup>-</sup> leu1::kanMX6-P3nmt1-pkc1(HR1-C2)-mECitrine ade6-M210 leu1-32 ura4-D18</i>	Chapter 3
JW6004	<i>ync13Δ::kanMX6 leu1::kanMX6-P3nmt1-pkc1(HR1-C2)-mECitrine ade6 leu1-32 ura4-D18</i>	Chapter 3
JW5928	<i>h<sup>+</sup> rho1-596-natMX6 ync13-mECitrine-kanMX6 ade6-210 leu1-32 ura4-D18</i>	Chapter 3
JW5249	<i>GFP-bgs1-leu1<sup>+</sup> bgs1Δ::ura4<sup>+</sup> rlc1-tdTomato-natMX6 ade6-M210 leu1-32 ura4-D18</i>	Chapter 3
JW6616	<i>GFP-bgs1-leu1<sup>+</sup> bgs1Δ::ura4<sup>+</sup> ync13Δ::kanMX6 rlc1-tdTomato-natMX6 ade6 ura4-D18</i>	Chapter 3
JW6153	<i>bgs4Δ::ura4<sup>+</sup> Pbgs4<sup>+</sup>::GFP-bgs4<sup>+</sup>-leu1<sup>+</sup> rlc1-tdTomato-natMX6 leu1-32 ura4-D18</i>	Chapter 3
JW6152	<i>bgs4Δ::ura4<sup>+</sup> Pbgs4<sup>+</sup>::GFP-bgs4<sup>+</sup>-leu1<sup>+</sup> ync13Δ::kanMX6 rlc1-tdTomato-natMX6 leu1-32 ura4-D18 his3-D1 ade6</i>	Chapter 3
JW6808	<i>ync13Δ::kanMX6 rlc1-tdTomato-natMX6 ags1Δ 3'UTRags1<sup>+</sup>::ags1<sup>+</sup>-GFP:leu1<sup>+</sup>:ura4<sup>+</sup>ade6 leu1-32 ura4-D18</i>	Chapter 3
JW6810	<i>rlc1-tdTomato-natMX6 ags1Δ 3'UTRags1<sup>+</sup>::ags1<sup>+</sup>-GFP:leu1<sup>+</sup>:ura4<sup>+</sup>ade6 leu1-32 ura4-D18</i>	Chapter 3
JW6747	<i>ync13Δ::kanMX6 eng1-GFP-kanMX6 rlc1-tdTomato-natMX6 ade6 leu1-32 ura4-D18</i>	Chapter 3
		Continued

---

---

**Table 3.2: Continued**

JW6748	<i>eng1-GFP-kanMX6 rlc1-tdTomato-natMX6 ade6 leu1-32 ura4-D18</i>	Chapter 3
JW1696	<i>h<sup>+</sup> bgs1-191 ade6-M210 leu1-32 ura4-D18</i>	Chapter 3
JW6778	<i>ync13-4-his5-kanMX6 bgs1-191 ade6-M210 leu1-32 ura4</i>	Chapter 3
JW7551	<i>cwg1-2 ade6-M210 leu1-32 ura4</i>	Chapter 3
JW7549	<i>ync13-4-his5-kanMX6 cwg1-2 ade6-M210 leu1-32 ura4</i>	Chapter 3
JW7577	<i>h<sup>-</sup> mok1-664 ync13-4-his5-kanMX6 leu1</i>	Chapter 3
DH664	<i>h<sup>-</sup> leu1 mok1-664</i>	Katayama <i>et al.</i> , 1999
JW2319	<i>h<sup>+</sup> eng1Δ::kanMX4 ade6 leu1-32 ura4-D18</i>	Chapter 3
JW6745	<i>ync13Δ::kanMX6 eng1Δ::kanMX4 rlc1-tdTomato-natMX6 ade6 leu1-32 ura4-D18</i>	Chapter 3
JW3915	<i>h<sup>+</sup> sec8-1 leu1-32 ura4-D18</i>	Lab stock
JW5931	<i>sec8-1 ync13-4-his5-kanMX6 ade6 leu1-32 ura4-D18</i>	Chapter 3
JW7294	<i>sec8-1 GFP-bgs1-leu1<sup>+</sup> bgs1Δ::ura4<sup>+</sup> rlc1-tdTomato-natMX6 ade6-M210 leu1-32 ura4-D18</i>	Chapter 3
JW5911	<i>h<sup>+</sup> ync13-4-his5-kanMX6 GFP-bgs1-leu1<sup>+</sup> bgs1Δ::ura4<sup>+</sup> rlc1-tdTomato-natMX6 ade6-M210 leu1-32 ura4</i>	Chapter 3
JW7516	<i>sec8-1 ync13-4-his5-kanMX6 GFP-bgs1-leu1<sup>+</sup> bgs1Δ::ura4<sup>+</sup> rlc1-tdTomato-natMX6 ade6-M210 leu1-32 ura4</i>	Chapter 3
JW6550	<i>h<sup>-</sup> GFP-syb1-kanMX6 ade6 leu1-32 ura4-D18</i>	Chapter 3
JW7339	<i>ync13-19-his5-kanMX6 GFP-syb1-kanMX6 sec8-1 ade6 leu1-32 ura4</i>	Chapter 3
JW7341	<i>ync13-19-his5-kanMX6 GFP-syb1-kanMX6 ade6 leu1-32 ura4</i>	Chapter 3
JW6549	<i>GFP-syb1-kanMX6 sec8-1 ade6 leu1-32 ura4-D18</i>	Chapter 3
JW2716	<i>h<sup>+</sup> exo70Δ::kanMX4 ade6 leu1-32 ura4-D18</i>	Lab stock
JW5929	<i>exo70Δ::kanMX4 ync13-4-his5-kanMX6 ade6 leu1-32 ura4-D18</i>	Chapter 3
JW7062	<i>sec3-GFP-kanMX6 rlc1-tdTomato-natMX6 ade6 leu1-32 ura4-D18</i>	Chapter 3

Continued

**Table 3.2: Continued**

JW7066	<i>sec3-GFP-kanMX6 ync13Δ::kanMX6 rlc1-tdTomato-natMX6 ade6 leu1-32 ura4-D18</i>	Chapter 3
JW7061	<i>h<sup>-</sup> sec8-GFP-ura4<sup>+</sup> rlc1-tdTomato-natMX6 leu1-32 ura4-D18</i>	Chapter 3
JW7065	<i>sec8-GFP-ura4<sup>+</sup> ync13Δ::kanMX6 rlc1-tdTomato-natMX6 leu1-32 ura4-D18</i>	Chapter 3
JW7320	<i>trs120-3GFP-kanMX6 rlc1-tdTomato-natMX6 ade6 leu1-32 ura4-D18</i>	Wang <i>et al.</i> , 2016
JW7318	<i>ync13Δ::kanMX6 trs120-3GFP-kanMX6 rlc1-tdTomato-natMX6 ade6 leu1-32 ura4-D18</i>	Chapter 3
JW6208	<i>ync13Δ::kanMX6 GFP-syb1-kanMX6 rlc1-tdTomato-natMX6 ade6 leu1-32</i>	Chapter 3
JW6548	<i>h<sup>+</sup> GFP-syb1-kanMX6 rlc1-tdTomato-natMX6 ade6 leu1-32 ura4-D18</i>	Chapter 3
JW7356	<i>kanMX6-Pypt3-mEGFP-ypt3 rlc1-tdTomato-natMX6 ade6 leu1-32 ura4-D18</i>	Wang <i>et al.</i> , 2016
JW7357	<i>kanMX6-Pypt3-mEGFP-ypt3 ync13Δ::kanMX6 rlc1-tdTomato-natMX6 ade6 leu1-32 ura4-D18</i>	Chapter 3
JW7056	<i>h<sup>-</sup> rlc1-tdTomato-natMX6 fim1-mEGFP-kanMX6 ade6 leu1-32 ura4-D18</i>	Chapter 3
JW7057	<i>fim1-mEGFP-kanMX6 rlc1-tdTomato-natMX6 ync13Δ::kanMX6 ade6 leu1-32 ura4-D18</i>	Chapter 3
JW7191	<i>ede1-mGFP-kanMX6 ync13Δ::kanMX6 rlc1-tdTomato-natMX6 ade6 leu1-32 ura4-D18</i>	Chapter 3
JW7194	<i>ede1-mGFP-kanMX6 rlc1-tdTomato-natMX6 ade6 leu1-32 ura4-D18</i>	Chapter 3
JW7193	<i>pan1-mGFP-kanMX6 rlc1-tdTomato-natMX6 ade6 leu1-32 ura4-D18</i>	Chapter 3
JW7190	<i>pan1-mGFP-kanMX6 ync13Δ::kanMX6 rlc1-tdTomato-natMX6 ade6 leu1-32 ura4-D18</i>	Chapter 3
JW7192	<i>end4-mGFP-kanMX6 rlc1-tdTomato-natMX6 ade6 leu1-32 ura4-D18</i>	Chapter 3
JW7189	<i>end4-mGFP-kanMX6 ync13Δ::kanMX6 rlc1-tdTomato-natMX6 ade6 leu1-32 ura4-D18</i>	Chapter 3
JW7242	<i>ede1-mGFP-kanMX6 ync13Δ::kanMX6 rlc1-tdTomato-natMX6 spn1-Δ2::kanMX6 leu1-32 ura4-D18</i>	Chapter 3
JW7243	<i>ede1-mGFP-kanMX6 rlc1-tdTomato-natMX6 spn1-Δ2::kanMX6 leu1-32 ura4-D18</i>	Chapter 3
JW7523	<i>rlc1-tdTomato-natMX6 fim1-mEGFP-kanMX6 spn1-Δ2::kanMX6 ade6 leu1-32 ura4-D18</i>	Chapter 3
		Continued

**Table 3.2: Continued**

---

JW7522	<i>fim1-mEGFP-kanMX6 rlc1-tdTomato-natMX6 ync13Δ::kanMX6 spn1-Δ2::kanMX6 ade6 leu1-32 ura4-D18</i>	Chapter 3
JW5888	<i>myo2-E1 ync13-4-his5-kanMX6 ade6 leu1-32 ura4</i>	Chapter 3
JW2252	<i>myo2-E1 ade6 leu1-32 ura4-D18</i>	Chapter 3
JW5887	<i>cdc15-140 ync13-4-his5-kanMX6 ade6-M210 leu1-32 ura4</i>	Chapter 3
JW1743	<i>cdc15-140 ade6-M210 leu1-32 ura4-D18</i>	Chapter 3
JD141	<i>h<sup>-</sup> imp2Δ::ura4<sup>+</sup> ade6-M216 leu1-32 ura4-D18</i>	Lab stock
JW3563	<i>h<sup>-</sup> art1Δ::kanMX6 ade6-210 leu1-32 ura4-D18</i>	Chapter 3
JW4028	<i>h<sup>-</sup> rga7Δ::kanMX6 ade6-M210 leu1-32 ura4-D18</i>	Chapter 3
JW3039	<i>h<sup>+</sup> pck1Δ::kanMX4 ade6 leu1-32 ura4-D18</i>	Chapter 3
JW5996	<i>pck2-Δ1::kanMX6 ync13-4-his5-kanMX6 ade6 leu1-32 ura4-D18</i>	Chapter 3
JW376	<i>h<sup>+</sup> pck2-Δ1::kanMX6 ade6 leu1-32 ura4-D18</i>	Chapter 3
IJ767	<i>h<sup>-</sup> sec3-913-hphMX6 ade6-M216 leu1-32 ura4-D18</i>	Jourdain, <i>et al.</i> , 2012
JW6517	<i>sec3-913-hphMX6 ync13-4-his5-kanMX6 ade6 leu1-32 ura4</i>	Chapter 3
IJ1032	<i>h<sup>-</sup> sec3-916-hphMX6 ade6-M216 leu1-32 ura4-D18</i>	Jourdain, <i>et al.</i> , 2012
JW6519	<i>sec3-916-hphMX6 ync13-4-his5-kanMX6 ade6 leu1-32 ura4</i>	Chapter 3
JW6002	<i>h<sup>-</sup> rho3Δ::natMX6 ade6-210 leu1-32 ura4-D18</i>	Chapter 3
JW6515	<i>h<sup>-</sup> rho3Δ::natMX6 ync13-4-his5-kanMX6 ade6-210 leu1-32 ura4</i>	Chapter 3
JW7036	<i>h<sup>-</sup> trs120-ts1-his5-kanMX6 his5D ade6-M210 leu1-32 ura4</i>	Chapter 3
JW7383	<i>ync13-4-his5-kanMX6 trs120-ts1-his5-kanMX6 ade6-M210 leu1-32 ura4</i>	Chapter 3
VS845	<i>h<sup>+</sup> end4Δ::kanMX6 ade6-M210 leu1-32 ura4-D18 his3-D1</i>	V. Sirotkin Lab
JW7526	<i>h<sup>-</sup> ync13-4-his5-kanMX6 end4Δ::kanMX6 ade6 leu1-32 ura4 his3-D1</i>	Chapter 3
		Continued

---

**Table 3.2: Continued**

VS822	<i>h<sup>+</sup> pan1ΔACV::kanMX6 ade6-M210 leu1-32 ura4-D18 his3-D1</i>	V. Sirotkin Lab
JW7524	<i>h<sup>+</sup> ync13-4-his5-kanMX6 pan1ΔACV::kanMX6 ade6-M210 leu1-32 ura4</i>	Chapter 3
JW2244	<i>h<sup>+</sup> fic1Δ::kanMX4 ade6 leu1-32 ura4-D18</i>	Chapter 3
JW6617	<i>h<sup>+</sup> fic1Δ::kanMX4 ync13-4-his5-kanMX6ade6 leu1-32 ura4</i>	Chapter 3
JW2640	<i>h<sup>+</sup> pxl1Δ::kanMX4 ade6 leu1-32 ura4-D18</i>	Chapter 3
JW6622	<i>h<sup>+</sup> pxl1Δ::kanMX4 ync13-4-his5-kanMX6 ade6 leu1-32 ura4</i>	Chapter 3
JW3962	<i>rho2Δ::kanMX4 ade6 leu1-32 ura4-D18</i>	Chapter 3
JW6060	<i>h<sup>-</sup> rho2Δ::hphMX6 ade6-210 leu1-32 ura4-D18</i>	Chapter 3
JW6116	<i>ync13-4-his5-kanMX6 rho2D::hphMX6 ade6-M210 leu1-32 ura4-D18</i>	Chapter 3
JW1272	<i>h<sup>-</sup> myo52Δ::ura4<sup>+</sup> ade6-M210 leu1-32 ura4-D18</i>	Chapter 3
JW6818	<i>ync13-4-his5-kanMX6 myo52Δ::ura4<sup>+</sup> ade6-M210 leu1-32 ura4</i>	Chapter 3
JW144	<i>h<sup>-</sup> fim1-Δ1::kanMX6 ade6 leu1-32 ura4-D18</i>	Lab stock
JW6710	<i>ync13-4-his5-kanMX6 fim1-Δ1::kanMX6 ade6 leu1-32 ura4</i>	Chapter 3
JW1234	<i>h<sup>+</sup> arp2-1 mam2::leu2 ade6 leu1-32 ura4-D18</i>	Lab stock
JW6683	<i>ync13-4-his5-kanMX6 arp2-1 mam2::LEU2 ade6 leu1-32 ura4</i>	Chapter 3
JW1319	<i>h<sup>+</sup> acp2Δ::kanMX6 his7-366 leu1-32 ura4-D18 ade6-M210</i>	Lab stock
JW6682	<i>ync13-4-his5-kanMX6 acp2Δ::kanMX6 ade6-210 leu1-32 ura4</i>	Chapter 3
JW1240	<i>h<sup>-</sup> wsp1Δ::kanMX6 ade6-M216 leu1-32 ura4-D18 his3-D1</i>	Lab stock
JW6684	<i>ync13-4-his5-kanMX6 wsp1Δ::kanMX6 ade6 leu1-32 ura4-D18 his3-D1</i>	Chapter 3
JW6654	<i>eng1Δ::kanMX4 ync13-4-his5-kanMX6 ade6 leu1-32 ura4</i>	Chapter 3
JW2318	<i>h<sup>+</sup> agn1Δ::kanMX4 ade6 leu1-32 ura4-D18</i>	Lab stock

Continued

---

**Table 3.2: Continued**

JW6653	<i>h<sup>+</sup> agn1Δ::kanMX4 ync13-4-his5-kanMX6 ade6 leu1-32 ura4</i>	Chapter 3
JW1256	<i>h<sup>-</sup> its3-1 leu1-32</i>	Lab stock
JW5968	<i>h<sup>-</sup> its3-1 ync13-4-his5-kanMX6 leu1-32</i>	Chapter 3
JW289	<i>h<sup>+</sup> spn1-Δ2::kanMX6 leu1-32 ura4-D18</i>	Lab stock
JW5889	<i>spn1-Δ2::kanMX6 ync13-4-his5-kanMX6 ade6-M210 leu1-32 ura4</i>	Chapter 3
JW3054	<i>h<sup>+</sup> cdc42-1625(A158V)-kanMX leu1-32 ura4-D18</i>	Lab stock
JW3091	<i>h<sup>-</sup> rho4::kanMX6 leu1-32 ura4-D18</i>	Chapter 3
JW6514	<i>rho4Δ::kanMX6 ync13-4-his5-kanMX6 ade6 leu1-32 ura4</i>	Chapter 3
JW6066	<i>ync13Δ::kanMX6 ade6 leu1-32 ura4-D18</i>	Chapter 3
JW4751	<i>h<sup>-</sup> rgf3(lad1-1) ade6-M210 leu1-32 ura4-D18</i>	Lab stock
JW6547	<i>rgf3(lad1-1) ync13Δ::kanMX6 ade6 leu1-32 ura4-D18</i>	Chapter 3
JW6746	<i>ync13Δ::kanMX6 agn1Δ::kanMX4 ade6 leu1-32 ura4-D18</i>	Chapter 3

---

## Chapter 4: Conclusions and Future Directions

### 4.1 The roles of putative Rho GEF Gef2 and its binding partner Nod1 during early and late cytokinesis

In Chapter 2, I report a novel type-II node protein Nod1, which forms a complex with the Rho GEF Gef2 for regulating fission yeast cytokinesis. Nod1 and Gef2 interact via their C termini and are interdependent for their localization to the interphase nodes. At the G2/M transition, the Gef2-Nod1 complex coordinates with the POLO kinase Plo1 for the division site selection by maintaining the Anillin Mid1 at the medial cortex. The finding in my work that a GEF works with a small binding partner for its localization and functions provides a new perspective on the mechanisms of regulations on the Rho GEFs. In budding yeast, the Cdc42 GEF Cdc24 interacts with Bem1 for localization and GEF activities (Shimada *et al.*, 2004; Rapali *et al.*, 2017). Shortly after the publication of this work, another two studies suggested that the fission yeast Rho GEF Rgf3 and Rho GAP Rga7 both require a binding partner, Art1 and Rng10, respectively, for their localization (Davidson *et al.*, 2015; Liu *et al.*, 2016). It will be tempting to examine if the GEF/GAP-adaptor patterns exist for other Rho GEFs/GAPs in yeasts and higher model organisms. In addition, how Gef2-Nod1 complex localizes to the interphase nodes requires further investigation. Gef2 interacts with Mid1 (Ye *et al.*, 2012), and another node protein Blt1 recruits Gef2 and Nod1 (Guzman-Vendrell *et al.*, 2013; Jourdain *et al.*, 2013; Goss *et al.*, 2014). Further examination of the interphase nodes organizations and the structures of

Gef2-Mid1 and Gef2-Nod1-Blt1 interactions will shed more light on the mechanisms of division site selection.

During the later stages, the Gef2-Nod1 complex helps stabilize the contractile ring during ring constriction together with the F-BAR protein Cdc15. Cdc15, recruited by Mid1, is an important component in the cytokinesis nodes and contractile ring. Along with the other Pombe Cdc15 Homology (PCH) protein Imp2, Cdc15 interacts with multiple downstream partners to ensure the contractile ring stability and anchorage to the medial cortex (Arasada and Pollard, 2014; Martin-Garcia *et al.*, 2014; Ren *et al.*, 2015). In addition, Cdc15 facilitates the delivery of the cell wall synthase Bgs1 to the division site and prevent the contractile ring sliding (Arasada and Pollard, 2014). I found that Nod1 N terminus binds to Cdc15 for its contractile ring localization during ring constriction, and the contractile ring stability gets compromised when both Cdc15 and Gef2-Nod1 were mutated. Thus, the Cdc15-Nod1 interaction may also help recruit and stabilize Cdc15 at the division site. Further experiments are needed to examine the level and dynamics of Cdc15 and its downstream network in *nod1Δ*. Alternatively, Gef2 could affect Cdc15 levels through Mid1 (Ye *et al.*, 2012), or directly the cell wall synthesis through its potential activity on Rho1 during the late stages of cytokinesis.

The Gef2 GEF domain interacts with Rho1, Rho4 and Rho5. Gef2 also affects Rho4 localization to the division site, which suggests that Gef2 may be a potential GEF for Rho4. Indeed, our lab later identified Gef3 as a GEF for Rho4, and Gef3 collaborates with Gef2 to regulate Rho4 activity and localization (data unpublished) (Wang *et al.*, 2015). Although Rho GTPases regulate the early stages of cytokinesis by promoting the actin filament nucleation, myosin-II activation and targeted exocytosis at the division site

in budding yeast and animals, no such roles are reported in fission yeast (Imamura *et al.*, 1997; Kosako *et al.*, 2000; Piekny *et al.*, 2005; Pollard, 2010; Watanabe *et al.*, 2010).

Gef2 is the GEF that localizes to the division site during cytokinesis the earliest. We previously showed that Gef2 GEF domain is important for cleavage site selection (Ye *et al.*, 2012). Thus, it will be of great interest to know if Gef2 activates any Rho GTPases at this stage.

#### **4.2 The novel role of UNC-13/Munc13 protein during cytokinesis**

In Chapter 3, I report that the yeast UNC-13/Munc13 protein Ync13 maintains the homogenous distribution of exocytosis and endocytosis during cytokinesis, and prevents the accumulation of the cell wall synthases at the center of the division plane for proper cell wall formation. The UNC-13/Munc13 proteins are essential priming factors for the neuron transmitter release, insulin secretion and cytotoxic T cell functions (Richmond *et al.*, 1999; Sheu *et al.*, 2003; Rossner *et al.*, 2004; Dudenhoffer-Pfeifer *et al.*, 2013). They promote the SNARE complex assembly by opening the syntaxin-Munc18 closed conformation (Ma *et al.*, 2011; Yang *et al.*, 2015; Xu *et al.*, 2017). As a fungal member of the UNC-13/Munc13 family, Ync13 has a distinguished domain structure compared to its animal homologs where the characteristic MUN domain is separated by a C2 domain (Pei *et al.*, 2009). This may explain why the MHD1C2MHD2 domain fails in lipid mixing, content mixing or even lipid clustering in vitro unlike Munc13-1 does. However, it is still possible that Ync13 needs its N terminus aa1-590 to help the SNARE complex assembly. The N terminus of UNC-13/Munc13 proteins are responsible for protein-protein interactions and essential for protein localization in animal cells (Shen *et al.*, 2005; Lu *et al.*, 2006; Kwan *et al.*, 2007; Shin *et al.*, 2010). The deletion of Ync13 N

terminus is lethal, and causes a significant decrease of Ync13 local concentration at the division site. Thus, future work is needed to identify the role of Ync13 N terminus and its potential binding partners, and whether the full length Ync13 can promote the vesicle fusion and tethering.

What is the exact role of Ync13 during cytokinesis? The cell wall defects in *ync13Δ* cells result from the uneven distribution of cell wall enzymes and the membrane trafficking machinery. I propose two hypotheses for Ync13 function. First, Ync13 could affect membrane dynamics on the division site as it alters the distribution of exocytosis and endocytosis during cytokinesis. Previously our lab showed that the t-SNARE Psy1 is more dynamic at the division site than along the cell axis in FRAP assays (Wang *et al.*, 2016). Such analysis in *ync13Δ* cells will help examine the dynamic and diffusion of membrane markers along the division plane. Second, Ync13 may serve as a landmark for exocytosis and endocytosis. The interaction between Ync13 and the components of exocytosis, endocytosis and the SNARE complex, albeit transient, should be investigated.

Membrane trafficking is of great importance to cytokinesis as it provides the membrane and the materials needed for furrow ingression and extracellular matrix formation (Shuster and Burgess, 2002; Li *et al.*, 2006; Robinett *et al.*, 2009; Wu *et al.*, 2014). I show in Chapter 3 that improper delivery and unbalanced membrane trafficking cause cytokinesis defects. In *ync13Δ* cells, the TRAPP-II complex accumulates at the leading edge of the septum whereas the exocyst is not affected at the rim of the division plane. This observation supports our previous notion that the two complexes work redundantly but independently for vesicle delivery during cytokinesis (Wang *et al.*, 2016). In addition, the endocytic events are significantly reduced at the center region of

the division site in *ync13Δ* cells. The establishment of endocytosis has not been extensively studied in fission yeast compared to other model organisms. The discovery in Chapter 3 raises questions about how endocytosis contribute to cytokinesis. The combined defects in *ync13Δ* with biased exocytosis and absent endocytosis along the division plane emphasize the importance of membrane trafficking during cytokinesis.

Septins are important scaffold and barrier proteins during cytokinesis (Joo *et al.*, 2005; DeMay *et al.*, 2011; Bridges and Gladfelter, 2015). In *S. pombe*, the septins form a non-constricting ring at the division site and restrict the localization of the exocyst complex and glucanases (Martin-Cuadrado *et al.*, 2005). Unexpectedly, I found that the deletion of septins resumes endocytosis along the division plane in *ync13Δ*. Whether the septins directly regulate endocytosis or this is an indirect effect from mislocalized exocytosis is unknown. Interestingly, a recent study showed that the septins associate with several components of the endocytic pathway in budding yeast from mass spectrometry (Renz *et al.*, 2016; Song *et al.*, 2016). Thus, more work is needed to explore the roles of the septins in membrane trafficking during cytokinesis.

In summary, I characterize the functions of two novel proteins during different stages of fission yeast cytokinesis. Nod1 forms a complex with Rho GEF Gef2, and regulates the division site positioning and the contractile ring stability. The yeast UNC-13/Munc13 protein Ync13 ensures the proper distribution of the plasma membrane and cell wall materials on the division plane through both exocytosis and endocytosis. These findings complement our understanding of Rho GTPase regulation, exocytosis and endocytosis pathways, septins and cytokinesis, and hopefully, will provide new insights on future studies in the field.

## References

### Reference for Chapter 1

Adamo JE, Rossi G, and Brennwald P (1999). The Rho GTPase Rho3 has a direct role in exocytosis that is distinct from its role in actin polarity. *Mol Biol Cell* 10, 4121-4133.

Akamatsu M, Berro J, Pu KM, Tebbs IR, and Pollard TD (2014). Cytokinetic nodes in fission yeast arise from two distinct types of nodes that merge during interphase. *J Cell Biol* 204, 977-988.

Albertson R, Riggs B, and Sullivan W (2005). Membrane traffic: a driving force in cytokinesis. *Trends Cell Biol* 15, 92-101.

Almonacid M, Celton-Morizur S, Jakubowski JL, Dingli F, Loew D, Mayeux A, Chen JS, Gould KL, Clifford DM, and Paoletti A (2011). Temporal control of contractile ring assembly by Plo1 regulation of myosin II recruitment by Mid1/anillin. *Curr Biol* 21, 473-479.

Almonacid M, Moseley JB, Janvore J, Mayeux A, Fraisier V, Nurse P, and Paoletti A (2009). Spatial control of cytokinesis by Cdr2 kinase and Mid1/anillin nuclear export. *Curr Biol* 19, 961-966.

Aravamudan B, Fergestad T, Davis WS, Rodesch CK, and Broadie K (1999). *Drosophila* Unc-13 is essential for synaptic transmission. *Nat Neurosci* 2, 965-971.

- Archbold JK, Whitten AE, Hu SH, Collins BM, and Martin JL (2014). SNARE-ing the structures of Sec1/Munc18 proteins. *Curr Opin Struct Biol* 29, 44-51.
- Arellano M, Duran A, and Pérez P (1996). Rho1 GTPase activates the (1-3)beta-D-glucan synthase and is involved in *Schizosaccharomyces pombe* morphogenesis. *EMBO J* 15, 4584-4591.
- Bähler J, Steever AB, Wheatley S, Wang Y, Pringle JR, Gould KL, and McCollum D (1998). Role of polo kinase and Mid1p in determining the site of cell division in fission yeast. *J Cell Biol* 143, 1603-1616.
- Baro B, Queralt E, and Monje-Casas F (2017). Regulation of Mitotic Exit in *Saccharomyces cerevisiae*. *Methods Mol Biol* 1505, 3-17.
- Bedhomme M, Jouannic S, Champion A, Simanis V, and Henry Y (2008). Plants, MEN and SIN. *Plant Physiol Biochem* 46, 1-10.
- Betz A, Telemenakis I, Hofmann K, and Brose N (1996). Mammalian Unc-13 homologues as possible regulators of neurotransmitter release. *Biochem Soc Trans* 24, 661-666.
- Bhatia P, Hachet O, Hersch M, Rincón SA, Berthelot-Grosjean M, Dalessi S, Basterra L, Bergmann S, Paoletti A, and Martin SG (2013). Distinct levels in Pom1 gradients limit Cdr2 activity and localization to time and position division. *Cell Cycle* 13.
- Bidone TC, Tang H, and Vavylonis D (2014). Dynamic network morphology and tension buildup in a 3D model of cytokinetic ring assembly. *Biophys J* 107, 2618-2628.
- Bidone TC, Tang H, and Vavylonis D (2015). Insights into the Mechanics of Cytokinetic Ring Assembly Using 3D Modeling. *Proc Asme Int Mech Eng Congress Expo*, 2014, Vol 9.

- Boeke D, Trautmann S, Meurer M, Wachsmuth M, Godlee C, Knop M, and Kaksonen M (2014). Quantification of cytosolic interactions identifies Ede1 oligomers as key organizers of endocytosis. *Mol Syst Biol* 10.
- Bohnert KA, Grzegorzewska AP, Willet AH, Vander Kooi CW, Kovar DR, and Gould KL (2013). SIN-dependent phosphoinhibition of formin multimerization controls fission yeast cytokinesis. *Genes Dev* 27, 2164-2177.
- Boucrot E, and Kirchhausen T (2007). Endosomal recycling controls plasma membrane area during mitosis. *Proc Natl Acad Sci U S A* 104, 7939-7944.
- Brose N, Hofmann K, Hata Y, and Sudhof TC (1995). Mammalian homologues of *Caenorhabditis elegans* unc-13 gene define novel family of C2-domain proteins. *J Biol Chem* 270, 25273-25280.
- Calonge TM, Nakano K, Arellano M, Arai R, Katayama S, Toda T, Mabuchi I, and Pérez P (2000). *Schizosaccharomyces pombe* Rho2p GTPase regulates cell wall alpha-glucan biosynthesis through the protein kinase Pck2p. *Mol Biol Cell* 11, 4393-4401.
- Cerutti L, and Simanis V (1999). Asymmetry of the spindle pole bodies and spg1p GAP segregation during mitosis in fission yeast. *J Cell Sci* 112 ( Pt 14), 2313-2321.
- Chen CT, Feoktistova A, Chen JS, Shim YS, Clifford DM, Gould KL, and McCollum D (2008). The SIN kinase Sid2 regulates cytoplasmic retention of the *S. pombe* Cdc14-like phosphatase Clp1. *Curr Biol* 18, 1594-1599.
- Chen YA, and Scheller RH (2001). SNARE-mediated membrane fusion. *Nat Rev Mol Cell Biol* 2, 98-106.

- Coffman VC, Sees JA, Kovar DR, and Wu J-Q (2013). The formins Cdc12 and For3 cooperate during contractile ring assembly in cytokinesis. *J Cell Biol* 203, 101-114.
- Coffman VC, and Wu J-Q (2014). Every laboratory with a fluorescence microscope should consider counting molecules. *Mol Biol Cell* 25, 1545-1548.
- Cole GT. (1996). Basic Biology of Fungi. In: Medical Microbiology, ed. S. Baron, Galveston (TX).
- Coll PM, Trillo Y, Ametzazurra A, and Pérez P (2003). Gef1p, a new guanine nucleotide exchange factor for Cdc42p, regulates polarity in *Schizosaccharomyces pombe*. *Mol Biol Cell* 14, 313-323.
- Cortés JC, Sato M, Munoz J, Moreno MB, Clemente-Ramos JA, Ramos M, Okada H, Osumi M, Duran A, and Ribas JC (2012). Fission yeast Ags1 confers the essential septum strength needed for safe gradual cell abscission. *J Cell Biol* 198, 637-656.
- Cortés JCG, Carnero E, Ishiguro J, Sánchez Y, Duran A, and Ribas JC (2005). The novel fission yeast (1,3)beta-D-glucan synthase catalytic subunit Bgs4p is essential during both cytokinesis and polarized growth. *J Cell Sci* 118, 157-174.
- Cortés JCG, Ishiguro J, Duran A, and Ribas JC (2002). Localization of the (1,3)beta-D-glucan synthase catalytic subunit homologue Bgs1p/Cps1p from fission yeast suggests that it is involved in septation, polarized growth, mating, spore wall formation and spore germination. *J Cell Sci* 115, 4081-4096.
- Cortés JCG, Konomi M, Martins IM, Munoz J, Moreno MB, Osumi M, Duran A, and Ribas JC (2007). The (1,3)beta-D-glucan synthase subunit Bgs1p is responsible for the fission yeast primary septum formation. *Mol Microbiol* 65, 201-217.

- D'Agostino JL, and Goode BL (2005). Dissection of Arp2/3 complex actin nucleation mechanism and distinct roles for its nucleation-promoting factors in *Saccharomyces cerevisiae*. *Genetics* 171, 35-47.
- D'Avino PP, Giansanti MG, and Petronczki M (2015). Cytokinesis in animal cells. *Cold Spring Harb Perspect Biol* 7, a015834.
- Davidson R, Laporte D, and Wu J-Q (2015). Regulation of Rho-GEF Rgf3 by the arrestin Art1 in fission yeast cytokinesis. *Mol Biol Cell* 26, 453-466.
- De Franceschi N, Hamidi H, Alanko J, Sahgal P, and Ivaska J (2015). Integrin traffic - the update. *J Cell Sci* 128, 839-852.
- Deng L, and Moseley JB (2013). Compartmentalized nodes control mitotic entry signaling in fission yeast. *Mol Biol Cell*.
- Doi A, Kita A, Kanda Y, Uno T, Asami K, Satoh R, Nakano K, and Sugiura R (2015). Geranylgeranyltransferase Cwg2-Rho4/Rho5 module is implicated in the Pmk1 MAP kinase-mediated cell wall integrity pathway in fission yeast. *Genes Cells* 20, 310-323.
- Duncan MC, Cope MJ, Goode BL, Wendland B, and Drubin DG (2001). Yeast Eps15-like endocytic protein, Pan1p, activates the Arp2/3 complex. *Nat Cell Biol* 3, 687-690.
- Fielding AB, Schonteich E, Matheson J, Wilson G, Yu XZ, Hickson GRX, Srivastava S, Baldwin SA, Prekeris R, and Gould GW (2005). Rab11-FIP3 and FIP4 interact with Arf6 and the Exocyst to control membrane traffic in cytokinesis. *EMBO J* 24, 3389-3399.

- Foltman M, and Sánchez-Díaz A (2017). Studying the role of the mitotic exit network in cytokinesis. *Methods Mol Biol* 1505, 245-262.
- Fujiwara T, Bandi M, Nitta M, Ivanova EV, Bronson RT, and Pellman D (2005). Cytokinesis failure generating tetraploids promotes tumorigenesis in p53-null cells. *Nature* 437, 1043-1047.
- Furge KA, Cheng Q-C, Jwa M, Shin S, Song K, and Albright CF (1999). Regions of Byr4, a regulator of septation in fission yeast, that bind Spg1 or Cdc16 and form a two-component GTPase-activating protein with Cdc16. *J Biol Chem* 274, 11339-11343.
- Ganem NJ, Storchova Z, and Pellman D (2007). Tetraploidy, aneuploidy and cancer. *Curr Opin Genet Dev* 17, 157-162.
- García P, García I, Marcos F, de Garibay GR, and Sánchez Y (2009). Fission yeast *rgf2p* is a *rho1p* guanine nucleotide exchange factor required for spore wall maturation and for the maintenance of cell integrity in the absence of *rgf1p*. *Genetics* 181, 1321-1334.
- García P, Tajadura V, García I, and Sánchez Y (2006a). *Rgf1p* is a specific Rho1-GEF that coordinates cell polarization with cell wall biogenesis in fission yeast. *Mol Biol Cell* 17, 1620-1631.
- García P, Tajadura V, García I, and Sánchez Y (2006b). Role of Rho GTPases and Rho-GEFs in the regulation of cell shape and integrity in fission yeast. *Yeast* 23, 1031-1043.
- Giansanti MG, Vanderleest TE, Jewett CE, Sechi S, Frappaolo A, Fabian L, Robinett CC, Brill JA, Loerke D, Fuller MT, and Blankenship JT (2015). Exocyst-dependent

- membrane addition is required for anaphase cell elongation and cytokinesis in *Drosophila*. *Plos Genetics* 11 (11): e1005632.
- Goode BL, Eskin JA, and Wendland B (2015). Actin and Endocytosis in Budding Yeast. *Genetics* 199, 315-358.
- Goss JW, Kim S, Bledsoe H, and Pollard TD (2014). Characterization of the roles of Blt1p in fission yeast cytokinesis. *Mol Biol Cell* 25, 1946-1957.
- Gromley A, Yeaman C, Rosa J, Redick S, Chen CT, Mirabelle S, Guha M, Sillibourne J, and Doxsey SJ (2005). Centriolin anchoring of exocyst and SNARE complexes at the midbody is required for secretory-vesicle-mediated abscission. *Cell* 123, 75-87.
- Guertin DA, Chang L, Irshad F, Gould KL, and McCollum D (2000). The role of the sid1p kinase and cdc14p in regulating the onset of cytokinesis in fission yeast. *EMBO J* 19, 1803-1815.
- Guo W, Roth D, Walch-Solimena C, and Novick P (1999). The exocyst is an effector for Sec4p, targeting secretory vesicles to sites of exocytosis. *EMBO J* 18, 1071-1080.
- Guo W, Tamanoi F, and Novick P (2001). Spatial regulation of the exocyst complex by Rho1 GTPase. *Nat Cell Biol* 3, 353-360.
- Guzman-Vendrell M, Baldissard S, Almonacid M, Mayeux A, Paoletti A, and Moseley JB (2013). Blt1 and Mid1 provide overlapping membrane anchors to position the division plane in fission yeast. *Mol Cell Biol* 33, 418-428.
- Hachet O, and Simanis V (2008). Mid1p/anillin and the septation initiation network orchestrate contractile ring assembly for cytokinesis. *Genes Dev* 22, 3205-3216.
- Hall A (2012). Rho family GTPases. *Biochem Soc Trans* 40, 1378-1382.

- Harbury PA (1998). Springs and zippers: coiled coils in SNARE-mediated membrane fusion. *Structure* 6, 1487-1491.
- He B, and Guo W (2009). The exocyst complex in polarized exocytosis. *Curr Opin Cell Biol* 21, 537-542.
- Hirota K, Tanaka K, Ohta K, and Yamamoto M (2003). Gef1p and Scd1p, the Two GDP-GTP exchange factors for Cdc42p, form a ring structure that shrinks during cytokinesis in *Schizosaccharomyces pombe*. *Mol Biol Cell* 14, 3617-3627.
- Holly RM, Mavor LM, Zuo ZY, and Blankenship JT (2015). A rapid, membrane-dependent pathway directs furrow formation through RalA in the early *Drosophila* embryo. *Development* 142, 2316-2328.
- Hou MC, Salek J, and McCollum D (2000). Mob1p interacts with the Sid2p kinase and is required for cytokinesis in fission yeast. *Curr Biol* 10, 619-622.
- Imamura H, Tanaka K, Hihara T, Umikawa M, Kamei T, Takahashi K, Sasaki T, and Takai Y (1997). Bni1p and Bnr1p: downstream targets of the Rho family small G-proteins which interact with profilin and regulate actin cytoskeleton in *Saccharomyces cerevisiae*. *EMBO J* 16, 2745-2755.
- Iwaki T, Tanaka N, Takagi H, Giga-Hama Y, and Takegawa K (2004). Characterization of *end4<sup>+</sup>*, a gene required for endocytosis in *Schizosaccharomyces pombe*. *Yeast* 21, 867-881.
- James DJ, and Martin TF (2013). CAPS and Munc13: CATCHRs that SNARE Vesicles. *Front Endocrinol (Lausanne)* 4, 187.
- Johnson AE, McCollum D, and Gould KL (2012). Polar opposites: Fine-tuning cytokinesis through SIN asymmetry. *Cytoskeleton (Hoboken)* 69, 686-699.

- Jordan SN, and Canman JC (2012). Rho GTPases in animal cell cytokinesis: an occupation by the one percent. *Cytoskeleton (Hoboken)* 69, 919-930.
- Jordan SN, Olson S, and Canman JC (2011). Cytokinesis: thinking outside the cell. *Curr Biol* 21, R119-121.
- Jourdain I, Brzezinska EA, and Toda T (2013). Fission yeast Nod1 is a component of cortical nodes involved in cell size control and division site placement. *PLoS One* 8, e54142.
- Jurgens G, Park M, Richter S, Touihri S, Krause C, El Kasmi F, and Mayer U (2015). Plant cytokinesis: a tale of membrane traffic and fusion. *Biochem Soc Trans* 43, 73-78.
- Kabachinski G, Yamaga M, Kielar-Grevstad DM, Bruinsma S, and Martin TF (2013). CAPS and Munc13 utilize distinct PIP2-linked mechanisms to promote vesicle exocytosis. *Mol Biol Cell* 25, 508-521.
- Kao RS, Morreale E, Wang L, Ivey FD, and Hoffman CS (2006). *Schizosaccharomyces pombe* Git1 is a C2-domain protein required for glucose activation of adenylate cyclase. *Genetics* 173, 49-61.
- Kita A, Li C, Yu Y, Umeda N, Doi A, Yasuda M, Ishiwata S, Taga A, Horiuchi Y, and Sugiura R (2011). Role of the small GTPase Rho3 in Golgi/Endosome trafficking through functional interaction with Adaptin in fission yeast. *PLoS One* 6, e16842.
- Krapp A, and Simanis V (2008). An overview of the fission yeast septation initiation network (SIN). *Biochem Soc Trans* 36, 411-415.
- Laplante C, Huang F, Tebbs IR, Bewersdorf J, and Pollard TD (2016). Molecular organization of cytokinesis nodes and contractile rings by super-resolution

- fluorescence microscopy of live fission yeast. *Proc Natl Acad Sci U S A* 113, E5876-E5885.
- Laporte D, Coffman VC, Lee IJ, and Wu J-Q (2011). Assembly and architecture of precursor nodes during fission yeast cytokinesis. *J Cell Biol* 192, 1005-1021.
- Lee I-J, Coffman VC, and Wu J-Q (2012). Contractile-ring assembly in fission yeast cytokinesis: Recent advances and new perspectives. *Cytoskeleton (Hoboken)* 69, 751-763.
- Lee I-J, and Wu J-Q (2012). Characterization of Mid1 domains for targeting and scaffolding in fission yeast cytokinesis. *J Cell Sci* 125, 2973-2985.
- Lepore D, Spassibojko O, Pinto G, and Collins RN (2016). Cell cycle-dependent phosphorylation of Sec4p controls membrane deposition during cytokinesis. *J Cell Biol* 214, 691-703.
- Li WM, Webb SE, Lee KW, and Miller AL (2006). Recruitment and SNARE-mediated fusion of vesicles in furrow membrane remodeling during cytokinesis in zebrafish embryos. *Exp Cell Res* 312, 3260-3275.
- Liu XX, Seven AB, Camacho M, Esser V, Xu JJ, Trimbuch T, Quade B, Su LJ, Ma C, Rosenmund C, and Rizo J (2016). Functional synergy between the Munc13 C-terminal C-1 and C-2 domains. *Elife* 5, e13696.
- Lu R, and Drubin DG (2017). Selection and stabilization of endocytic sites by Ede1, a yeast functional homologue of human Eps15. *Mol Biol Cell* 28, 567-575.
- Lu R, Drubin DG, and Sun YD (2016). Clathrin-mediated endocytosis in budding yeast at a glance. *J Cell Sci* 129, 1531-1536.

- Lu X, Zhang Y, and Shin YK (2008). Supramolecular SNARE assembly precedes hemifusion in SNARE-mediated membrane fusion. *Nat Struct Mol Biol* 15, 700-706.
- Madison JM, Nurrish S, and Kaplan JM (2005). UNC-13 interaction with syntaxin is required for synaptic transmission. *Curr Biol* 15, 2236-2242.
- Mardilovich K, Olson MF, and Baugh M (2012). Targeting Rho GTPase signaling for cancer therapy. *Future Oncol* 8, 165-177.
- Martin-Cuadrado AB, Morrell JL, Konomi M, An H, Petit C, Osumi M, Balasubramanian M, Gould KL, Del Rey F, and de Aldana CR (2005). Role of septins and the exocyst complex in the function of hydrolytic enzymes responsible for fission yeast cell separation. *Mol Biol Cell* 16, 4867-4881.
- McNew JA (2008). Regulation of SNARE-mediated membrane fusion during exocytosis. *Chem Rev* 108, 1669-1686.
- Mehta S, and Gould KL (2006). Identification of functional domains within the septation initiation network kinase, Cdc7. *J Biol Chem* 281, 9935-9941.
- Montagnac G, Echard A, and Chavrier P (2008). Endocytic traffic in animal cell cytokinesis. *Curr Opin Cell Biol* 20, 454-461.
- Morrell-Falvey JL, Ren L, Feoktistova A, Haese GD, and Gould KL (2005). Cell wall remodeling at the fission yeast cell division site requires the Rho-GEF Rgf3p. *J Cell Sci* 118, 5563-5573.
- Moseley JB, Mayeux A, Paoletti A, and Nurse P (2009). A spatial gradient coordinates cell size and mitotic entry in fission yeast. *Nature* 459, 857-860.

- Munoz S, Manjon E, and Sánchez Y (2014). The putative exchange factor Gef3p interacts with Rho3p GTPase and the septin ring during cytokinesis in fission yeast. *J Biol Chem* 289, 21995-22007.
- Mutoh T, Nakano K, and Mabuchi I (2005). Rho1-GEFs Rgf1 and Rgf2 are involved in formation of cell wall and septum, while Rgf3 is involved in cytokinesis in fission yeast. *Genes Cells* 10, 1189-1202.
- Nakano K, Arai R, and Mabuchi I (2005). Small GTPase Rho5 is a functional homologue of Rho1, which controls cell shape and septation in fission yeast. *Febs Letters* 579, 5181-5186.
- Nakayama K (2016). Regulation of cytokinesis by membrane trafficking involving small GTPases and the ESCRT machinery. *Crit Rev Biochem Mol Biol* 51, 1-6.
- Naqvi SN, Zahn R, Mitchell DA, Stevenson BJ, and Munn AL (1998). The WASp homologue Las17p functions with the WIP homologue End5p/verprolin and is essential for endocytosis in yeast. *Curr Biol* 8, 959-962.
- Neto H, Balmer G, and Gould G (2013). Exocyst proteins in cytokinesis: Regulation by Rab11. *Commun Integr Biol* 6, e27635.
- Ojkic N, Wu J-Q, and Vavylonis D (2011). Model of myosin node aggregation into a contractile ring: the effect of local alignment. *J Phys Condens Matter* 23, 374103.
- Pei JM, Ma C, Rizo J, and Grishin NV (2009). Remote Homology between Munc13 MUN Domain and Vesicle Tethering Complexes. *J Mol Biol* 391, 509-517.
- Pellinen T, Tuomi S, Arjonen A, Wolf M, Edgren H, Meyer H, Grosse R, Kitzing T, Rantala JK, Kallioniemi O, Fassler R, Kallio M, and Ivaska J (2008). Integrin trafficking regulated by Rab21 is necessary for cytokinesis. *Dev Cell* 15, 371-385.

- Pérez P, Portales E, and Santos B (2015). Rho4 interaction with exocyst and septins regulates cell separation in fission yeast. *Microbiology* 161, 948-959.
- Piekny A, Werner M, and Glotzer M (2005). Cytokinesis: welcome to the Rho zone. *Trends Cell Biol* 15, 651-658.
- Pollard TD (2010). Mechanics of cytokinesis in eukaryotes. *Curr Opin Cell Biol* 22, 50-56.
- Pollard TD, and Wu J-Q (2010). Understanding cytokinesis: lessons from fission yeast. *Nat Rev Mol Cell Biol* 11, 149-155.
- Proctor SA, Minc N, Boudaoud A, and Chang F (2012). Contributions of turgor pressure, the contractile ring, and septum assembly to forces in cytokinesis in fission yeast. *Curr Biol* 22, 1601-1608.
- Pu KM, Akamatsu M, and Pollard TD (2015). The septation initiation network controls the assembly of nodes containing Cdr2p for cytokinesis in fission yeast. *J Cell Sci* 128, 441-446.
- Rincón S, Coll PM, and Pérez P (2007). Spatial regulation of Cdc42 during cytokinesis. *Cell Cycle* 6, 1687-1691.
- Rincón SA, Estravis M, Dingli F, Loew D, Tran PT, and Paoletti A (2017). SIN-Dependent Dissociation of the SAD Kinase Cdr2 from the Cell Cortex Resets the Division Plane. *Curr Biol* 27, 534-542.
- Rincón SA, Santos B, and Pérez P (2006). Fission yeast Rho5p GTPase is a functional paralogue of Rho1p that plays a role in survival of spores and stationary-phase cells. *Eukaryot Cell* 5, 435-446.

- Rizo J, and Sudhof TC (2012). The Membrane Fusion Enigma: SNAREs, Sec1/Munc18 Proteins, and Their Accomplices-Guilty as Charged? *Annu Rev Cell Dev Biol* 28, 279-308.
- Rizo J, and Xu J (2015). The Synaptic Vesicle Release Machinery. *Annu Rev Biophys* 44, 339-367.
- Robinett CC, Giansanti MG, Gatti M, and Fuller MT (2009). TRAPPII is required for cleavage furrow ingression and localization of Rab11 in dividing male meiotic cells of *Drosophila*. *J Cell Sci* 122, 4526-4534.
- Roncero C, and Sánchez Y (2010). Cell separation and the maintenance of cell integrity during cytokinesis in yeast: the assembly of a septum. *Yeast* 27, 521-530.
- Rossner S, Fuchsbrunner K, Lange-Dohna C, Hartlage-Rubsamen M, Bigl V, Betz A, Reim K, and Brose N (2004). Munc13-1-mediated vesicle priming contributes to secretory amyloid precursor protein processing. *J Biol Chem* 279, 27841-27844.
- Rybak K, Steiner A, Synek L, Klaeger S, Kulich I, Facher E, Wanner G, Kuster B, Zarsky V, Persson S, and Assaad FF (2014). Plant cytokinesis is orchestrated by the sequential action of the TRAPPII and exocyst tethering complexes. *Dev Cell* 29, 607-620.
- Saha S, and Pollard TD (2012a). Anillin-related protein Mid1p coordinates the assembly of the cytokinetic contractile ring in fission yeast. *Mol Biol Cell* 23, 3982-3992.
- Saha S, and Pollard TD (2012b). Characterization of structural and functional domains of the anillin-related protein Mid1p that contribute to cytokinesis in fission yeast. *Mol Biol Cell* 23, 3993-4007.

- Scott BL, Van Komen JS, Irshad H, Liu S, Wilson KA, and McNew JA (2004). Sec1p directly stimulates SNARE-mediated membrane fusion in vitro. *J Cell Biol* 167, 75-85.
- Simanis V (2015). *Pombe's* thirteen - control of fission yeast cell division by the septation initiation network. *J Cell Sci* 128, 1465-1474.
- Sipiczki M (2007). Splitting of the fission yeast septum. *FEMS Yeast Res* 7, 761-770.
- Skop AR, Bergmann D, Mohler WA, and White JG (2001). Completion of cytokinesis in *C. elegans* requires a brefeldin A-sensitive membrane accumulation at the cleavage furrow apex. *Curr Biol* 11, 735-746.
- Sparks CA, Morphew M, and McCollum D (1999). Sid2p, a spindle pole body kinase that regulates the onset of cytokinesis. *J Cell Biol* 146, 777-790.
- Stachowiak MR, Laplante C, Chin HF, Guirao B, Karatekin E, Pollard TD, and O'Shaughnessy B (2014). Mechanism of cytokinetic contractile ring constriction in fission yeast. *Dev Cell* 29, 547-561.
- Su K-C, Takaki T, and Petronczki M (2011). Targeting of the RhoGEF Ect2 to the equatorial membrane controls cleavage furrow formation during cytokinesis. *Dev Cell* 21, 1104-1115.
- Tajadura V, García B, García I, García P, and Sánchez Y (2004). *Schizosaccharomyces pombe* Rgf3p is a specific Rho1 GEF that regulates cell wall beta-glucan biosynthesis through the GTPase Rho1p. *J Cell Sci* 117, 6163-6174.
- Tang BL (2012). Membrane trafficking components in cytokinesis. *Cell Physiol Biochem* 30, 1097-1108.

- TerBush DR, Maurice T, Roth D, and Novick P (1996). The Exocyst is a multiprotein complex required for exocytosis in *Saccharomyces cerevisiae*. EMBO J 15, 6483-6494.
- Thiyagarajan S, Munteanu EL, Arasada R, Pollard TD, and O'Shaughnessy B (2015). The fission yeast cytokinetic contractile ring regulates septum shape and closure. J Cell Sci 128, 3672-3681.
- Thumkeo D, Watanabe S, and Narumiya S (2013). Physiological roles of Rho and Rho effectors in mammals. Eur J Cell Biol 92, 303-315.
- Toshima JY, Furuya E, Kanno C, Nagano M, and Toshima JY (2015). Pan1p regulates the interaction between endocytic vesicles, endosomes and the actin cytoskeleton. Mol Biol Cell 26.
- Toshima JY, Furuya E, Nagano M, Kanno C, Sakamoto Y, Ebihara M, Siekhaus DE, and Toshima J (2016). Yeast Eps15-like endocytic protein Pan1p regulates the interaction between endocytic vesicles, endosomes and the actin cytoskeleton. Elife 5, e10276.
- Vavylonis D, Wu J-Q, Hao S, O'Shaughnessy B, and Pollard TD (2008). Assembly mechanism of the contractile ring for cytokinesis by fission yeast. Science 319, 97-100.
- Vogel BE, Wagner C, Paterson JM, Xu X, and Yanowitz JL (2011). An extracellular matrix protein prevents cytokinesis failure and aneuploidy in the *C. elegans* germline. Cell Cycle 10, 1916-1920.

- Wachtler V, Huang Y, Karagiannis J, and Balasubramanian MK (2006). Cell cycle-dependent roles for the FCH-domain protein Cdc15p in formation of the actomyosin ring in *Schizosaccharomyces pombe*. *Mol Biol Cell* 17, 3254-3266.
- Walther A, and Wendland J (2003). Septation and cytokinesis in fungi. *Fungal Genet Biol* 40, 187-196.
- Wang N, Lee I-J, Rask G, and Wu J-Q (2016). Roles of the TRAPP-II Complex and the Exocyst in Membrane Deposition during Fission Yeast Cytokinesis. *PLoS Biol* 14, e1002437.
- Wang N, Wang M, Zhu Y-H, Grosel TW, Sun D, Kudryashov DS, and Wu J-Q (2015). The Rho-GEF Gef3 interacts with the septin complex and activates the GTPase Rho4 during fission yeast cytokinesis. *Mol Biol Cell* 26, 238-255.
- Wei B, Hercyk BS, Mattson N, Mohammadi A, Rich J, DeBruyne E, Clark MM, and Das M (2016). Unique spatiotemporal activation pattern of Cdc42 by Gef1 and Scd1 promotes different events during cytokinesis. *Mol Biol Cell* 27, 1235-1245.
- Weinberg J, and Drubin DG (2012). Clathrin-mediated endocytosis in budding yeast. *Trends Cell Biol* 22, 1-13.
- Wu B, and Guo W (2015). The Exocyst at a Glance. *J Cell Sci* 128, 2957-2964.
- Wu J, Tan X, Wu C, Cao K, Li Y, and Bao Y (2013). Regulation of cytokinesis by exocyst subunit SEC6 and KEULE in *Arabidopsis thaliana*. *Mol Plant* 6, 1863-1876.
- Wu J-Q, and Pollard TD (2005). Counting cytokinesis proteins globally and locally in fission yeast. *Science* 310, 310-314.

- Wu J-Q, Sirotkin V, Kovar DR, Lord M, Beltzner CC, Kuhn JR, and Pollard TD (2006).  
Assembly of the cytokinetic contractile ring from a broad band of nodes in fission  
yeast. *J Cell Biol* 174, 391-402.
- Xu J, Camacho M, Xu Y, Esser V, Liu X, Trimbuch T, Pan YZ, Ma C, Tomchick DR,  
Rosenmund C, and Rizo J (2017). Mechanistic insights into neurotransmitter  
release and presynaptic plasticity from the crystal structure of Munc13-1  
C1C2BMUN. *Elife* 6, e22567.
- Xu X, and Vogel BE (2011). A new job for ancient extracellular matrix proteins:  
Hemicentins stabilize cleavage furrows. *Commun Integr Biol* 4, 433-435.
- Yang CB, Zheng YT, Li GY, and Mower GD (2002). Identification of Munc 13-3 as a  
candidate gene for critical-period neuroplasticity in visual cortex. *J Neurosci* 22,  
8614-8618.
- Yang X, Wang S, Sheng Y, Zhang M, Zou W, Wu L, Kang L, Rizo J, Zhang R, Xu T,  
and Ma C (2015). Syntaxin opening by the MUN domain underlies the function of  
Munc13 in synaptic-vesicle priming. *Nat Struct Mol Biol* 22, 547-554.
- Ye Y, Lee I-J, Runge KW, and Wu J-Q (2012). Roles of putative Rho-GEF Gef2 in  
division-site positioning and contractile-ring function in fission yeast cytokinesis.  
*Mol Biol Cell* 23, 1181-1195.
- Zarsky V, Kulich I, Fendrych M, and Pecenkova T (2013). Exocyst complexes multiple  
functions in plant cells secretory pathways. *Curr Opin Plant Biol* 16, 726-733.
- Zhang X, Bi E, Novick P, Du L, Kozminski KG, Lipschutz JH, and Guo W (2001).  
Cdc42 interacts with the exocyst and regulates polarized secretion. *J Biol Chem*  
276, 46745-46750.

Zhou Z, Munteanu EL, He J, Ursell T, Bathe M, Huang KC, and Chang F (2015). The contractile ring coordinates curvature-dependent septum assembly during fission yeast cytokinesis. *Mol Biol Cell* 26, 78-90.

Zhu Y-H, Ye Y, Wu Z, and Wu J-Q (2013). Cooperation between Rho-GEF Gef2 and its binding partner Nod1 in the regulation of fission yeast cytokinesis. *Mol Biol Cell* 24, 3187-3204.

## **Reference for Chapter 2**

Almonacid M, Celton-Morizur S, Jakubowski JL, Dingli F, Loew D, Mayeux A, Chen JS, Gould KL, Clifford DM, and Paoletti A (2011). Temporal control of contractile ring assembly by Plo1 regulation of myosin II recruitment by Mid1/anillin. *Curr Biol* 21, 473-479.

Almonacid M, Moseley JB, Janvore J, Mayeux A, Fraisier V, Nurse P, and Paoletti A (2009). Spatial control of cytokinesis by Cdr2 kinase and Mid1/anillin nuclear export. *Curr Biol* 19, 961-966.

Arasada R, and Pollard TD (2011). Distinct roles for F-BAR proteins Cdc15p and Bzz1p in actin polymerization at sites of endocytosis in fission yeast. *Curr Biol* 21, 1450-1459.

Arellano M, Duran A, and Pérez P (1997). Localisation of the *Schizosaccharomyces pombe* rho1p GTPase and its involvement in the organisation of the actin cytoskeleton. *J Cell Sci* 110, 2547-2555.

- Bähler J, Steever AB, Wheatley S, Wang Y-L, Pringle JR, Gould KL, and McCollum D (1998a). Role of polo kinase and Mid1p in determining the site of cell division in fission yeast. *J Cell Biol* 143, 1603-1616.
- Bähler J, Wu J-Q, Longtine MS, Shah NG, McKenzie A III, Steever AB, Wach A, Philippsen P, and Pringle JR (1998b). Heterologous modules for efficient and versatile PCR-based gene targeting in *Schizosaccharomyces pombe*. *Yeast* 14, 943-951.
- Balasubramanian MK, McCollum D, Chang L, Wong KC, Naqvi NI, He X, Sazer S, and Gould KL (1998). Isolation and characterization of new fission yeast cytokinesis mutants. *Genetics* 149, 1265-1275.
- Bement WM, Benink HA, and von Dassow G (2005). A microtubule-dependent zone of active RhoA during cleavage plane specification. *J Cell Biol* 170, 91-101.
- Bezanilla M, Forsburg SL, and Pollard TD (1997). Identification of a second myosin-II in *Schizosaccharomyces pombe*: Myp2p is conditionally required for cytokinesis. *Mol Biol Cell* 8, 2693-2705.
- Bi E, and Park H-O (2012). Cell polarization and cytokinesis in budding yeast. *Genetics* 191, 347-387.
- Butty AC, Perrinjaquet N, Petit A, Jaquenoud M, Segall JE, Hofmann K, Zwahlen C, and Peter M (2002). A positive feedback loop stabilizes the guanine-nucleotide exchange factor Cdc24 at sites of polarization. *EMBO J* 21, 1565-1576.
- Calonge TM, Nakano K, Arellano M, Arai R, Katayama S, Toda T, Mabuchi I, and Pérez P (2000). *Schizosaccharomyces pombe* Rho2p GTPase regulates cell wall  $\alpha$ -

- glucan biosynthesis through the protein kinase Pck2p. *Mol Biol Cell* 11, 4393-4401.
- Carnahan RH, and Gould KL (2003). The PCH family protein, Cdc15p, recruits two F-actin nucleation pathways to coordinate cytokinetic actin ring formation in *Schizosaccharomyces pombe*. *J Cell Biol* 162, 851-862.
- Cerutti L, and Simanis V (1999). Asymmetry of the spindle pole bodies and spg1p GAP segregation during mitosis in fission yeast. *J Cell Sci* 112, 2313-2321.
- Chang F, Wollard A, and Nurse P (1996). Isolation and characterization of fission yeast mutants defective in the assembly and placement of the contractile actin ring. *J Cell Sci* 109, 131-142.
- Chang L, and Gould KL (2000). Sid4p is required to localize components of the septation initiation pathway to the spindle pole body in fission yeast. *Proc Natl Acad Sci USA* 97, 5249-5254.
- Chen C-T, Feoktistova A, Chen J.S, Shim YS, Clifford DM, Gould KL, and McCollum D (2008). The SIN kinase Sid2 regulates cytoplasmic retention of the *S. pombe* Cdc14-like phosphatase Clp1. *Curr Biol* 18, 1594-1599.
- Chen Q, and Pollard TD (2011). Actin filament severing by cofilin is more important for assembly than constriction of the cytokinetic contractile ring. *J Cell Biol* 195, 485-498.
- Coffman VC, Nile AH, Lee I-J, Liu HY, and Wu J-Q (2009). Roles of formin nodes and myosin motor activity in Mid1p-dependent contractile-ring assembly during fission yeast cytokinesis. *Mol Biol Cell* 20, 5195-5210.

Coll PM, Trillo Y, Ametzazurra A, and Pérez P (2003). Gef1p, a new guanine nucleotide exchange factor for Cdc42p, regulates polarity in *Schizosaccharomyces pombe*. Mol Biol Cell 14, 313-323.

Deng L, and Moseley JB (2013). Compartmentalized nodes control mitotic entry signaling in fission yeast. Mol Biol Cell 24,1872-1881.

Eng K, Naqvi NI, Wong KC, and Balasubramanian MK (1998). Rng2p, a protein required for cytokinesis in fission yeast, is a component of the actomyosin ring and the spindle pole body. Curr Biol 8, 611-621.

Fankhauser C, Reymond A, Cerutti L, Utzig S, Hofmann K, and Simanis V (1995). The *S. pombe cdc15* gene is a key element in the reorganization of F-actin at mitosis. Cell 82, 435-444.

Fankhauser C, and Simanis V (1993). The *Schizosaccharomyces pombe cdc14* gene is required for septum formation and can also inhibit nuclear division. Mol Biol Cell 4, 531-539.

Fankhauser C, and Simanis V (1994). The *cdc7* protein kinase is a dosage dependent regulator of septum formation in fission yeast. EMBO J 13, 3011-3019.

Furge KA, Cheng Q-C, Jwa M, Shin S, Song K, and Albright CF (1999). Regions of Byr4, a regulator of septation in fission yeast, that bind Spg1 or Cdc16 and form a two-component GTPase-activating protein with Cdc16. J Biol Chem 274, 11339-11343.

Furge KA, Wong K, Armstrong J, Balasubramanian M, and Albright CF (1998). Byr4 and Cdc16 form a two-component GTPase-activating protein for the Spg1 GTPase that controls septation in fission yeast. Curr Biol 8, 947-954.

- García P, García I, Marcos F, de Garibay GR, and Sánchez Y (2009). Fission yeast *rgf2p* is a rho1p guanine nucleotide exchange factor required for spore wall maturation and for the maintenance of cell integrity in the absence of *rgf1p*. *Genetics* 181, 1321-1334.
- García P, Tajadura V, García I, and Sánchez Y (2006a). *Rgf1p* is a specific Rho1-GEF that coordinates cell polarization with cell wall biogenesis in fission yeast. *Mol Biol Cell* 17, 1620-1631.
- García P, Tajadura V, García I, and Sánchez Y (2006b). Role of Rho GTPases and Rho-GEFs in the regulation of cell shape and integrity in fission yeast. *Yeast* 23, 1031-1043.
- Goyal A, and Simanis V (2012). Characterization of *ypa1* and *ypa2*, the *Schizosaccharomyces pombe* orthologs of the peptidyl prolyl isomerases that activate PP2A, reveals a role for Ypa2p in the regulation of cytokinesis. *Genetics* 190, 1235-1250.
- Green RA, Paluch E, and Oegema K (2012). Cytokinesis in animal cells. *Annu Rev Cell Dev Biol* 28, 29-58.
- Guertin DA, Chang L, Irshad F, Gould KL, and McCollum D (2000). The role of the Sid1p kinase and Cdc14p in regulating the onset of cytokinesis in fission yeast. *EMBO J* 19, 1803-1815.
- Guzman-Vendrell M, Baldissard S, Almonacid M, Mayeux A, Paoletti A, and Moseley JB (2013). Blt1 and Mid1 provide overlapping membrane anchors to position the division plane in fission yeast. *Mol Cell Biol* 33, 418-428.

- Hachet O, Berthelot-Grosjean M, Kokkoris K, Vincenzetti V, Moosbrugger J, and MartinSG (2011). A phosphorylation cycle shapes gradients of the DYRK family kinase Pom1 at the plasma membrane. *Cell* 145, 1116-1128.
- Hachet O, and Simanis V (2008). Mid1p/anillin and the septation initiation network orchestrate contractile ring assembly for cytokinesis. *Genes Dev* 22, 3205-3216.
- Hirota K, Tanaka K, Ohta K, and Yamamoto M (2003). Gef1p and Scd1p, the Two GDP-GTP exchange factors for Cdc42p, form a ring structure that shrinks during cytokinesis in *Schizosaccharomyces pombe*. *Mol Biol Cell* 14, 3617-3627.
- Hou M-C, Salek J, and McCollum D (2000). Mob1p interacts with the Sid2p kinase and is required for cytokinesis in fission yeast. *Curr Biol* 10, 619-622.
- Huang Y, Yan H, and Balasubramanian MK (2008). Assembly of normal actomyosin rings in the absence of Mid1p and cortical nodes in fission yeast. *J Cell Biol* 183, 979-988.
- Imamura H, Tanaka K, Hihara T, Umikawa M, Kamei T, Takahashi K, Sasaki T, and Takai Y (1997). Bni1p and Bnr1p: downstream targets of the Rho family small G-proteins which interact with profilin and regulate actin cytoskeleton in *Saccharomyces cerevisiae*. *EMBO J* 16, 2745-2755.
- Iwaki N, Karatsu K, and Miyamoto M (2003). Role of guanine nucleotide exchange factors for Rho family GTPases in the regulation of cell morphology and actin cytoskeleton in fission yeast. *Biochem Biophys Res Commun* 312, 414-420.
- Jiang W, and Hallberg RL (2001). Correct regulation of the septation initiation network in *Schizosaccharomyces pombe* requires the activities of *par1* and *par2*. *Genetics* 158, 1413-1429.

- Jin Q-W, and McCollum D (2003). Scw1p antagonizes the septation initiation network to regulate septum formation and cell separation in the fission yeast *Schizosaccharomyces pombe*. *Eukaryot Cell* 2, 510-520.
- Jin Q-W, Zhou M, Bimbo A, Balasubramanian MK, and McCollum D (2006). A role for the septation initiation network in septum assembly revealed by genetic analysis of *sid2-250* suppressors. *Genetics* 172, 2101-2112.
- Johnson AE, McCollum D, and Gould KL (2012). Polar opposites: Fine-tuning cytokinesis through SIN asymmetry. *Cytoskeleton (Hoboken)* 69, 686-699.
- Jones DT (1999). Protein secondary structure prediction based on position-specific scoring matrices. *J Mol Biol* 292, 195-202.
- Jourdain I, Brzezinska EA, and Toda T (2013). Fission yeast Nod1 is a component of cortical nodes involved in cell size control and division site placement. *PLoS One* 8, e54142.
- Jwa M, and Song K (1998). Byr4, a dosage-dependent regulator of cytokinesis in *S. pombe*, interacts with a possible small GTPase pathway including Spg1 and Cdc16. *Mol cells* 8, 240-245.
- Kim DU *et al.* (2010). Analysis of a genome-wide set of gene deletions in the fission yeast *Schizosaccharomyces pombe*. *Nat Biotechnol* 28, 617-623.
- Kita A, Li C, Yu Y, Umeda N, Doi A, Yasuda M, Ishiwata S, Taga A, Horiuchi Y, and Sugiura R (2011). Role of the Small GTPase Rho3 in Golgi/Endosome Trafficking through Functional Interaction with Adaptin in Fission Yeast. *PLoS One* 6, e16842.

- Kovar DR, Kuhn JR, Tichy AL, and Pollard TD (2003). The fission yeast cytokinesis formin Cdc12p is a barbed end actin filament capping protein gated by profilin. *J Cell Biol* 161, 875-887.
- Krapp A, Collin P, Cano Del Rosario E, and Simanis V (2008). Homeostasis between the GTPase Spg1p and its GAP in the regulation of cytokinesis in *S. pombe*. *J Cell Sci* 121, 601-608.
- Krapp A, Schmidt S, Cano E, and Simanis V (2001). *S. pombe* cdc11p, together with sid4p, provides an anchor for septation initiation network proteins on the spindle pole body. *Curr Biol* 11, 1559-1568.
- Krapp A, and Simanis V (2008). An overview of the fission yeast septation initiation network (SIN). *Biochem Soc Trans* 36, 411-415.
- Laporte D, Coffman VC, Lee I-J, and Wu J-Q (2011). Assembly and architecture of precursor nodes during fission yeast cytokinesis. *J Cell Biol* 192, 1005-1021.
- Laporte D, Ojkic N, Vavylonis D, and Wu J-Q (2012).  $\alpha$ -Actinin and fimbrin cooperate with myosin II to organize actomyosin bundles during contractile-ring assembly. *Mol Biol Cell* 23, 3094-3110.
- Lee I-J, Coffman VC, and Wu J-Q (2012). Contractile-ring assembly in fission yeast cytokinesis: Recent advances and new perspectives. *Cytoskeleton (Hoboken)* 69, 751-763.
- Lee I-J, and Wu J-Q (2012). Characterization of Mid1 domains for targeting and scaffolding in fission yeast cytokinesis. *J Cell Sci* 125, 2973-2985.
- Lehner CF (1992). The *pebble* gene is required for cytokinesis in *Drosophila*. *J Cell Sci* 103, 1021-1030.

- MacIver FH, Tanaka K, Robertson AM, and Hagan IM (2003). Physical and functional interactions between polo kinase and the spindle pole component Cut12 regulate mitotic commitment in *S. pombe*. *Genes Dev* 17, 1507-1523.
- Mana-Capelli S, McLean JR, Chen C-T, Gould KL, and McCollum D (2012). The kinesin-14 Klp2 is negatively regulated by the SIN for proper spindle elongation and telophase nuclear positioning. *Mol Biol Cell* 23, 4592-4600.
- Martin SG, and Berthelot-Grosjean M (2009). Polar gradients of the DYRK-family kinase Pom1 couple cell length with the cell cycle. *Nature* 459, 852-856.
- Maudrell K (1990). *nmt1* of fission yeast. A highly transcribed gene completely repressed by thiamine. *J Biol Chem* 265, 10857-10864.
- Mehta S, and Gould KL (2006). Identification of functional domains within the septation initiation network kinase, Cdc7. *J Biol Chem* 281, 9935-9941.
- Moreno S, Klar A, and Nurse P (1991). Molecular genetic analysis of fission yeast *Schizosaccharomyces pombe*. *Methods Enzymol* 194, 795-823.
- Morrell-Falvey JL, Ren L, Feoktistova A, Haese GD, and Gould KL (2005). Cell wall remodeling at the fission yeast cell division site requires the Rho-GEF Rgf3p. *J Cell Sci* 118, 5563-5573.
- Morrell JL *et al* (2004). Sid4p-Cdc11p assembles the septation initiation network and its regulators at the *S. pombe* SPB. *Curr Biol* 14, 579-584.
- Moseley JB, Mayeux A, Paoletti A, and Nurse P (2009). A spatial gradient coordinates cell size and mitotic entry in fission yeast. *Nature* 459, 857-860.

- Motegi F, Mishra M, Balasubramanian MK, and Mabuchi I (2004). Myosin-II reorganization during mitosis is controlled temporally by its dephosphorylation and spatially by Mid1 in fission yeast. *J Cell Biol* 165, 685-695.
- Mutoh T, Nakano K, and Mabuchi I (2005). Rho1-GEFs Rgf1 and Rgf2 are involved in formation of cell wall and septum, while Rgf3 is involved in cytokinesis in fission yeast. *Genes Cells* 10, 1189-1202.
- Nakano K, Arai R, and Mabuchi I (1997). The small GTP-binding protein Rho1 is a multifunctional protein that regulates actin localization, cell polarity, and septum formation in the fission yeast *Schizosaccharomyces pombe*. *Genes Cells* 2, 679-694.
- Nakano K, Arai R, and Mabuchi I (2005). Small GTPase Rho5 is a functional homologue of Rho1, which controls cell shape and septation in fission yeast. *FEBS Lett* 579, 5181-5186.
- Nakano K, Imai J, Arai R, Toh EA, Matsui Y, and Mabuchi I (2002). The small GTPase Rho3 and the diaphanous/formin For3 function in polarized cell growth in fission yeast. *J Cell Sci* 115, 4629-4639.
- Nakano K, Mutoh T, Arai R, and Mabuchi I (2003). The small GTPase Rho4 is involved in controlling cell morphology and septation in fission yeast. *Genes Cells* 8, 357-370.
- Nishimura Y, and Yonemura S (2006). Centralspindlin regulates ECT2 and RhoA accumulation at the equatorial cortex during cytokinesis. *J Cell Sci* 119, 104-114.
- O'Keefe L, Somers WG, Harley A, and Saint R (2001). The pebble GTP exchange factor and the control of cytokinesis. *Cell Struct Funct* 26, 619-626.

- Ojkie N, Wu J-Q, and Vavylonis D (2011). Model of myosin node aggregation into a contractile ring: the effect of local alignment. *J Phys Condens Matter* 23, 374103.
- Padmanabhan A, Bakka K, Sevugan M, Naqvi NI, D'Souza V, Tang X, Mishra M, and Balasubramanian MK (2011). IQGAP-related Rng2p organizes cortical nodes and ensures position of cell division in fission yeast. *Curr Biol* 21, 467-472.
- Paoletti A, and Chang F (2000). Analysis of mid1p, a protein required for placement of the cell division site, reveals a link between the nucleus and the cell surface in fission yeast. *Mol Biol Cell* 11, 2757-2773.
- Pérez P, and Rincón SA (2010). Rho GTPases: regulation of cell polarity and growth in yeasts. *Biochem J* 426, 243-253.
- Piekny A, Werner M, and Glotzer M (2005). Cytokinesis: welcome to the Rho zone. *Trends Cell Biol* 15, 651-658.
- Pinar M, Coll PM, Rincón SA, and Pérez P (2008). *Schizosaccharomyces pombe* Pxl1 is a paxillin homologue that modulates Rho1 activity and participates in cytokinesis. *Mol Biol Cell* 19, 1727-1738.
- Pollard TD, and Wu J-Q (2010). Understanding cytokinesis: lessons from fission yeast. *Nat Rev Mol Cell Biol* 11, 149-155.
- Proctor SA, Minc N, Boudaoud A, and Chang F (2012). Contributions of turgor pressure, the contractile ring, and septum assembly to forces in cytokinesis in fission yeast. *Curr Biol* 22, 1601-1608.
- Rincón S, Coll PM, and Pérez P (2007). Spatial regulation of Cdc42 during cytokinesis. *Cell Cycle* 6, 1687-1691.

- Rincón SA, Santos B, and Pérez P (2006). Fission yeast Rho5p GTPase is a functional paralogue of Rho1p that plays a role in survival of spores and stationary-phase cells. *Eukaryot Cell* 5, 435-446.
- Roberts-Galbraith RH, Chen J-S, Wang J, and Gould KL (2009). The SH3 domains of two PCH family members cooperate in assembly of the *Schizosaccharomyces pombe* contractile ring. *J Cell Biol* 184, 113-127.
- Roberts-Galbraith RH, and Gould KL (2008). Stepping into the ring: the SIN takes on contractile ring assembly. *Genes Dev* 22, 3082-3088.
- Roberts-Galbraith RH, Ohi MD, Ballif BA, Chen J-S, McLeod I, McDonald WH, Gygi SP, Yates JR III, and Gould KL (2010). Dephosphorylation of F-BAR protein Cdc15 modulates its conformation and stimulates its scaffolding activity at the cell division site. *Mol Cell* 39, 86-99.
- Saha S, and Pollard TD (2012a). Anillin-related protein Mid1p coordinates the assembly of the cytokinetic contractile ring in fission yeast. *Mol Biol Cell* 23, 3982-3992.
- Saha S, and Pollard TD (2012b). Characterization of structural and functional domains of the anillin-related protein Mid1p that contribute to cytokinesis in fission yeast. *Mol Biol Cell* 23, 3993-4007.
- Salimova E, Sohrmann M, Fournier N, and Simanis V (2000). The *S. pombe* orthologue of the *S. cerevisiae mob1* gene is essential and functions in signalling the onset of septum formation. *J Cell Sci* 113, 1695-1704.
- Santos B, Gutierrez J, Calonge TM, and Pérez P (2003). Novel Rho GTPase involved in cytokinesis and cell wall integrity in the fission yeast *Schizosaccharomyces pombe*. *Eukaryot Cell* 2, 521-533.

- Santos B, Martin-Cuadrado AB, Vazquez de Aldana CR, del Rey F, and Pérez P (2005). Rho4 GTPase is involved in secretion of glucanases during fission yeast cytokinesis. *Eukaryot Cell* 4, 1639-1645.
- Schmidt S, Sohrmann M, Hofmann K, Woollard A, and Simanis V (1997). The Spg1p GTPase is an essential, dosage-dependent inducer of septum formation in *Schizosaccharomyces pombe*. *Genes Dev* 11, 1519-1534.
- Slaughter BD, Smith SE, and Li R (2009). Symmetry breaking in the life cycle of the budding yeast. *Cold Spring Harb Perspect Biol* 1, a003384.
- Sohrmann M, Fankhauser C, Brodbeck C, and Simanis V (1996). The *dmf1/mid1* gene is essential for correct positioning of the division septum in fission yeast. *Genes Dev* 10, 2707-2719.
- Sparks CA, Morpew M, and McCollum D (1999). Sid2p, a spindle pole body kinase that regulates the onset of cytokinesis. *J Cell Biol* 146, 777-790.
- Su K-C, Takaki T, and Petronczki M (2011). Targeting of the RhoGEF Ect2 to the equatorial membrane controls cleavage furrow formation during cytokinesis. *Dev Cell* 21, 1104-1115.
- Tajadura V, García B, García I, García P, and Sánchez Y (2004). *Schizosaccharomyces pombe* Rgf3p is a specific Rho1 GEF that regulates cell wall  $\beta$ -glucan biosynthesis through the GTPase Rho1p. *J Cell Sci* 117, 6163-6174.
- Tanaka K, Petersen J, MacIver F, Mulvihill D.P, Glover DM, and Hagan IM (2001). The role of Plo1 kinase in mitotic commitment and septation in *Schizosaccharomyces pombe*. *EMBO J* 20, 1259-1270.

- Tebbs IR, and Pollard TD (2013). Separate roles of IQGAP Rng2p in forming and constricting the *Schizosaccharomyces pombe* cytokinetic contractile ring. *Mol Biol Cell* 24, 1904-1917.
- Tolliday N, VerPlank L, and Li R (2002). Rho1 directs formin-mediated actin ring assembly during budding yeast cytokinesis. *Curr Biol* 12, 1864-1870.
- Tomlin GC, Morrell JL, and Gould KL (2002). The spindle pole body protein Cdc11p links Sid4p to the fission yeast septation initiation network. *Mol Biol Cell* 13, 1203-1214.
- Vavylonis D, Wu J-Q, Hao S, O'Shaughnessy B, and Pollard TD (2008). Assembly mechanism of the contractile ring for cytokinesis by fission yeast. *Science* 319, 97-100.
- Wachtler V, Huang Y, Karagiannis J, and Balasubramanian MK (2006). Cell cycle-dependent roles for the FCH-domain protein Cdc15p in formation of the actomyosin ring in *Schizosaccharomyces pombe*. *Mol Biol Cell* 17, 3254-3266.
- Wang H, Tang X, and Balasubramanian MK (2003). Rho3p regulates cell separation by modulating exocyst function in *Schizosaccharomyces pombe*. *Genetics* 164, 1323-1331.
- Watanabe S, Okawa K, Miki T, Sakamoto S, Morinaga T, Segawa K, Arakawa T, Kinoshita M, Ishizaki T, and Narumiya S (2010). Rho and anillin-dependent control of mDia2 localization and function in cytokinesis. *Mol Biol Cell* 21, 3193-3204.
- Wloka C, and Bi E (2012). Mechanisms of cytokinesis in budding yeast. *Cytoskeleton (Hoboken)* 69, 710-726.

- Wood V *et al* (2012). PomBase: a comprehensive online resource for fission yeast. *Nucleic Acids Res* 40, D695-D699.
- Woods A, Sherwin T, Sasse R, MacRae TH, Baines AJ, and Gull K (1989). Definition of individual components within the cytoskeleton of *Trypanosoma brucei* by a library of monoclonal antibodies. *J Cell Sci* 93, 491-500.
- Wu J-Q, and Pollard TD (2005). Counting cytokinesis proteins globally and locally in fission yeast. *Science* 310, 310-314.
- Wu J-Q, Kuhn JR, Kovar DR, and Pollard TD (2003). Spatial and temporal pathway for assembly and constriction of the contractile ring in fission yeast cytokinesis. *Dev Cell* 5, 723-734.
- Wu J-Q, McCormick C, and Pollard TD (2008). Counting Proteins in Living Cells by Quantitative Fluorescence Microscopy with Internal Standards. *Methods Cell Biol* 89, 253-273.
- Wu J-Q, Sirotkin V, Kovar DR, Lord M, Beltzner CC, Kuhn JR, and Pollard TD (2006). Assembly of the cytokinetic contractile ring from a broad band of nodes in fission yeast. *J Cell Biol* 174, 391-402.
- Wu J-Q, Ye Y, Wang N, Pollard TD, and Pringle JR (2010). Cooperation between the septins and the actomyosin ring and role of a cell-integrity pathway during cell division in fission yeast. *Genetics* 186, 897-915.
- Wu P, Zhao R, Ye Y, and Wu J-Q (2011). Roles of the DYRK kinase Pom2 in cytokinesis, mitochondrial morphology, and sporulation in fission yeast. *PLoS One* 6, e28000.

- Ye Y, Lee I-J, Runge KW, and Wu J-Q (2012). Roles of putative Rho-GEF Gef2 in division-site positioning and contractile-ring function in fission yeast cytokinesis. *Mol Biol Cell* 23, 1181-1195.
- Yoshida S, Kono K, Lowery DM, Bartolini S, Yaffe MB, Ohya Y, and Pellman D (2006). Polo like kinase Cdc5 controls the local activation of Rho1 to promote cytokinesis. *Science* 313, 108-111.
- Yuce O, Piekny A, and Glotzer M (2005). An ECT2-centralspindlin complex regulates the localization and function of RhoA. *J Cell Biol* 170, 571-582.

### **Reference for Chapter 3**

- Albertson R, Riggs B, and Sullivan W (2005). Membrane traffic: a driving force in cytokinesis. *Trends Cell Biol* 15, 92-101.
- Arasada R, and Pollard TD (2014). Contractile ring stability in *S. pombe* depends on F-BAR protein Cdc15p and Bgs1p transport from the Golgi complex. *Cell Rep* 8, 1533-1544.
- Aravamudan B, Fergestad T, Davis WS, Rodesch CK, and Broadie K (1999). *Drosophila* Unc-13 is essential for synaptic transmission. *Nat Neurosci* 2, 965-971.
- Arellano M, Durán A, and Pérez P (1996). Rho 1 GTPase activates the (1-3)beta-D-glucan synthase and is involved in *Schizosaccharomyces pombe* morphogenesis. *EMBO J* 15, 4584-4591.
- Arellano M, Valdivieso MH, Calonge TM, Coll PM, Durán A, and Pérez P (1999). *Schizosaccharomyces pombe* protein kinase C homologues, pck1p and pck2p, are targets of rho1p and rho2p and differentially regulate cell integrity. *J Cell Sci* 112, 3569-3578.

- Bähler J, Wu J-Q, Longtine MS, Shah NG, McKenzie A, 3<sup>rd</sup>, Steever AB, Wach A, Philippsen P, and Pringle JR (1998). Heterologous modules for efficient and versatile PCR-based gene targeting in *Schizosaccharomyces pombe*. *Yeast* 14, 943-951.
- Baluska F, Menzel D, and Barlow PW (2006). Cytokinesis in plant and animal cells: Endosomes 'shut the door'. *Dev Biol* 294, 1-10.
- Berro J, Sirotkin V, and Pollard TD (2010). Mathematical modeling of endocytic actin patch kinetics in fission yeast: disassembly requires release of actin filament fragments. *Mol Biol Cell* 21, 2905-2915.
- Betz A, Telemenakis I, Hofmann K, and Brose N (1996). Mammalian Unc-13 homologues as possible regulators of neurotransmitter release. *Biochem Soc Trans* 24, 661-666.
- Boucrot E, and Kirchhausen T (2007). Endosomal recycling controls plasma membrane area during mitosis. *Proc Natl Acad Sci U S A* 104, 7939-7944.
- Bridges AA, and Gladfelter AS (2015). Septin form and function at the cell cortex. *J Biol Chem* 290, 17173-17180.
- Brose N, Hofmann K, Hata Y, and Sudhof TC (1995). Mammalian homologues of *Caenorhabditis elegans* unc-13 gene define novel family of C2-domain proteins. *J Biol Chem* 270, 25273-25280.
- Brzezinska AA, Johnson JL, Munafo DB, Crozat K, Beutler B, Kiosses WB, Ellis BA, and Catz SD (2008). The Rab27a effectors JFC1/Slp1 and Munc13-4 regulate exocytosis of neutrophil granules. *Traffic* 9, 2151-2164.

- Calonge TM, Nakano K, Arellano M, Arai R, Katayama S, Toda T, Mabuchi I, and Pérez P (2000). *Schizosaccharomyces pombe* Rho2p GTPase regulates cell wall alpha-glucan biosynthesis through the protein kinase Pck2p. *Mol Biol Cell* 11, 4393-4401.
- Chang TY, Jaffray J, Woda B, Newburger PE, and Usmani GN (2011). Hemophagocytic lymphohistiocytosis with MUNC13-4 gene mutation or reduced natural killer cell function prior to onset of childhood leukemia. *Pediatr Blood Cancer* 56, 856-858.
- Chen YA, and Scheller RH (2001). SNARE-mediated membrane fusion. *Nat Rev Mol Cell Biol* 2, 98-106.
- Chicka MC, Ren Q, Richards D, Hellman LM, Zhang J, Fried MG, and Whiteheart SW (2016). Role of Munc13-4 as a Ca<sup>2+</sup>-dependent tether during platelet secretion. *Biochem J* 473, 627-639.
- Chou CS, Moore TI, Chang SD, Nie Q, and Yi TM (2012). Signaling regulated endocytosis and exocytosis lead to mating pheromone concentration dependent morphologies in yeast. *FEBS Lett* 586, 4208-4214.
- Coffman VC, Nile AH, Lee I-J, Liu HY, and Wu J-Q (2009). Roles of Formin Nodes and Myosin Motor Activity in Mid1p-dependent Contractile-Ring Assembly during Fission Yeast Cytokinesis. *Mol Biol Cell* 20, 5195-5210.
- Coffman VC, Sees JA, Kovar DR, and Wu J-Q (2013). The formins Cdc12 and For3 cooperate during contractile ring assembly in cytokinesis. *J Cell Biol* 203, 101-114.
- Coffman VC, and Wu J-Q (2014). Every laboratory with a fluorescence microscope should consider counting molecules. *Mol Biol Cell* 25, 1545-1548.

- Cortés JC, Ramos M, Osumi M, Pérez P, and Ribas JC (2016). Fission yeast septation. *Commun Integr Biol* 9, e1189045.
- Cortés JCG, Carnero E, Ishiguro J, Sánchez Y, Durán A, and Ribas JC (2005). The novel fission yeast (1,3)beta-D-glucan synthase catalytic subunit Bgs4p is essential during both cytokinesis and polarized growth. *J Cell Sci* 118, 157-174.
- D'Avino PP, Giansanti MG, and Petronczki M (2015). Cytokinesis in animal cells. *Cold Spring Harb Perspect Biol* 7, a015834.
- Danilchik MV, Bedrick SD, Brown EE, and Ray K (2003). Furrow microtubules and localized exocytosis in cleaving *Xenopus laevis* embryos. *J Cell Sci* 116, 273-283.
- Davidson R, Laporte D, and Wu J-Q (2015). Regulation of Rho-GEF Rgf3 by the arrestin Art1 in fission yeast cytokinesis. *Mol Biol Cell* 26, 453-466.
- Davidson R, Liu Y, Gerien KS, and Wu J-Q (2016). Real-Time visualization and quantification of contractile ring proteins in single living cells. *Methods Mol Biol* 1369, 9-23.
- de Leon N, Sharifmoghadam MR, Hoya M, Curto MA, Doncel C, and Valdivieso MH (2013). Regulation of cell wall synthesis by the clathrin light chain is essential for viability in *Schizosaccharomyces pombe*. *Plos One* 8, e71510.
- Dekker N, SpeI-Jer D, Grun CH, van den Berg M, de Haan A, and Hochstenbach F (2004). Role of the alpha-glucanase Agn1p in fission-yeast cell separation. *Mol Biol Cell* 15, 3903-3914.
- Deng L, Sugiura R, Ohta K, Tada K, Suzuki M, Hirata M, Nakamura S, Shuntoh H, and Kuno T (2005). Phosphatidylinositol-4-phosphate 5-kinase regulates fission yeast

cell integrity through a phospholipase C-mediated protein kinase C-independent pathway. *J Biol Chem* 280, 27561-27568.

Denis V, and Cyert MS (2005). Molecular analysis reveals localization of *Saccharomyces cerevisiae* protein kinase C to sites of polarized growth and Pkc1p targeting to the nucleus and mitotic spindle. *Eukaryot Cell* 4, 36-45.

Dimova K, Kalkhof S, Pottratz I, Ihling C, Rodriguez-Castaneda F, Liepold T, Griesinger C, Brose N, Sinz A, and Jahn O (2009). Structural insights into the calmodulin-Munc13 interaction obtained by cross-linking and mass spectrometry. *Biochemistry* 48, 5908-5921.

Donovan KW, and Bretscher A (2012). Myosin-V is activated by binding secretory cargo and released in coordination with Rab/Exocyst function. *Dev Cell* 23, 769-781.

Dudenhoffer-Pfeifer M, Schirra C, Pattu V, Halimani M, Maier-Peuschel M, Marshall MR, Matti U, Becherer U, Dirks J, Jung M, Lipp P, Hoth M, Sester M, Krause E, and Rettig J (2013). Different Munc13 isoforms function as priming factors in lytic granule release from murine cytotoxic T lymphocytes. *Traffic* 14, 798-809.

Echard A (2008). Membrane traffic and polarization of lipid domains during cytokinesis. *Biochem Soc Trans* 36, 395-399.

Elstak ED, Neeft M, Nehme NT, Voortman J, Cheung M, Goodarzifard M, Gerritsen HC, Henegouwen PMPVE, Callebaut I, de Saint Basile G, and van der Sluis P (2011). The munc13-4-rab27 complex is specifically required for tethering secretory lysosomes at the plasma membrane. *Blood* 118, 1570-1578.

Feng B, Schwarz H, and Jesuthasan S (2002). Furrow-specific endocytosis during cytokinesis of zebrafish blastomeres. *Exp Cell Res* 279, 14-20.

- Feyder S, De Craene JO, Bar S, Bertazzi DL, and Friant S (2015). Membrane trafficking in the yeast *Saccharomyces cerevisiae* model. *Int J Mol Sci* 16, 1509-1525.
- García P, Tajadura V, García I, and Sánchez Y (2006). Role of Rho GTPases and Rho-GEFs in the regulation of cell shape and integrity in fission yeast. *Yeast* 23, 1031-1043.
- Gerald NJ, Damer CK, O'Halloran TJ, and De Lozanne A (2001). Cytokinesis failure in clathrin-minus cells is caused by cleavage furrow instability. *Cell Motil Cytoskeleton* 48, 213-223.
- Giansanti MG, Vanderleest TE, Jewett CE, Sechi S, Frappaolo A, Fabian L, Robinett CC, Brill JA, Loerke D, Fuller MT, and Blankenship JT (2015). Exocyst-dependent membrane addition is required for anaphase cell elongation and cytokinesis in *Drosophila*. *PLoS Genet* 11, e1005632.
- Giddings TH, Jr., O'Toole ET, Morpew M, Mastronarde DN, McIntosh JR, and Winey M (2001). Using rapid freeze and freeze-substitution for the preparation of yeast cells for electron microscopy and three-dimensional analysis. *Methods Cell Biol* 67, 27-42.
- Goode BL, Eskin JA, and Wendland B (2015). Actin and endocytosis in budding yeast. *Genetics* 199, 315-358.
- Grant BD, and Donaldson JG (2009). Pathways and mechanisms of endocytic recycling. *Nat Rev Mol Cell Biol* 10, 597-608.
- Gromley A, Yeaman C, Rosa J, Redick S, Chen CT, Mirabelle S, Guha M, Sillibourne J, and Doxsey SJ (2005). Centriolin anchoring of exocyst and SNARE complexes at

the midbody is required for secretory-vesicle-mediated abscission. *Cell* 123, 75-87.

Guan R, Dai H, and Rizo J (2008). Binding of the Munc13-1 MUN domain to membrane-anchored SNARE complexes. *Biochemistry* 47, 1474-1481.

Guo W, Grant A, and Novick P (1999a). Exo84p is an exocyst protein essential for secretion. *J Biol Chem* 274, 23558-23564.

Guo W, Roth D, Walch-Solimena C, and Novick P (1999b). The exocyst is an effector for Sec4p, targeting secretory vesicles to sites of exocytosis. *EMBO J* 18, 1071-1080.

Guo W, Tamanoi F, and Novick P (2001). Spatial regulation of the exocyst complex by Rho1 GTPase. *Nat Cell Biol* 3, 353-360.

Hall A (2012). Rho family GTPases. *Biochem Soc Trans* 40, 1378-1382.

Hartlage-Rubsamen M, Waniek A, and Rossner S (2013). Munc13 genotype regulates secretory amyloid precursor protein processing via postsynaptic glutamate receptors. *Int J Dev Neurosci* 31, 36-45.

Hayles J, Wood V, Jeffery L, Hoe KL, Kim DU, Park HO, Salas-Pino S, Heichinger C, and Nurse P (2013). A genome-wide resource of cell cycle and cell shape genes of fission yeast. *Open Biol* 3, 130053.

He B, and Guo W (2009). The exocyst complex in polarized exocytosis. *Curr Opin Cell Biol* 21, 537-542.

He J, Johnson JL, Monfregola J, Ramadass M, Pestonjamas K, Napolitano G, Zhang J, and Catz SD (2016). Munc13-4 interacts with syntaxin 7 and regulates late

- endosomal maturation, endosomal signaling, and TLR9-initiated cellular responses. *Mol Biol Cell* 27, 572-587.
- Herbst S, Lipstein N, Jahn O, and Sinz A (2014). Structural insights into calmodulin/Munc13 interaction. *Biol Chem* 395, 763-768.
- Hu Z, Tong XJ, and Kaplan JM (2013). UNC-13L, UNC-13S, and Tomosyn form a protein code for fast and slow neurotransmitter release in *Caenorhabditis elegans*. *Elife* 2, e00967.
- Huang J-Q, Sun MZ, Gumpfer K, Chi YJ, and Ma JJ (2015). 3D multifocus astigmatism and compressed sensing (3D MACS) based superresolution reconstruction. *Biomed Opt Express* 6, 902-917.
- Idrissi FZ, and Geli MI (2014). Zooming in on the molecular mechanisms of endocytic budding by time-resolved electron microscopy. *Cell Mol Life Sci* 71, 641-657.
- Imamura H, Tanaka K, Hihara T, Umikawa M, Kamei T, Takahashi K, Sasaki T, and Takai Y (1997). Bni1p and Bnr1p: downstream targets of the Rho family small G-proteins which interact with profilin and regulate actin cytoskeleton in *Saccharomyces cerevisiae*. *EMBO J* 16, 2745-2755.
- Ishiguro J, Saitou A, Durán A, and Ribas JC (1997). *cps1(+)*, a *Schizosaccharomyces pombe* gene homolog of *Saccharomyces cerevisiae* FKS genes whose mutation confers hypersensitivity to cyclosporin A and papulacandin B. *J Bacteriol* 179, 7653-7662.
- James DJ, and Martin TF (2013). CAPS and Munc13: CATCHRs that SNARE vesicles. *Front Endocrinol (Lausanne)* 4, 187.

- Johansen J, Alfaro G, and Beh CT (2016). Polarized exocytosis induces compensatory endocytosis by Sec4p-regulated cortical actin polymerization. *PLoS Biol* 14, e1002534.
- Johnson JL, He J, Ramadass M, Pestonjamas K, Kiosses WB, Zhang J, and Catz SD (2016). Munc13-4 is a Rab11-binding protein that regulates Rab11-positive vesicle trafficking and docking at the plasma membrane. *J Biol Chem* 291, 3423-3438.
- Johnson JL, Hong H, Monfregola J, Kiosses WB, and Catz SD (2011). Munc13-4 restricts motility of Rab27a-expressing vesicles to facilitate lipopolysaccharide-induced priming of exocytosis in neutrophils. *J Biol Chem* 286, 5647-5656.
- Joo E, Tsang CW, and Trimble WS (2005). Septins: Traffic control at the cytokinesis intersection. *Traffic* 6, 626-634.
- Jordan SN, and Canman JC (2012). Rho GTPases in animal cell cytokinesis: an occupation by the one percent. *Cytoskeleton (Hoboken)* 69, 919-930.
- Kao RS, Morreale E, Wang L, Ivey FD, and Hoffman CS (2006). *Schizosaccharomyces pombe* Git1 is a C2-domain protein required for glucose activation of adenylate cyclase. *Genetics* 173, 49-61.
- Kashiwazaki J, Yamasaki Y, Itadani A, Teraguchi E, Maeda Y, Shimoda C, and Nakamura T (2011). Endocytosis is essential for dynamic translocation of a syntaxin 1 orthologue during fission yeast meiosis. *Mol Biol Cell* 22, 3658-3670.
- Katayama S, Hirata D, Arellano M, Pérez P, and Toda T (1999). Fission yeast alpha-glucan synthase Mok1 requires the actin cytoskeleton to localize the sites of

growth and plays an essential role in cell morphogenesis downstream of protein kinase C function. *J Cell Bio* 144, 1173-1186.

Kawabe H, Mitkovski M, Kaeser PS, Hirrlinger J, Opazo F, Nestvogel D, Kalla S, Fejtova A, Verrier SE, Bungers SR, Cooper BH, Varoqueaux F, Wang Y, Nehring RB, Gundelfinger ED, Rosenmund C, Rizzoli SO, Sudhof TC, Rhee JS, and Brose N (2017). ELKS1 localizes the synaptic vesicle priming protein bMunc13-2 to a specific subset of active zones. *J Cell Biol* 216, 1143-1161.

Kohli J, Hottinger H, Munz P, Strauss A, and Thuriaux P (1977). Genetic-mapping in *Schizosaccharomyces pombe* by mitotic and meiotic analysis and induced haploidization. *Genetics* 87, 471-489.

Kwan EP, Xie L, Sheu L, Ohtsuka T, and Gaisano HY (2007). Interaction between munc13-1 and RIM is critical for glucagon-like peptide-1-mediated rescue of exocytotic defects in munc13-1-deficient pancreatic beta-cells. *Diabetes* 56, 2579-2588.

Laporte D, Coffman VC, Lee I-J, and Wu J-Q (2011). Assembly and architecture of precursor nodes during fission yeast cytokinesis. *J Cell Biol* 192, 1005-1021.

Layton AT, Savage NS, Howell AS, Carroll SY, Drubin DG, and Lew DJ (2011). Modeling vesicle traffic reveals unexpected consequences for Cdc42p-mediated polarity establishment. *Curr Biol* 21, 184-194.

Lee I-J, Coffman VC, and Wu J-Q (2012). Contractile-ring assembly in fission yeast cytokinesis: Recent advances and new perspectives. *Cytoskeleton (Hoboken)* 69, 751-763.

Lee I-J, Wang N, Hu W, Schott K, Bähler J, Giddings TH, Jr., Pringle JR, Du LL, and Wu J-Q (2014). Regulation of spindle pole body assembly and cytokinesis by the centrin-binding protein Sfi1 in fission yeast. *Mol Biol Cell* 25, 2735-2749.

Lee I-J, and Wu J-Q (2012). Characterization of Mid1 domains for targeting and scaffolding in fission yeast cytokinesis. *J Cell Sci* 125, 2973-2985

Levin DE (2011). Regulation of cell wall biogenesis in *Saccharomyces cerevisiae*: the cell wall integrity signaling pathway. *Genetics* 189, 1145-1175.

Levin DE, Bowers B, Chen CY, Kamada Y, and Watanabe M (1994). Dissecting the protein kinase C/MAP kinase signalling pathway of *Saccharomyces cerevisiae*. *Cell Mol Biol Res* 40, 229-239.

Li W, Ma C, Guan R, Xu YB, Tomchick DR, and Rizo J (2011). The Crystal Structure of a Munc13 C-terminal Module Exhibits a Remarkable Similarity to Vesicle Tethering Factors. *Structure* 19, 1443-1455.

Liu JH, Tang X, Wang HY, Oliferenko S, and Balasubramanian MK (2002). The localization of the integral membrane protein Cps1p to the cell division site is dependent on the actomyosin ring and the septation-inducing network in *Schizosaccharomyces pombe*. *Mol Biol Cell* 13, 989-1000.

Liu JH, Wang HY, McCollum D, and Balasubramanian MK (1999). Drc1p/Cps1p, a 1,3-beta-glucan synthase subunit, is essential for division septum assembly in *Schizosaccharomyces pombe*. *Genetics* 153, 1193-1203.

Liu XX, Seven AB, Camacho M, Esser V, Xu JJ, Trimbuch T, Quade B, Su LJ, Ma C, Rosenmund C, and Rizo J (2016a). Functional synergy between the Munc13 C-terminal C-1 and C-2 domains. *Elife* 5, e13696.

- Liu Y, Lee I-J, Sun M, Lower CA, Runge KW, Ma J, and Wu J-Q (2016b). Roles of the novel coiled-coil protein Rng10 in septum formation during fission yeast cytokinesis. *Mol Biol Cell* 27, 2528-2541.
- Lu J, Machius M, Dulubova I, Dai H, Sudhof TC, Tomchick DR, and Rizo J (2006). Structural basis for a Munc13-1 homodimer to Munc13-1/RIM heterodimer switch. *PLoS Biol* 4, 1159-1172.
- Lu R, and Drubin DG (2017). Selection and stabilization of endocytic sites by Ede1, a yeast functional homologue of human Eps15. *Mol Biol Cell* 28, 567-575.
- Lu R, Drubin DG, and Sun YD (2016). Clathrin-mediated endocytosis in budding yeast at a glance. *J Cell Sci* 129, 1531-1536.
- Ma C, Li W, Xu Y, and Rizo J (2011). Munc13 mediates the transition from the closed syntaxin-Munc18 complex to the SNARE complex. *Nat Struct Mol Biol* 18, 542-549.
- Madison JM, Nurrish S, and Kaplan JM (2005). UNC-13 interaction with syntaxin is required for synaptic transmission. *Curr Biol* 15, 2236-2242.
- Maeda Y, Kashiwazaki J, Shimoda C, and Nakamura T (2009). The *Schizosaccharomyces pombe* syntaxin 1 homolog, Psy1, is essential in the development of the forespore membrane. *Biosci Biotechnol Biochem* 73, 339-345.
- Maimaitiyiming M, Kobayashi Y, Kumanogoh H, Nakamura S, Morita M, and Maekawa S (2013). Identification of dynamin as a septin-binding protein. *Neurosci Lett* 534, 322-326.

- Martin-Cuadrado AB, Duenas E, Sipiczki M, de Aldana CRV, and del Rey F (2003). The endo-beta-1,3-glucanase eng1p is required for dissolution of the primary septum during cell separation in *Schizosaccharomyces pombe*. *J Cell Sci* 116, 1689-1698.
- Martin-Cuadrado AB, Morrell JL, Konomi M, An H, Petit C, Osumi M, Balasubramanian M, Gould KL, Del Rey F, and de Aldana CR (2005). Role of septins and the exocyst complex in the function of hydrolytic enzymes responsible for fission yeast cell separation. *Mol Biol Cell* 16, 4867-4881.
- Martin-García R, Coll PM, and Pérez P (2014). F-BAR domain protein Rga7 collaborates with Cdc15 and Imp2 to ensure proper cytokinesis in fission yeast. *J Cell Sci* 127, 4146-4158.
- Martin TF (2015). PI(4,5)P(2)-binding effector proteins for vesicle exocytosis. *Biochim Biophys Acta* 1851, 785-793.
- Maruyama H, Rakow TL, and Maruyama IN (2001). Synaptic exocytosis and nervous system development impaired in *Caenorhabditis elegans* unc-13 mutants. *Neuroscience* 104, 287-297.
- Matsuyama A, Arai R, Yashiroda Y, Shirai A, Kamata A, Sekido S, Kobayashi Y, Hashimoto A, Hamamoto M, Hiraoka Y, Horinouchi S, and Yoshida M (2006). ORFeome cloning and global analysis of protein localization in the fission yeast *Schizosaccharomyces pombe*. *Nat Biotechnol* 24, 841-847.
- McCollum D, Feoktistova A, Morpew M, Balasubramanian M, and Gould KL (1996). The *Schizosaccharomyces pombe* actin-related protein, Arp3, is a component of the cortical actin cytoskeleton and interacts with profilin. *EMBO J* 15, 6438-6446.

- McCusker D, Royou A, Velours C, and Kellogg D (2012). Cdk1-dependent control of membrane-trafficking dynamics. *Mol Biol Cell* 23, 3336-3347.
- McDonald NA, Vander Kooi CW, Ohi MD, and Gould KL (2015). Oligomerization but not membrane bending underlies the function of certain F-BAR proteins in cell motility and cytokinesis. *Dev Cell* 35, 725-736.
- McMullan R, Hiley E, Morrison P, and Nurrish SJ (2006). Rho is a presynaptic activator of neurotransmitter release at pre-existing synapses in *C. elegans*. *Genes Dev* 20, 65-76.
- Meitinger F, and Palani S (2016). Actomyosin ring driven cytokinesis in budding yeast. *Semin Cell Dev Biol* 53,19-27.
- Mishra M, Huang J, and Balasubramanian MK (2014). The yeast actin cytoskeleton. *FEMS Microbiol Rev* 38, 213-227.
- Montagnac G, Echard A, and Chavrier P (2008). Endocytic traffic in animal cell cytokinesis. *Curr Opin Cell Biol* 20, 454-461.
- Moreno S, Klar A, and Nurse P (1991). Molecular genetic analysis of fission yeast *Schizosaccharomyces pombe*. *Methods Enzymol* 194, 795-823.
- Morrell-Falvey JL, Ren L, Feoktistova A, Haese GD, and Gould KL (2005). Cell wall remodeling at the fission yeast cell division site requires the Rho-GEF Rgf3p. *J Cell Sci* 118, 5563-5573.
- Mutoh T, Nakano K, and Mabuchi I (2005). Rho1-GEFs Rgf1 and Rgf2 are involved in formation of cell wall and septum, while Rgf3 is involved in cytokinesis in fission yeast. *Genes Cells* 10, 1189-1202.

- Nakamura T, Kashiwazaki J, and Shimoda C (2005). A fission yeast SNAP-25 homologue, SpSec9, is essential for cytokinesis and sporulation. *Cell Struct Funct* 30, 15-24.
- Neeft M, Wieffer M, de Jong AS, Negroiu G, Metz CHG, van Loon A, Griffith J, KrI-Jgsveld J, Wulffraat N, Koch H, Heckt AJR, Brose N, KleI-Jmeer M, and van der SluI-Js P (2005). Munc13-4 is an effector of Rab27a and controls secretion of lysosomes in hematopoietic cells. *Mol Biol Cell* 16, 731-741.
- Neto H, Balmer G, and Gould G (2013). Exocyst proteins in cytokinesis: Regulation by Rab11. *Commun Integr Biol* 6, e27635.
- Netrakanti PR, Cooper BH, Dere E, Poggi G, Winkler D, Brose N, and Ehrenreich H (2015). Fast cerebellar reflex circuitry requires synaptic vesicle priming by Munc13-3. *Cerebellum* 14, 264-283.
- Nishimura S, Tokukura M, Ochi J, Yoshida M, and Kakeya H (2014). Balance between exocytosis and endocytosis determines the efficacy of sterol-targeting antibiotics. *Chem Biol* 21, 1690-1699.
- Nonaka H, Tanaka K, Hirano H, Fujiwara T, Kohno H, Umikawa M, Mino A, and Takai Y (1995). A downstream target of Rho1 small GTP-binding protein is Pkc1, a homolog of protein-kinase-C, which leads to activation of the MAP Kinase cascade in *Saccharomyces cerevisiae*. *EMBO J* 14, 5931-5938.
- Onishi M, Koga T, Hirata A, Nakamura T, Asakawa H, Shimoda C, Bähler J, Wu J-Q, Takegawa K, Tachikawa H, Pringle JR, and Fukui Y (2010). Role of septins in the orientation of forespore membrane extension during sporulation in fission yeast. *Mol Cel Biol* 30, 2057-2074.

- Pei JM, Ma C, Rizo J, and Grishin NV (2009). Remote homology between Munc13 MUN domain and vesicle tethering complexes. *J Mol Biol* 391, 509-517.
- Pérez P, Cortés JC, Martín-García R, and Ribas JC (2016). Overview of fission yeast septation. *Cell Microbiol* 18, 1201-1207.
- Pérez P, and Rincón SA (2010). Rho GTPases: regulation of cell polarity and growth in yeasts. *Biochem J* 426, 243-253.
- Pollard TD, and Wu J-Q (2010). Understanding cytokinesis: lessons from fission yeast. *Nat Rev Mol Cell Biol* 11, 149-155.
- Prosser DC, Drivas TG, Maldonado-Baez L, and Wendland B (2011). Existence of a novel clathrin-independent endocytic pathway in yeast that depends on Rho1 and formin. *J Cell Biol* 195, 657-671.
- Prosser DC, and Wendland B (2012). Conserved roles for yeast Rho1 and mammalian RhoA GTPases in clathrin-independent endocytosis. *Small GTPases* 3, 229-235.
- Ren L, Willet AH, Roberts-Galbraith RH, McDonald NA, Feoktistova A, Chen JS, Huang H, Guillen R, Boone C, Sidhu SS, Beckley JR, and Gould KL (2015). The Cdc15 and Imp2 SH3 domains cooperatively scaffold a network of proteins that redundantly ensure efficient cell division in fission yeast. *Mol Biol Cell* 26, 256-269.
- Renz C, Oeljeklaus S, Grinhagens S, Warscheid B, Johnsson N, and Gronemeyer T (2016). Identification of cell cycle dependent interaction partners of the septins by quantitative mass spectrometry. *PLoS One* 11, e0148340.

- Ribas JC, Diaz M, Durán A, and Pérez P (1991). Isolation and characterization of *Schizosaccharomyces pombe* mutants defective in cell wall (1-3)beta-D-glucan. *J Bacteriol* 173, 3456-3462.
- Richmond JE, Davis WS, and Jorgensen EM (1999). UNC-13 is required for synaptic vesicle fusion in *C-elegans*. *Nat Neurosci* 2, 959-964.
- Rincón SA, and Paoletti A (2016). Molecular control of fission yeast cytokinesis. *Semin Cell Dev Biol* 53, 28-38.
- Rizo J, and Sudhof TC (2012). The Membrane fusion enigma: SNAREs, Sec1/Munc18 proteins, and their accomplices-guilty as charged? *Annu Rev Cell Dev Biol*, 28, 279-308.
- Rizo J, and Xu J (2015). The Synaptic Vesicle Release Machinery. *Annu Rev Biophys* 44, 339-367.
- Rossner S, Fuchsbrunner K, Lange-Dohna C, Hartlage-Rubsamen M, Bigl V, Betz A, Reim K, and Brose N (2004). Munc13-1-mediated vesicle priming contributes to secretory amyloid precursor protein processing. *J Biol Chem* 279, 27841-27844.
- Sánchez-Mir L, Soto T, Franco A, Madrid M, Viana RA, Vicente J, Gacto M, Pérez P, and Cansado J (2014). Rho1 GTPase and PKC ortholog Pck1 are upstream activators of the cell integrity MAPK pathway in fission yeast. *PLoS One* 9, e88020.
- Schweitzer JK, Burke EE, Goodson HV, and D'Souza-Schorey C (2005). Endocytosis resumes during late mitosis and is required for cytokinesis. *J Biol Chem* 280, 41628-41635.

- Shen N, Guryev O, and Rizo J (2005). Intramolecular occlusion of the diacylglycerol-binding site in the C1 domain of munc13-1. *Biochemistry* 44, 1089-1096.
- Sheu L, Pasyk EA, Ji JZ, Haung XH, Gao XD, Varoqueaux F, Brose N, and Gaisano HY (2003). Regulation of insulin exocytosis by Munc13-1. *J Biol Chem* 278, 27556-27563.
- Shin OH, Lu J, Rhee JS, Tomchick DR, Pang ZP, Wojcik SM, Camacho-Pérez M, Brose N, Machius M, Rizo J, Rosenmund C, and Sudhof TC (2010). Munc13 C2B domain is an activity-dependent Ca<sup>2+</sup> regulator of synaptic exocytosis. *Nat Struct Mol Biol* 17, 280-288.
- Shuster CB, and Burgess DR (2002). Targeted new membrane addition in the cleavage furrow is a late, separate event in cytokinesis. *Proc Natl Acad Sci U S A* 99, 3633-3638.
- Simanis V (2015). *Pombe's* thirteen - control of fission yeast cell division by the septation initiation network. *J Cell Sci* 128, 1465-1474.
- Sipiczki M (2007). Splitting of the fission yeast septum. *FEMS Yeast Res* 7, 761-770.
- Skop AR, Bergmann D, Mohler WA, and White JG (2001). Completion of cytokinesis in *C. elegans* requires a brefeldin A-sensitive membrane accumulation at the cleavage furrow apex. *Curr Biol* 11, 735-746.
- Song K, Russo G, and Krauss M (2016). Septins as modulators of endo-lysosomal membrane traffic. *Front Cell Dev Biol* 4, 124.
- Sun L, Guan R, Lee I-J, Liu Y, Chen M, Wang J, Wu J-Q, and Chen Z (2015). Mechanistic insights into the anchorage of the contractile ring by anillin and Mid1. *Dev Cell* 33, 413-426.

- Tajadura V, García B, García I, García P, and Sánchez Y (2004). *Schizosaccharomyces pombe* Rgf3p is a specific Rho1 GEF that regulates cell wall beta-glucan biosynthesis through the GTPase Rho1p. *J Cell Sci* 117, 6163-6174.
- Takeda T, Kawate T, and Chang F (2004). Organization of a sterol-rich membrane domain by cdc15p during cytokinesis in fission yeast. *Nat Cell Biol* 6, 1142-1144.
- Tang X, Huang J, Padmanabhan A, Bakka K, Bao Y, Tan BY, Cande WZ, and Balasubramanian MK (2011). Marker reconstitution mutagenesis: a simple and efficient reverse genetic approach. *Yeast* 28, 205-212.
- TerBush DR, Maurice T, Roth D, and Novick P (1996). The Exocyst is a multiprotein complex required for exocytosis in *Saccharomyces cerevisiae*. *EMBO J* 15, 6483-6494.
- VerPlank L, and Li R (2005). Cell cycle-regulated trafficking of Chs2 controls actomyosin ring stability during cytokinesis. *Mol Biol Cell* 16, 2529-2543.
- Wachtler V, Huang Y, Karagiannis J, and Balasubramanian MK (2006). Cell cycle-dependent roles for the FCH-domain protein Cdc15p in formation of the actomyosin ring in *Schizosaccharomyces pombe*. *Mol Biol Cell* 17, 3254-3266.
- Wang HY, Tang X, Liu JH, Trautmann S, Balasundaram D, McCollum D, and Balasubramanian MK (2002). The multiprotein exocyst complex is essential for cell separation in *Schizosaccharomyces pombe*. *Mol Biol Cell* 13, 515-529.
- Wang N, Lee I-J, Rask G, and Wu J-Q (2016). Roles of the TRAPP-II complex and the Exocyst in membrane deposition during fission yeast cytokinesis. *PLoS Biol* 14, e1002437.

- Wang N, Lo Presti L, Zhu Y-H, Kang M, Wu Z, Martin SG, and Wu J-Q (2014). The novel proteins Rng8 and Rng9 regulate the myosin-V Myo51 during fission yeast cytokinesis. *J Cell Biol* 205, 357-375.
- Wang N, Wang M, Zhu Y-H, Grosel TW, Sun D, Kudryashov DS, and Wu J-Q (2015). The Rho-GEF Gef3 interacts with the septin complex and activates the GTPase Rho4 during fission yeast cytokinesis. *Mol Biol Cell* 26, 238-255.
- Weinberg J, and Drubin DG (2012). Clathrin-mediated endocytosis in budding yeast. *Trends Cell Biol* 22, 1-13.
- Wienke DC, Knetsch MLW, Neuhaus EM, Reedy MC, and Manstein DJ (1999). Disruption of a dynamin homologue affects endocytosis, organelle morphology, and cytokinesis in *Dictyostelium discoideum*. *Mol Biol Cell* 10, 225-243.
- Wu J-Q, and Pollard TD (2005). Counting cytokinesis proteins globally and locally in fission yeast. *Science* 310, 310-314.
- Wu J-Q, Sirotkin V, Kovar DR, Lord M, Beltzner CC, Kuhn JR, and Pollard TD (2006). Assembly of the cytokinetic contractile ring from a broad band of nodes in fission yeast. *J Cell Biol* 174, 391-402.
- Wu J-Q, Ye Y, Wang N, Pollard TD, and Pringle JR (2010). Cooperation between the septins and the actomyosin ring and role of a cell-integrity pathway during cell division in fission yeast. *Genetics* 186, 897-915.
- Wu LG, Hamid E, Shin W, and Chiang HC (2014). Exocytosis and endocytosis: modes, functions, and coupling mechanisms. *Annu Rev Physiol* 76, 301-331.
- Xie Z, Long J, Liu J, Chai Z, Kang X, and Wang C (2017). Molecular mechanisms for the coupling of endocytosis to exocytosis in neurons. *Front Mol Neurosci* 10, 47.

- Xu J, Camacho M, Xu Y, Esser V, Liu X, Trimbuch T, Pan YZ, Ma C, Tomchick DR, Rosenmund C, and Rizo J (2017). Mechanistic insights into neurotransmitter release and presynaptic plasticity from the crystal structure of Munc13-1 C1C2BMUN. *Elife* 6, e22567.
- Yamaoka T, Imada K, Fukunishi K, Yamasaki Y, Shimoda C, and Nakamura T (2013). The fission yeast synaptobrevin ortholog Syb1 plays an important role in forespore membrane formation and spore maturation. *Eukaryot Cell* 12, 1162-1170.
- Yang CB, Kiser PJ, Zheng YT, Varoqueaux F, and Mower GD (2007). Bidirectional regulation of munc13-3 protein expression by age and dark rearing during the critical period in mouse visual cortex. *Neuroscience* 150, 603-608.
- Yang CB, Zheng YT, Li GY, and Mower GD (2002). Identification of Munc 13-3 as a candidate gene for critical-period neuroplasticity in visual cortex. *J Neurosci* 22, 8614-8618.
- Yang X, Wang S, Sheng Y, Zhang M, Zou W, Wu L, Kang L, Rizo J, Zhang R, Xu T, and Ma C (2015). Syntaxin opening by the MUN domain underlies the function of Munc13 in synaptic-vesicle priming. *Nat Struct Mol Biol* 22, 547-554.
- Zhang Y, Sugiura R, Lu Y, Asami M, Maeda T, Itoh T, Takenawa T, Shuntoh H, and Kuno T (2000). Phosphatidylinositol 4-phosphate 5-kinase Its3 and calcineurin Ppb1 coordinately regulate cytokinesis in fission yeast. *J Biol Chem* 275, 35600-35606.

Zhou K, Stawicki TM, Goncharov A, and Jin Y (2013). Position of UNC-13 in the active zone regulates synaptic vesicle release probability and release kinetics. *Elife* 2, e01180.

Zhu Y-H, Ye Y, Wu Z, and Wu J-Q (2013). Cooperation between Rho-GEF Gef2 and its binding partner Nod1 in the regulation of fission yeast cytokinesis. *Mol Biol Cell* 24, 3187-3204.

#### **Reference for Chapter 4**

Arasada R, and Pollard TD (2014). Contractile ring stability in *S. pombe* depends on F-BAR protein Cdc15p and Bgs1p transport from the Golgi complex. *Cell Rep* 8, 1533-1544.

Bridges AA, and Gladfelter AS (2015). Septin form and function at the cell cortex. *J Biol Chem* 290, 17173-17180.

Davidson R, Laporte D, and Wu J-Q (2015). Regulation of Rho-GEF Rgf3 by the arrestin Art1 in fission yeast cytokinesis. *Mol Biol Cell* 26, 453-466.

DeMay BS, Bai XB, Howard L, Occhipinti P, Meseroll RA, Spiliotis ET, Oldenbourg R, and Gladfelter AS (2011). Septin filaments exhibit a dynamic, paired organization that is conserved from yeast to mammals. *J Cell Biol* 193, 1065-1081.

Dudenhoffer-Pfeifer M, Schirra C, Pattu V, Halimani M, Maier-Peuschel M, Marshall MR, Matti U, Becherer U, Dirks J, Jung M, Lipp P, Hoth M, Sester M, Krause E, and Rettig J (2013). Different Munc13 isoforms function as priming factors in lytic granule release from murine cytotoxic T lymphocytes. *Traffic* 14, 798-809.

Goss JW, Kim S, Bledsoe H, and Pollard TD (2014). Characterization of the roles of Blt1p in fission yeast cytokinesis. *Mol Biol Cell* 25, 1946-1957.

- Guzman-Vendrell M, Baldissard S, Almonacid M, Mayeux A, Paoletti A, and Moseley JB (2013). Blt1 and Mid1 provide overlapping membrane anchors to position the division plane in fission yeast. *Mol Cell Biol* 33, 418-428.
- Imamura H, Tanaka K, Hihara T, Umikawa M, Kamei T, Takahashi K, Sasaki T, and Takai Y (1997). Bni1p and Bnr1p: downstream targets of the Rho family small G-proteins which interact with profilin and regulate actin cytoskeleton in *Saccharomyces cerevisiae*. *EMBO J* 16, 2745-2755.
- Joo E, Tsang CW, and Trimble WS (2005). Septins: Traffic control at the cytokinesis intersection. *Traffic* 6, 626-634.
- Jourdain I, Brzezinska EA, and Toda T (2013). Fission yeast Nod1 is a component of cortical nodes involved in cell size control and division site placement. *PLoS One* 8, e54142.
- Kosako H, Yoshida T, Matsumura F, Ishizaki T, Narumiya S, and Inagaki M (2000). Rho-kinase/ROCK is involved in cytokinesis through the phosphorylation of myosin light chain and not ezrin/radixin/moesin proteins at the cleavage furrow. *Oncogene* 19, 6059-6064.
- Kwan EP, Xie L, Sheu L, Ohtsuka T, and Gaisano HY (2007). Interaction between munc13-1 and RIM is critical for glucagon-like peptide-1-mediated rescue of exocytotic defects in munc13-1-deficient pancreatic beta-cells. *Diabetes* 56, 2579-2588.
- Li WM, Webb SE, Lee KW, and Miller AL (2006). Recruitment and SNARE-mediated fusion of vesicles in furrow membrane remodeling during cytokinesis in zebrafish embryos. *Exp Cell Res* 312, 3260-3275.

- Liu Y, Lee I-J, Sun M, Lower CA, Runge KW, Ma J, and Wu J-Q (2016). Roles of the novel coiled-coil protein Rng10 in septum formation during fission yeast cytokinesis. *Mol Biol Cell* 27, 2528-2541.
- Lu J, Machius M, Dulubova I, Dai H, Sudhof TC, Tomchick DR, and Rizo J (2006). Structural basis for a Munc13-1 homodimer to Munc13-1/RIM heterodimer switch. *PLoS Biol* 4, 1159-1172.
- Ma C, Li W, Xu Y, and Rizo J (2011). Munc13 mediates the transition from the closed syntaxin-Munc18 complex to the SNARE complex. *Nat Struct Mol Biol* 18, 542-549.
- Martin-Cuadrado AB, Morrell JL, Konomi M, An H, Petit C, Osumi M, Balasubramanian M, Gould KL, Del Rey F, and de Aldana CR (2005). Role of septins and the exocyst complex in the function of hydrolytic enzymes responsible for fission yeast cell separation. *Mol Biol Cell* 16, 4867-4881.
- Martin-Garcia R, Coll PM, and Perez P (2014). F-BAR domain protein Rga7 collaborates with Cdc15 and Imp2 to ensure proper cytokinesis in fission yeast. *J Cell Sci* 127, 4146-4158.
- Pei JM, Ma C, Rizo J, and Grishin NV (2009). Remote homology between Munc13 MUN domain and vesicle tethering complexes. *J Mol Biol* 391, 509-517.
- Piekny A, Werner M, and Glotzer M (2005). Cytokinesis: welcome to the Rho zone. *Trends Cell Biol* 15, 651-658.
- Pollard TD (2010). Mechanics of cytokinesis in eukaryotes. *Curr Opin Cell Biol* 22, 50-56.

- Rapali P, Mitteau R, Braun C, Massoni-Laporte A, Unlu C, Bataille L, Saint Arramon F, Gyg SP, and McCusker D (2017). Scaffold-mediated gating of Cdc42 signalling flux. *Elife* 6, e25257.
- Ren L, Willet AH, Roberts-Galbraith RH, McDonald NA, Feoktistova A, Chen JS, Huang H, Guillen R, Boone C, Sidhu SS, Beckley JR, and Gould KL (2015). The Cdc15 and Imp2 SH3 domains cooperatively scaffold a network of proteins that redundantly ensure efficient cell division in fission yeast. *Mol Biol Cell* 26, 256-269.
- Renz C, Oeljeklaus S, Grinhagens S, Warscheid B, Johnsson N, and Gronemeyer T (2016). Identification of Cell Cycle Dependent Interaction Partners of the Septins by Quantitative Mass Spectrometry. *PLoS One* 11, e0148340.
- Richmond JE, Davis WS, and Jorgensen EM (1999). UNC-13 is required for synaptic vesicle fusion in *C. elegans*. *Nat Neurosci* 2, 959-964.
- Robinett CC, Giansanti MG, Gatti M, and Fuller MT (2009). TRAPPII is required for cleavage furrow ingression and localization of Rab11 in dividing male meiotic cells of *Drosophila*. *J Cell Sci* 122, 4526-4534.
- Rossner S, Fuchsbrunner K, Lange-Dohna C, Hartlage-Rubsamen M, Bigl V, Betz A, Reim K, and Brose N (2004). Munc13-1-mediated vesicle priming contributes to secretory amyloid precursor protein processing. *J Biol Chem* 279, 27841-27844.
- Shen N, Guryev O, and Rizo J (2005). Intramolecular occlusion of the diacylglycerol-binding site in the C1 domain of munc13-1. *Biochemistry* 44, 1089-1096.

- Sheu L, Pasyk EA, Ji JZ, Haung XH, Gao XD, Varoqueaux F, Brose N, and Gaisano HY (2003). Regulation of insulin exocytosis by Munc13-1. *J Biol Chem* 278, 27556-27563.
- Shimada Y, Wiget P, Gulli MP, Bi ER, and Peter M (2004). The nucleotide exchange factor Cdc24p may be regulated by auto-inhibition. *EMBO J* 23, 1051-1062.
- Shin OH, Lu J, Rhee JS, Tomchick DR, Pang ZP, Wojcik SM, Camacho-Perez M, Brose N, Machius M, Rizo J, Rosenmund C, and Sudhof TC (2010). Munc13 C2B domain is an activity-dependent Ca<sup>2+</sup> regulator of synaptic exocytosis. *Nat Struct Mol Biol* 17, 280-288.
- Shuster CB, and Burgess DR (2002). Targeted new membrane addition in the cleavage furrow is a late, separate event in cytokinesis. *Proc Natl Acad Sci U S A* 99, 3633-3638.
- Song K, Russo G, and Krauss M (2016). Septins as modulators of endo-lysosomal membrane traffic. *Front Cell Dev Biol* 4, 124.
- Wang N, Lee I-J, Rask G, and Wu J-Q (2016). Roles of the TRAPP-II complex and the exocyst in membrane deposition during fission yeast cytokinesis. *PLoS Biol* 14, e1002437.
- Wang N, Wang M, Zhu Y-H, Grosel TW, Sun D, Kudryashov DS, and Wu J-Q (2015). The Rho-GEF Gef3 interacts with the septin complex and activates the GTPase Rho4 during fission yeast cytokinesis. *Mol Biol Cell* 26, 238-255.
- Watanabe S, Okawa K, Miki T, Sakamoto S, Morinaga T, Segawa K, Arakawa T, Kinoshita M, Ishizaki T, and Narumiya S (2010). Rho and anillin-dependent

- control of mDia2 localization and function in cytokinesis. *Mol Biol Cell* 21, 3193-3204.
- Wu LG, Hamid E, Shin W, and Chiang HC (2014). Exocytosis and endocytosis: modes, functions, and coupling mechanisms. *Annu Rev Physiol* 76, 301-331.
- Xu J, Camacho M, Xu Y, Esser V, Liu X, Trimbuch T, Pan YZ, Ma C, Tomchick DR, Rosenmund C, and Rizo J (2017). Mechanistic insights into neurotransmitter release and presynaptic plasticity from the crystal structure of Munc13-1 C1C2BMUN. *Elife* 6, e22567.
- Yang X, Wang S, Sheng Y, Zhang M, Zou W, Wu L, Kang L, Rizo J, Zhang R, Xu T, and Ma C (2015). Syntaxin opening by the MUN domain underlies the function of Munc13 in synaptic-vesicle priming. *Nat Struct Mol Biol* 22, 547-554.
- Ye Y, Lee I-J, Runge KW, and Wu J-Q (2012). Roles of putative Rho-GEF Gef2 in division-site positioning and contractile-ring function in fission yeast cytokinesis. *Mol Biol Cell* 23, 1181-1195.